Classification of the Chiral $\mathbb{Z}_2 \times \mathbb{Z}_2$ Heterotic String Models

SANDER E.M. NOOIJ TRINITY 2004

Classification of the Chiral $\mathbb{Z}_2 \times \mathbb{Z}_2$ Heterotic String Models

SANDER E.M. NOOIJ
ORIEL COLLEGE
TRINITY 2004

RUDOLF PEIERLS CENTRE FOR THEORETICAL PHYSICS
UNIVERSITY OF OXFORD

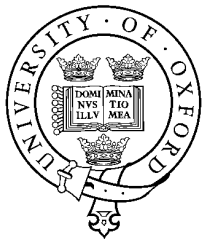

Thesis submitted in partial fulfillment of the requirements
for the Degree of Doctor of Philosophy
at the University of Oxford

Abstract

The Standard Model has been shown to be consistent with observations up to the electroweak scale. The $SO(10)$ grand unification group provides an elegant way to unify the gauge interactions and the particle content of the Standard Model. The replication of the three generations of the Standard Model cannot be explained in this framework. At present the best candidate for providing a unified theory for matter and its interactions is string theory.

Among the most advanced realistic string models that have three generations with a $SO(10)$ embedding are the heterotic free fermionic $\mathbb{Z}_2 \times \mathbb{Z}_2$ orbifold models. This thesis provides a classification of the chiral content of the heterotic $\mathbb{Z}_2 \times \mathbb{Z}_2$ orbifold models. We show that the chiral content of the heterotic $\mathbb{Z}_2 \times \mathbb{Z}_2$ orbifold models at any point in the moduli space can be described by a free fermionic model. We present a direct translation between the orbifold formulation and the free fermionic construction. We use the free fermionic description for the classification wherein we consider orbifolds with symmetric shifts.

We show that perturbative three generation models are not obtained in the case of $\mathbb{Z}_2 \times \mathbb{Z}_2$ orbifolds with symmetric shifts on complex tori, and that the perturbative three generation models in this class necessarily employ an asymmetric shift. We show that the freedom in the modular invariant phases in the $N = 1$ vacua that control the chiral content, can be interpreted as vacuum expectation values of background fields of the underlying $N = 4$ theory, whose dynamical components are projected out by the $\mathbb{Z}_2$ fermionic projections. In this class of vacua the chiral content of the models is determined by the underlying $N = 4$ mother theory.

Publications

This thesis is the culmination of my years at the University of Oxford. It is based on several papers that have been written during that time. Chapter 5 is based on a paper published in Nuclear Physics B [13]. The chapters 6, 7 and the results in chapters 8 and 9 are based on three papers. The first paper reports on a talk given at the second String Phenomenology Conference in Durham, UK [29]. The second paper is published in Nuclear Physics B [30]. The last paper on which parts of this thesis are based, is currently in preparation [31].

Acknowledgements

During my time at the University of Oxford I have enjoyed the support of many people and institutions, allowing me to complete this work. I would like to thank my supervisor Alon Faraggi for his guidance and many useful discussions. The enlightening conversations and meetings with both Costas and Ioannis have proven essential for the completion of this work. I would like to thank Richard and Dave for many interesting discussions as well as Filipe for helping me out even while he was in Portugal.

This work could not have been completed without the financial support I have recieved from many institutions as well as my father Hans. I would like to thank him especially for his fabulous support while I was working on my research. Furthermore, this work would not have been possible without the support of the Pieter Langerhuizen Lambertszoon Fund of the Royal Holland Society of Sciences and Humanities, the VSBfonds, the Fundatie van de Vrijvrouwe van Renswoude te 's Gravenhage and the Noorthey Academy. I would also like to thank Oriel College for their support and generosity. I am thankful that the Rudolf Peierls Centre for Theoretical Physics at the University of Oxford made it possible for me to strengthen my knowledge outside of Oxford during summer.

I would like to thank my beloved Carolijn for supporting me while I was in Oxford. It was a delight having her around in Oxford during my second year. While she was in the Netherlands, I truly enjoyed our many great conversations on the phone as well as her presence during her frequent visits. The support from my mother Kiek and our many conversations I enjoyed hugely. The interest and support from my sister Claire were remarkable, our conversations good fun. Oxford has been a very interesting and stimulating place, notably because of its highly international environment. The many conversations I had with Josef were very intriguing and I would like to thank him for introduc-

ing me to the world of politics. I have had many wonderfull evenings with both chaps Geoff and Mark. I would like to thank Geoff for his insistence on rationality and silly dances, and Mark for his skills in the English language as well as sometimes being a simulacrum of the cerebral and the abstract. When I was not working on my research, I had many great times on the hockey pitch. I would like to thank both Tony and Oli of New College Hockey Club for their enthousiasm. During the year I played at Rover Hockey Club, I had some many good games and evenings with Rich and Tom. I would also like to thank Bernhard and Kudrat for our many conversations and their generosity at the end of my time in Oxford.

Having completed my Doctor of Philosophy at the Universty of Oxford, I will leave behind a place that has given me many invaluable experiences. I will treasure these for the rest of my life.

Contents

Chapter 1

Introduction

One of the most remarkable achievements in physics has been the development of the Standard Model that describes the strong, weak and electromagnetic forces. These three forces together with the matter content of the Standard Model have been shown to be consistent with experimental observations up to the electroweak scale.

In the Standard Model the interactions are invariant under the gauge group $SU(3)_C \times SU(2)_L \times U(1)_Y$ above the electroweak scale. In the Standard Model there are three families of chiral leptons and quarks. Each family has two $SU(2)_L$ weak doublets, of which one weak doublet transforms as a strong $SU(3)_C$ triplet, and three $SU(2)_L$ singlets, two of which transform as strong $SU(3)_C$ triplets. The Higgs weak doublet gives mass to particles below the electroweak scale. The forces are mediated by the gauge bosons of the Standard Model gauge group. The chiral matter content for each family is summarized in table 1.0.1.

Below the electroweak scale the $SU(2)_L \times U(1)_Y$ symmetry is broken to $U(1)_{QED}$ thereby giving mass to the $W^{\pm}$ and Z gauge bosons of the broken symmetry through the Higgs mechanism. The Higgs mechanism furthermore ensures that matter in the Standard Model acquires a mass. In this process the $SU(2)_L$ gauge bosons mix with the $U(1)_Y$ gauge boson giving rise to the Weinberg or weak mixing angle θ_W.

To fully determine the Standard Model we need to fix its parameters. Three gauge couplings determine the strength of the gauge interactions. Nine Yukawa couplings describe the mass of three electron type chiral matter, three down type chiral matter and three up type chiral mat-

	$SU(3)_C$	$SU(2)_L$	$U(1)_Y$
$L = \binom{\nu_e}{e}_L$	1	2	$-\frac{1}{2}$
$Q = \binom{u}{d}_L$	3	2	$\frac{1}{6}$
$\bar{e}_L$	1	1	1
$\bar{u}_L$	$\bar{3}$	1	$-\frac{2}{3}$
$\bar{d}_L$	$\bar{3}$	1	$\frac{1}{3}$

Table 1.0.1: The chiral matter content of the Standard Model decomposed under the gauge group $SU(3)_C \times SU(2)_L \times U(1)_Y$ for each family.

ter. The Standard Model requires three mixing angles and one weak CP violating phase for the CKM matrix. The θ_{QCD} phase parameterizes possible CP violation in the strong sector. Additionally, there are two parameters in the Higgs potential setting the electroweak symmetry breaking scale. All these parameters are measured by experiments and one would like to have a theoretical explanation for their origin. The results of the experiments done at LEP show a repetition of 2.994 ± 0.012 light neutrinos in the Standard Model adding strong experimental support to the existence of just three families of quarks and leptons.[48] This thesis focuses on the replication of three generations in the Standard Model.

An elegant way to explain the gauge couplings and the chiral matter content of the Standard Model is by introducing a $SO(10)$ grand unified theory (GUT). The chiral matter content of a three family $SO(10)$ model is described by three chiral 16 representations of $SO(10)$. Each chiral 16 $SO(10)$ representation contains the chiral matter of the Standard Model plus a right handed neutrino. Breaking each $SO(10)$ to the Standard Model gauge group $SU(3)_C \times SU(2)_L \times U(1)_Y$ decomposes each 16 of $SO(10)$ multiplet into the Standard Model multiplet structure listed in table 1.0.1 plus the right handed neutrino which is a singlet under each Standard Model gauge group. The right handed neutrino allows for massive neutrinos. A nonzero mass for the neutrino has been supported by the observation of neutrinos oscillations.[39, 15] However, the $SO(10)$ grand unified theory cannot explain the number of generations observed in nature.

Ever since the first GUT was proposed, physicists have been troubled by the existence of two mass scales, the electroweak scale and the Planck scale, that differ by approximately thirteen orders of magnitude. This is known as the hierarchy problem. In terms of perturbative field theory, this implies an almost exact cancellation between the bare mass of the

Higgs boson, determining the electroweak scale, and its radiative corrections from the GUT scale. In order to stop the mass of the Higgs boson from becoming too large, an intermediate scale between the Planck and the electroweak scale should be introduced. At this intermediate scale a symmetry between bosons and fermions, known as supersymmetry (SUSY), is present. If supersymmetry is exact then diagrams with boson loops exactly cancel diagrams with fermion loops. In the case of broken global supersymmetry the boson and fermion loops will cancel up to corrections from the broken SUSY scale. The introduction of supersymmetry therefore solves the hierarchy problem by suppressing radiative corrections to the Higgs mass terms above the SUSY breaking scale. A promising feature of $SO(10)$ unification, with supersymmetry included, is that by giving the Standard Model couplings in terms of the $SO(10)$ coupling, it predicts the weak mixing angle $\sin^2\theta_W$ that agrees with observations to a very high precision.[70, 1] However, supersymmetry cannot explain the number of generations.

Although this scheme of unification and the introduction of supersymmetry at an intermediate scale gives very good results, we have left out the force of gravity in our description of elementary matter and its interactions. Unifying the four forces using the highly successful method of field quantization as used in the Standard Model has been shown to give a nonrenormalizable theory.[9] At present the best candidate for unifying the four forces is string theory. In string theory the fundamental objects are one dimensional particles, known as strings. The Lagrangian describing string theory has only one parameter, known as the string tension. However, a consistent string theory has enough degrees of freedom to describe a ten dimensional target space. One way to reduce the ten dimensional target space to the observed four dimensional target space is by compactifying the additional six dimensions. Another way to describe a string in four space time dimensions is by treating the additional degrees of freedom in the Lagrangian as fields on the world sheet not related to any spacetime coordinate a priori. The two descriptions have been shown to be equivalent in a wide class of models.[61, 30] There are many different ways of reducing the number of dimensions. Consequently we have introduced even more degrees of freedom than we started out with in the Standard Model. The problem of finding the correct vacuum of string theory is one of the major problems in string theory today.

Among the most realistic phenomenological string models to date are the three generation heterotic string models, constructed in the free-fermion formulation. These models have been the subject of detailed studies, showing that they can, at least in principle, account for de-

sirable physical features including the small neutrino masses, the consistency of gauge-coupling unification with the experimental data from LEP and elsewhere. An important property of the fermionic construction is the standard SO(10) embedding of the Standard Model spectrum, which ensures natural consistency with the experimental values for $\sin^2\theta_W$ at the electroweak scale and allows neutrinos to have a nonzero mass below the electroweak scale.[70]

A key property of the realistic free fermionic models is their underlying $\mathbb{Z}_2 \times \mathbb{Z}_2$ orbifold structure. The emergence of the three chiral generations in a large class of fermionic constructions is correlated with the existence of three twisted sectors in the $\mathbb{Z}_2 \times \mathbb{Z}_2$ orbifold of the six dimensional internal space. Each twisted sector produces exactly one of the light chiral generations and there is no additional chiral matter. Thus, the fermionic construction offers a plausible and compelling explanation for the existence of three generations in nature. However, the geometrical structures that underlies the realistic free fermionic models are not fully understood. This thesis tries to shed light on this aspect and on the geometrical mechanism that reduces the number of generations in the $\mathbb{Z}_2 \times \mathbb{Z}_2$ orbifold models.

We are interested in the net number of chiral generations. In the $\mathbb{Z}_2 \times \mathbb{Z}_2$ orbifold models, the net number of generations comes from the twisted sectors. The untwisted sector has an equal number of generations and anti-generations. By compactifying the heterotic string on a $\mathbb{Z}_2 \times \mathbb{Z}_2$ orbifold we are left with the moduli of the three planes (T_i, U_i), where i runs over the three twisted planes. We argue in section 3.4 that the matter spectrum of the twisted sectors does not depend on the moduli. Consequently we can choose any value for the moduli space to investigate the chiral content of the $\mathbb{Z}_2 \times \mathbb{Z}_2$ orbifold. We choose the maximal symmetry point in the moduli space as this point can be described by a free fermionic model. By selecting a specific free fermionic model and describing its chiral content we have therefore described the chiral content of all models that are related to the selected free fermionic model by a change of the moduli (T_i, U_i) of the internal space.

In this thesis we classify the chiral content of the heterotic $\mathbb{Z}_2 \times \mathbb{Z}_2$ $N = 1$ supersymmetric orbifolds. This classification is possible since we can choose any point in the moduli space to describe the chiral content as explained above. This choice gives us the opportunity to describe the chiral content of the heterotic $\mathbb{Z}_2 \times \mathbb{Z}_2$ orbifolds in the free fermionic construction. We argue in section 5.4 that in the realistic free fermionic models the number of generations is reduced by symmetric shifts. In the orbifold description symmetric shifts on the internal space are well

known. We show in chapter 6 the correspondence between symmetric shifts on the internal space and symmetric shifts in the free fermionic description. As the hidden $\mathbb{E}_8$ gauge group is broken to $SO(16)$ and then further broken to $SO(8) \times SO(8)$ in the realistic free fermionic models we include these possibilities of symmetry breaking in our classification. The classification of the chiral content therefore includes all $N = 1$ $\mathbb{Z}_2 \times \mathbb{Z}_2$ models where symmetric shifts are realized on the internal space and where the hidden gauge group is at most broken to $SO(8) \times SO(8)$ at *any* point in the moduli space.

In the classification we define four subclasses of $\mathbb{Z}_2 \times \mathbb{Z}_2$ orbifolds. The first subclass of models has spinorial representations on each plane. The second subclass has spinorial representations on two of the three planes. The third subclass has spinorial representations on only one of the three planes. The fourth subclass does not have spinorial representations on any of the three planes. In chapter 4 we explain that a free fermionic model is defined by a set of basis vectors and a set of generalized GSO coefficients. We show in chapter 6 that in each subclass of models, the basis vectors that induce the $\mathbb{Z}_2 \times \mathbb{Z}_2$ twists are *completely* fixed. The basis vectors describing the symmetric shifts on the internal space and the Wilson lines in the hidden sector are *completely* fixed as well. The only free parameters in the classification are therefore the generalized GSO coefficients in the free fermionic formulation. We classify the chiral content of the heterotic $\mathbb{Z}_2 \times \mathbb{Z}_2$ orbifolds by looking at all possible values for these GSO coefficients. This is done using a computer program written in FORTRAN. We show that a subclass of $\mathbb{Z}_2 \times \mathbb{Z}_2$ orbifold models have a geometrical interpretation at the $N = 4$ level. In these models the symmetric shifts on the internal space and the Wilson lines that break the hidden $\mathbb{E}_8 \to SO(8) \times SO(8)$ are completely separated from the twists on the internal space. We show that the freedom in the modular invariant phases in the $N = 1$ vacua that control the chiral content, can be interpreted as vacuum expectation values of background fields of the underlying $N = 4$ theory, whose dynamical components are projected out by the $\mathbb{Z}_2$ fermionic projections. In this class of vacua the chiral content of the models is predetermined at the $N = 4$ level. We restrict the numerical classification to those models that have a geometrical interpretation at the $N = 4$ level due to computational limitations.

The results of the classification show that three generation models can be realized using symmetric shifts. The observable gauge group in these models cannot be broken perturbatively to the Standard Model gauge group while preserving the matter content. Additionally, the complex structure of the internal space is necessarily broken, thereby splitting

the internal $\Gamma_{6,6}$ lattice into six $\Gamma_{1,1}$ lattices. The classification shows that in the context of the realistic free fermionic $\mathbb{Z}_2 \times \mathbb{Z}_2$ models the reduction of the number of generations to the observed three, *necessarily* requires asymmetric shifts on the internal space. This is one of the main results of the analysis and it reveals, at least in the context of the three generation free fermionic models, that the geometrical structures that underly these models may not be simple Calabi–Yau manifolds, but it corresponds to geometries that are yet to be defined.

This thesis is organized as follows. In chapter 2 we give a short review of the heterotic string. We show that in a conformal field theory bosons can be interchanged by fermions. We give a short overview of the closed string models. In chapter 3 we discuss the orbifold formulation of a string on a compact space. We discuss the construction of the free fermionic models in chapter 4. Chapter 5 contains a typical derivation of the particle content of a free fermionic model. Two models are discussed in detail. In chapter 6 we isolate the free parameters of $\mathbb{Z}_2 \times \mathbb{Z}_2$ orbifolds in the heterotic string using the orbifold description. In chapter 7 we translate this orbifold description to the fermionic formulation. We then focus on the chiral content of these models. Using the formulas derived in chapter 7, we give in chapter 8 an example of a model that has 48 families as well as a model that has 3 generations. Similar examples of models with a particular number of generations are given. In chapter 9 we discuss the results we obtained from our analysis. We end this thesis with chapter 10 giving some suggestions for future work and an overall conclusion. In appendix A we give the full spectrum of two sample free fermionic models of the heterotic string. We give the explicit results of the classification of the chiral $\mathbb{Z}_2 \times \mathbb{Z}_2$ fermionic models of the heterotic super string in appendix B.

Part I

Introduction to the Orbifold and Free Fermionic Construction

Chapter 2

The Heterotic String

In this chapter we construct the heterotic string. We describe the bosonic string. We show how bosons are related to fermions in a conformal field theory description. This will be one of the building blocks for the free fermionic description of the heterotic string. The four different closed strings are discussed. We explain how the different string theories are related by dualities.

2.1 The String

We construct the string from basic principles. We introduce the operator product expansion of two operators that will allow us to explain the equivalence between bosons and fermions. We refer to [66] for more details.

Considering higher dimensional objects as elementary particles, where the world manifold is scale invariant leads automatically to the notion of strings. These strings have necessarily a 2 dimensional world sheet and their action is described as

$$S = \frac{1}{2\pi\alpha'} \int_M d^2\sigma \left(-\det \partial_a X^\mu \partial_b X_\mu\right)^{\frac{1}{2}} , \tag{2.1.1}$$

where α' is the string tension, M is the string world sheet. The bosonic fields X^μ are maps from the world sheet to the target space and μ runs over the number of spacetime dimensions and a runs over the number of world sheet dimensions i.e. 2. σ parameterizes the world sheet. This

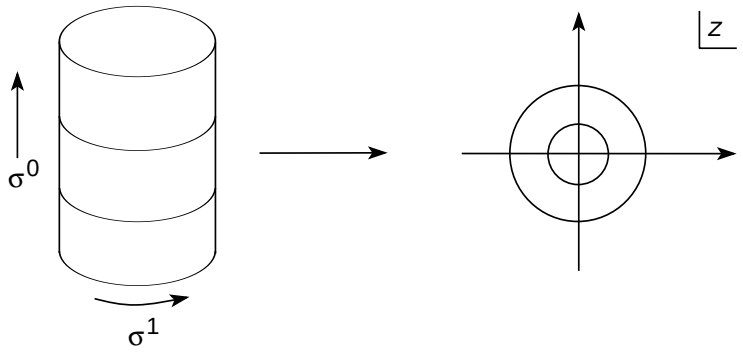

Figure 2.1: The map from the cylinder to the compactified complex plane

action is known as the Nambu-Goto action. The α' is the string tension and M is the string world sheet. This action is rewritten as the Polyakov action

$$S_P = \frac{1}{4\pi\alpha'} \int_M d^2\sigma \ (-\gamma)^{1/2} \gamma^{ab} \partial_a X^\mu \partial_b X_\mu, \tag{2.1.2}$$

where γ^{ab} is the metric on the world sheet. From now on we consider only closed strings. This means that the world sheet becomes a cylinder. In this case, the Polyakov action can be rewritten as an integral over the complex plane by first defining light cone coordinates following a Wick rotation. We then map the world sheet to the complex plane by mapping the *in* state to the origin and the *out* state to infinity as is done in figure 2.1

$$z = e^{-iw} = z^1 + iz^2, \tag{2.1.3}$$

where $w = i\sigma^0 + \sigma^1$. This can be realized due to the scale or conformal invariance of the theory. We then complexify the fields on the world sheet. Deriving the equations of motion shows that the fields split into left and right moving sectors. Since the left and right moving sectors are pure holomorphic and anti-holomorphic functions on the world sheet respectively, we can expand these fields into a Laurent series.

An interesting feature has arisen when we projected the world sheet to the complex plane. When calculating the integral of equation (2.1.2) on the complex plane the integral in the radial direction is trivial while the contour integral only picks up residues. Since we have mapped the *in* state to the origin we have effectively removed the origin from the complex plane and replaced this with a residue, or *in* state. This contour integral therefore picks up the residue at the origin. The *in* state is therefore realized by the residue. In a similar fashion we can replace

each incoming or outgoing state on the world sheet by a residue on the complex plane. The only requirement induced by time like ordering of the QFT is that the poles are ordered radially. The interesting part of the theory therefore is encrypted in the poles of the fields on the complex plane.

The operator product expansion is a result of this realization. First consider a field ϕ. Any change of this field induced by a conformal transformation is identical to the commutator of the field with the conformal Noether charge

$$\partial_\epsilon \phi(z,\bar{z}) = [Q_\epsilon, \phi(z,\bar{z})], \tag{2.1.4}$$

where ∂_ϵ is the infinitesimal flow along the conformal direction and Q_ϵ is the conformal charge which generates the conformal transformations. This can be seen to be identical to the contour integral over the radially ordered product of the stress tensor with the field ϕ. Since the contour integral only picks up the values at the poles we can write the product of two operators $\mathcal{A}_{1,2}(\sigma_{1,2})$ defined at $\sigma_{1,2}$ on the world sheet as an expansion of the poles plus a regular part

$$\mathcal{A}_1(\sigma_1)\mathcal{A}_2(\sigma_2) = poles + \ :\mathcal{A}_1(\sigma_1)\mathcal{A}_2(\sigma_2):, \tag{2.1.5}$$

where : : defines the standard normal ordering of operators in a QFT and is known as the regular part. Usually the regular part is omitted and one only writes down the poles. For more details we refer to [52, 71]

2.2 Bosonization

In this section we describe the correspondence of fermions and bosons in a conformal field theory. We derive this equivalence from the operator products of both fermions and bosons.

We show that in a conformal field theory we can interchange bosonic fields with fermionic fields. This is important for the construction of the free fermionic models. In this section we set $\alpha' = 2$. We follow the methods employed in [67].

As we have explained in the previous section all information of the conformal field theory is embedded in the operator products. Let us now consider the operator product expansion of the bosonic fields $X(z)$, $X(w)$. We find.

$$X(z)X(0) = -\ln|z|^2 + \mathcal{O}(z). \tag{2.2.1}$$

Consider now the operators $e^{\pm iX(z)}$. Using the Campbell-Baker-Hausdorff formula

$$e^{ipX}e^{iqX} = e^{ipX(z)+iqX(0)+\frac{1}{2}pq[X(z),X(0)]+\ldots} \tag{2.2.2}$$

we find they have the operator product expansions

$$\begin{aligned} e^{iX(z)}e^{-iX(0)} &= \frac{1}{z} + \mathcal{O}(z), && \text{(2.2.3a)} \\ e^{iX(z)}e^{iX(0)} &= \mathcal{O}(z), && \text{(2.2.3b)} \\ e^{-iX(z)}e^{-iX(0)} &= \mathcal{O}(z). && \text{(2.2.3c)} \end{aligned}$$

Similarly, consider now the operator product expansion of two complexified Majorana-Weyl fermions $\psi^{1,2}(z)$

$$\psi = \frac{1}{\sqrt{2}}\left(\psi^1 + i\psi^2\right), \qquad \bar{\psi} = \frac{1}{\sqrt{2}}\left(\psi^1 - i\psi^2\right). \tag{2.2.4}$$

Their operator product expansions are

$$\begin{aligned} \psi(z)\bar{\psi}(0) &= \frac{1}{z} + \mathcal{O}(z), && \text{(2.2.5a)} \\ \psi(z)\psi(0) &= \mathcal{O}(z), && \text{(2.2.5b)} \\ \bar{\psi}(z)\bar{\psi}(0) &= \mathcal{O}(z). && \text{(2.2.5c)} \end{aligned}$$

We see that equations (2.2.3) are equal to equations (2.2.5). Therefore, we find the equivalence between bosons and fermions and write

$$\psi(z) \cong e^{iX(z)}, \qquad \bar{\psi}(z) \cong e^{-iX(z)}, \tag{2.2.6}$$

where the equal sign should be interpreted as being valid primarily as a statement for the expectation values of the two fields. This can be easily extended to the anti-holomorphic or right moving sector. From equation (2.2.6) we see that a shift around half the compactified dimension is realized by

$$X(z) \to X(z) + \pi \quad \leftrightarrow \quad \psi(z) \to -\psi(z) \tag{2.2.7}$$

and similarly for the right moving sector. Therefore *any* shift on the bosonic coordinates can be realized by a suitable choice of boundary conditions for the free fermionic degrees of freedom.

This boson-fermion equivalence is crucial for the further development of the construction of the heterotic string in lower than 10 dimensions.

2.3 The Closed String Models

In this section we give a small overview of the four different closed string models. We first discuss the two type II strings. The heterotic strings are then discussed. The Type I string is mentioned briefly.

In section 2.1 we have discussed that the left and right moving sectors are completely decoupled in the closed string. We can therefore construct several string theories by setting the configuration of the left and right moving sectors.

The type II strings are defined such that both their left and right moving sectors are $N = 1$ super symmetric. The different types of the Type II strings arise due to the chirality of the super current on the left and right moving sector. The type IIA strings have opposite chirality, while the Type IIB strings have the same chirality of the super current in the two sectors.

The heterotic strings are of a different form. In our formulation the left moving sector is defined to be super symmetric, while the right moving sector is non super symmetric. Since the left moving sector gives a 10 dimensional target space, the 16 additional degrees of freedom in the right moving sector are considered to be free. They can either make up an $SO(32)$ gauge group or a $\mathbb{E}_8 \times \mathbb{E}_8$. This gives rise to the two different heterotic string theories.

2.3.1 The type II string

Constructing a super symmetric string action puts constraints on the number of dimensions and as such, constraints on the type of world sheet fermions. It can be shown that the string action can be only super symmetric in $D = 3, 4, 6, 10$[43]. We consider only the case when $D = 10$. The super coordinates are then necessarily Majorana-Weyl which requires the assignment of chirality. Although chirality is a matter of convention the relative chirality of the two string directions, left and right, is physically different. The Type IIA string has opposite chirality for the left and right movers. Type IIB strings have the same chirality in the left and right moving sector. It can be shown that the type IIA strings are not chiral contrary to the type IIB strings.

In general relativity, space time spans up four dimensions. We there-

fore need to configure the target space of the super string in such a way that the low energy region of the theory exhibits effectively a four dimensional space. One way to reduce the number of dimensions is by the compactification of six dimensions. The simplest way to achieve this is to compactify the string on a torus[44]. It has been shown that the maximal number of space time super symmetries for the type II strings is $N = 8$[41, 72].

The Minimal Super Symmetric Standard model (MSSM) is realized with $N = 1$ spacetime super symmetry. There are several ways to reduce the number of super symmetries from $N = 8$ down to $N = 1$. In early works lattice constructions, orbifold methods, sigma models techniques, exactly solvable conformal blocks and notably the free fermionic formulation were used for this reduction[36]. More recently the connection between the free fermionic formulation and the orbifold construction has lead to the classification of the type II strings[46].

It is believed that all string models are related by duality. One duality which is easy to see is known as T-duality. This equivalence of two string theories is realized when the closed string is compactified on a circle. In this configuration not only the momenta contribute to the mass but also the winding modes of the string, i.e. how many times the string is wound on the circle. The spectrum of the string is then invariant under winding and momenta mode exchange by inverting the radius of the circle $R \rightarrow R' = \frac{\alpha'}{R}$. The result is that physically the $R \rightarrow \infty$ limit is equivalent to the $R' \rightarrow 0$ limit. This is purely due to the extended nature of the string.

Having constructed a theory with fields on a two dimensional world sheet, we would like to see what the low energy effective field theory description is. We can realise such a theory by describing the variation of the couplings as a function of the conformal invariance. Because we impose conformal invariance at the quantum level we find that the couplings in the $2D$ theory cannot run. This leads to constraints. Since constraints in general can be realised as equations of motion derived from an action we see that we have found an action that describes the low energy effective field theory in $D = 10$. The low energy effective field theory that is derived from the type IIA/B strings is known as type IIA/B super gravity.

The Type IIA/B string has a $D = 10$ target space as we have argued. This constraint is only realised at the perturbative limit. All the arguments were derived from the perturbative string. The perturbative regime is only valid when the string coupling is small. The string cou-

pling is directly related to the dilaton field $g_s = e^{<\phi>}$. Considering super symmetry in itself however, leads to the conclusion that we can have at most a $D = 11$ spacetime. Suppose now that the string coupling is directly related to the radius of a compactified eleventh dimension. We can then derive the low energy effective field theory from the string in the higher dimensional space. This would lead to a $11D$ super gravity theory with one compactified dimension. This indeed turns out to be correct for the Type IIA string. It can be shown that in the limit where the compactified eleventh dimension of the super gravity field theory is reduced to zero by dimensional reduction, we retrieve the $10D$ type IIA super gravity low energy effective action. For more details concerning this derivation we refer to [73].

2.3.2 The heterotic string

The heterotic string was first constructed by [47] and employs both the bosonic string and the super string. Since the left and right moving sectors are completely independent, we set in the formulation of this thesis, the left moving sector to be super symmetric and the the right moving sector to be purely bosonic. Note that this is mirrored in some standard works[47, 43, 44, 68, 67]. This gives us a ten dimensional theory with remaining degrees of freedom coming from the right moving sector. These remaining degrees of freedom either form a $SO(32)$ or a $\mathbb{E}_8 \times \mathbb{E}_8$ gauge group.

In the MSSM we find a $N = 1$ spacetime super symmetry and a $D = 4$ target space or space time. Again there has been considerable effort to reduce the number of dimensions and super symmetries. Although many different ways have been employed, we note here two that have been used extensively. Toroidal compactifications are the most widely used compactification scheme, in particular orbifold compactifications. They are identified as $\mathbb{Z}_M$ and $\mathbb{Z}_M \times \mathbb{Z}_N$ orbifolds. It has been shown that only a limited number of these types of orbifolds reduce the number of the super symmetries to the number of the MSSM.[69] Of particular interest for phenomenology are the $\mathbb{Z}_2 \times \mathbb{Z}_2$ orbifold compactifications. As this thesis is concerned with this last scheme of compactification we refer to chapter 5 for more details.

It has been shown that the $SO(32)$ and $\mathbb{E}_8 \times \mathbb{E}_8$ heterotic string theories are related by T-duality at all orders in perturbation theory. The reason for this lies in the fact that a compactified dimension allows for the presence of non-vanishing Wilson lines. These Wilson lines can break

$SO(32) \to SO(16) \times SO(16)$. A similar configuration can be realised by the $\mathbb{E}_8 \times \mathbb{E}_8$ model with a compactified dimension of radius $1/R$. For more detail see [73].

In order to have a unification of the five string theories, heterotic string theory has to have a description in the $11D$ stringy theory, from now on called M-theory, as well. This description is known as Hoŕava-Witten theory[49, 50]. To fully understand the rational for the exact description of this theory, an explanation of the different dualities of the five string theories is necessary. In section 2.4 we describe these issues in more detail. To obtain the type IIA string from M-theory we have compactified this theory on a circle. If we instead compactify on the orbifold S^1/Z_2 or a line segment we find a chiral $N = 1$ super gravity theory with $\mathbb{E}_8$ vector multiplets on each orbifold fixed plane or the boundaries of the line segment. It has been shown that the low energy effective field theory of heterotic $\mathbb{E}_8 \times \mathbb{E}_8$ string theory describes the same particle content and it is therefore believed that by compactifying M-theory on the $S^1/\mathbb{Z}_2$ orbifold, we obtain $\mathbb{E}_8 \times \mathbb{E}_8$ heterotic string theory. Similar to the type IIA case again the heterotic string coupling constant is proportional to the length of the line segment or radius.

2.4 Dualities

We have seen that the dimensional reduction of $11D$ super gravity is type IIA super gravity. In this construction we have compactified the $11D$ theory on a circle. We can also consider compactifying M-theory on a T^2 torus. We will follow [73] in our approach. One would expect that this would reduce the theory to a $9D$ super gravity theory. However since we are dealing with a stringy theory, membranes are naturally in the spectrum of the M-theory. Membranes appear more naturally in type I strings. This type I theory of strings has both open and closed strings. The open strings have end points and one can show that these end points are located on higher dimensional planes called membranes. Since we only consider closed string theories we do not explain them here in more detail. We refer to the books [68, 67, 43, 44] for more details. These branes can wrap the T^2 torus just as strings can wrap the circle as explained before. Reducing the size of the torus but maintaining its shape one can show that the wrapping modes become massless and complete the spectrum of the chiral Type IIB string spectrum. We have thus realised a connection, through M-theory with IIA and IIB string theory. The connection can be realised even at the $D = 10$ level.

It has been shown that the type IIA is T-dual to the type IIB string. The string coupling of the type IIB string is then $g_s^{(B)} = \frac{R_{11}}{R_{10}}$. Since a reparameterisation of the torus interchange R_{10} and R_{11} we can see that the type IIB string with string coupling g_s is dual to the type IIB string with string coupling $1/g_s$. This type of duality is known as S-duality. We see that the type II strings can be seen as different regions of a $11D$ theory.

In order to see how the heterotic strings are realised by dualities it is necessary to include type I strings. Open string theory can be constructed using the type IIB strings. The Type IIB string diagrams are orientable manifolds. The type I strings are equivalent except for the fact that their diagrams are unorientable. This renders the type I closed string sector anomalous. This can be countered by including the open string sector of the Type I strings. The $SO(32)$ gauge group arises by including Chan-Paton factors at the end points of the open strings. This was found in [42] and already then there was a hint of the heterotic string theories. It can be shown that the T-dual type I theory (Type IA) is equivalent to the Type IIA theory compactified on the orbifold $S^1/\mathbb{Z}_2$. The fixed points of this orbifold are 8-planes with a $SO(16)$ gauge group. Now again we can lift the Type IIA to M-theory and we find that type IA is M-theory compactified on a cylinder.

Although all string theories are different limits of this M-theory, it has not been possible yet to write down the M-theory explicitly. Consequently we are left with all sorts of different descriptions for the same thing. The benefit of all these different descriptions is that one description suits one purpose better than the other. In Type I string theory the gauge group arises from Chan-Paton factors attached to the end points of the open string. Consequently Type I string theory cannot describe a chiral spectrum. In heterotic string theory we do not find this obstacle as is shown in chapter 5 and subsequent chapters. Since the MSSM is a chiral theory, heterotic string theory provides a convenient description in the search for phenomenological string theories.

Chapter 3

The Orbifold Background

In this chapter we set up the orbifold description of the heterotic string. The total string amplitude is a sum over all possible Riemann surfaces, similar to the sum over all Feynman graphs in QFT, moded out by conformal invariance, which relates Riemann surfaces to each other. Only the tree amplitude and the first loop amplitude are well understood in string theory. The tree amplitude can be parameterised as a sphere by a stereographical projection. Since the tree amplitude does not take quantum corrections into account we will focus on the next simplest closed Riemann surface after the sphere, the torus. We discuss its symmetries. We then consider the bosonic string in one space time dimension as a toy model. We continue to extend this discussion to the higher dimensional case. This leads us to the fermionization and bosonization on the world sheet torus similar to what we have seen in section 2.2. We follow [54] in our approach. We first consider this equivalence in the one dimensional target space case after which we extend this to the two dimensional background case. We continue to introduce the construction of orbifolds and we explain the $S^1/\mathbb{Z}_2$ orbifold in detail. We define twists on the two dimensional target space. Having dealt with the higher dimensional orbifolds we introduce shifts on the compactified dimensions. Again we start with the one dimensional case which we generalise to the two dimensional case.

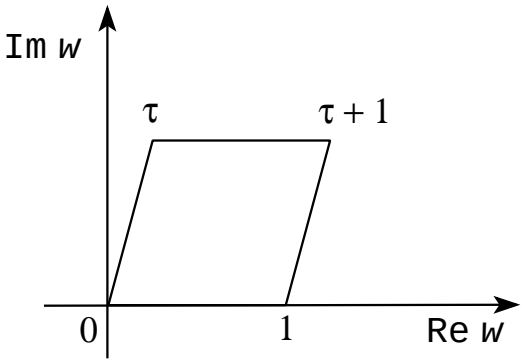

Figure 3.1: The torus as a quotient of the complex plane.

3.1 The Torus

In this section we show the symmetries of the torus that are derived from conformal invariance of the string and reparameterisation invariance of the torus. Since the surface of the one-loop string amplitude is conformally invariant we can set the surface area to 1. If we pick coordinates $\sigma_1, \sigma_2 \in [0,1]$ the area of the torus is 1 if the determinant of the torus metric is one. We parameterise the torus metric by a single complex number $\tau = \tau_1 + i\tau_2$ with $\tau_2 \geq 0$. The metric of the torus is then defined as

$$g^{ij} = \frac{1}{\tau_2} \begin{pmatrix} |\tau|^2 & -\tau_1 \\ -\tau_1 & 1 \end{pmatrix}. \tag{3.1.1}$$

In this parameterisation τ is known as the complex structure or modulus of the torus and is usually called the Teichmüller parameter.

We will now consider the symmetries of the torus. We can realise the torus by identifying points w on the complex plane with

$$w \to w + 1, \qquad\qquad w \to w + \tau \tag{3.1.2}$$

as is done in figure 3.1.

It is then easy to see that the translation $\tau \to \tau + 1$ realises the same torus. We have thus found one symmetry of the torus. A similar type of reformation of the torus leads to the second symmetry. In the first case we have moved the defining vector τ by a value of 1. The second reformation results in the transformation $\tau \to \frac{\tau}{\tau+1}$. We can now realise

the two orthogonal modular transformations

$$\tau \rightarrow \tau + 1, \tag{3.1.3a}$$

$$\tau \rightarrow -\frac{1}{\tau}. \tag{3.1.3b}$$

Another way to write these transformations exhibits the modular group more clearly. We can write equations (3.1.3) as

$$\tau' = \frac{a\tau + b}{c\tau + d}, \tag{3.1.4}$$

where we can put the numbers a, b, c, d in a matrix formulation

$$A = \begin{pmatrix} a & b \\ c & d \end{pmatrix}. \tag{3.1.5}$$

The matrix A has integer entries and has determinant 1 and forms the group $SL(2, \mathbb{Z})$. Since a change of sign does to affect the modular transformation we find that the modular group is $PSL(2, \mathbb{Z}) = SL(2, \mathbb{Z})/\mathbb{Z}_2$.

3.2 The String on a Compact Target Space

In this section we describe the compactified bosonic string and the free fermionic string. We start by setting the bosonic string in one compactified space dimension. We calculate the partition function starting with the action. We then extend this analysis to the two dimensional case. We employ a similar tactic with the free fermionic string. Again we derive the partition function of a string with two holomorphic and two anti-holomorphic free fermions on the world sheet starting with the action.

3.2.1 The bosonic string

We discuss the compactification of the bosonic string on one compact dimension. We set the string for convenience in a one dimensional target space and do not consider any anomalies. The field X takes its values on the circle with radius R. The Wick rotated Polyakov action for the string in a one-dimensional background is similar to equation (2.1.2)

$$S = \frac{1}{4\pi} \int d^2\sigma \sqrt{g} g^{ij} \partial_i X \partial_j X, \tag{3.2.1}$$

where X is again a map from the world sheet to the target space and g is the metric on the world sheet. Using equation (3.1.1) we evaluate the partition function of this configuration

$$Z(R) = \int \mathcal{D}X e^{-S}. \tag{3.2.2}$$

To evaluate this path integral we consider fluctuations of the classical field X_{class}

$$X = X_{class} + \chi. \tag{3.2.3}$$

Since the classical field is periodic when it goes around the two non-contractible loops of the torus we find that the classical equation of motion of the field X_{class} is realised when

$$X_{class} = 2\pi R\,(n\sigma_1 + m\sigma_2). \tag{3.2.4}$$

The action is separated into a quantum and a classical contribution. We can therefore write the partition function $Z(R)$ as

$$Z(R) = \sum_{m,n\in\mathbb{Z}} e^{-S_{m,n}} \int D\chi e^{-S(\chi)}, \tag{3.2.5}$$

where

$$S_{m,n} = \frac{\pi R^2}{\tau_2}|m - n\tau|^2, \tag{3.2.6}$$

which leaves us to solve the quantum contribution. We expand the quantum field χ in terms of eigenfunctions ψ_{m_1,m_2} of the Laplacian, defined by the equations of motion for the field X. The quantum contribution of the action is written in terms of the Fourier components and the eigenvalues λ_{m_1,m_2} of the eigenfunctions ψ_{m_1,m_2} of the Laplacian. Putting everything together we get

$$\int D\chi e^{-S(\chi)} = \frac{2\pi R}{\prod'_{m_1,m_2} \lambda^{1/2}_{m_1,m_2}} = \frac{2\pi R}{\sqrt{\det{}' \,\Box}}, \tag{3.2.7}$$

where the product runs over the eigenvalues of all but the zero modes. Using ζ-regularisation we find that the determinant is [40]

$$\det{}'\Box = 4\pi^2\tau_2\eta^2(\tau)\bar{\eta}^2(\bar{\tau}), \tag{3.2.8}$$

with the Dedekind eta function defined as

$$\eta = q^{\frac{1}{24}} \prod_{m>0} (1 - q^m), \qquad\qquad q = e^{2\pi i\tau}, \tag{3.2.9}$$

and we find that the partition function for the bosonic string on a one dimensional compactified target space is

$$Z(R) = \frac{R}{\sqrt{\tau_2}|\eta|^2} \sum_{m,n\in\mathbb{Z}} e^{-\frac{\pi R^2}{\tau_2}|m-n\tau|^2}. \tag{3.2.10}$$

We have written the partition function in the winding mode representation. Performing a Poisson resummation on m we write this in the momentum mode representation. We obtain, using the formula for Poisson resummation[54]

$$\sum_{m_i\in Z} e^{-\pi m_i m_j A_{ij} + \pi B_i m_i} = \frac{1}{\sqrt{\det A}} \sum_{m_i\in Z} e^{-\pi(m_k + iB_k/2)(A^{-1})_{kl}(m_l+iB_l/2)}, \tag{3.2.11}$$

the partition function

$$Z(R) \equiv \frac{\Gamma_{1,1}(R)}{|\eta|^2} = \sum_{m,n\in\mathbb{Z}} \frac{q^{\frac{P_L^2}{2}} \bar{q}^{\frac{P_R^2}{2}}}{\eta\bar{\eta}}, \tag{3.2.12}$$

where

$$P_L = \frac{1}{\sqrt{2}}\left(\frac{m}{R} + nR\right), \qquad P_R = \frac{1}{\sqrt{2}}\left(\frac{m}{R} - nR\right). \tag{3.2.13}$$

The modulus of the compactified dimension R has not been fixed. The quantum contribution of the partition function is encoded in the η functions while the classical contribution is described by the left and right moving momenta. T-duality is now realised by interchanging simultaneously $R \to 1/R$ and $m \leftrightarrow n$.

We have given the partition function of the bosonic string on one compactified dimension. We extend this discussion to the higher dimensional case.

Let us therefore parameterise the background by its metric G_{ij} and its anti-symmetric tensor B_{ij}, where i, j runs over the number of target space dimensions. For simplicity we require the entire background to be compact. We parameterise the world sheet in terms of its metric g_{ab} and its anti-symmetric tensor ϵ_{ab}. The action for this system is

$$S = \frac{1}{4\pi}\int d^2\sigma \sqrt{\det g}\; g^{ab} G_{ij}\partial_a X^i \partial_b X^j + \epsilon^{ab} B_{ij}\partial_a X^i \partial_b X^j. \tag{3.2.14}$$

We find that the partition function of the bosonic string in this configuration is

$$Z_{d,d}(G,B) = \frac{\sqrt{\det G}}{\left(\sqrt{\tau_2}\eta\bar{\eta}\right)^d} \sum_{\vec{m},\vec{n}} e^{-\frac{\pi\left(G_{ij}+B_{ij}\right)}{\tau_2}[m_i - n_i\tau][m_j + n_j\bar{\tau}]}. \tag{3.2.15}$$

Again we can do a Poisson resummation using equation (3.2.11), which leads to the momentum representation of the partition function

$$Z_{d,d}(G,B) \equiv \frac{\Gamma_{d,d}(G,B)}{\eta^d \bar{\eta}^d} = \sum_{\vec{m},\,\vec{n}\in\mathbb{Z}^d} \frac{q^{\frac{P_L^2}{2}} \bar{q}^{\frac{P_R^2}{2}}}{\eta^d \bar{\eta}^d}, \tag{3.2.16}$$

where

$$P^2_{L,R} = P^i_{L,R} G_{ij} P^j_{L,R}, \tag{3.2.17a}$$

$$P^i_L = \frac{G^{ij}}{\sqrt{2}} \left[m_j + (B_{jk} + G_{jk})\, n_k \right], \tag{3.2.17b}$$

$$P^i_R = \frac{G^{ij}}{\sqrt{2}} \left[m_j + (B_{jk} - G_{jk})\, n_k \right], \tag{3.2.17c}$$

where the $-$ sign difference in the left and right moving momenta is due to the fact that when we expand the product of equation (3.2.15) we find that the anti-symmetric tensor carries a factor i in front of it while the background metric does not. We have therefore realised an expression for the partition function of the compactified bosonic string in terms of both the winding modes as well as the momentum modes.

3.2.2 The free fermionic string

We discuss the partition function of two free Majorana-Weyl fermions on the torus. Although we can pursue a similar method as employed for the bosonic string, we use a different method here and follow [40] to which we refer for more intricate details. The action of two free left and right moving fermions is

$$S = \frac{1}{8\pi} \int d^2 z \;\; \psi^i \bar{\partial} \psi^i + \bar{\psi}^i \partial \bar{\psi}^i, \tag{3.2.18}$$

where i runs over the number of fermions. Again we are interested in the partition function of these free fermions. It can be shown that this becomes

$$\begin{aligned} Z = \int e^{-S} &= tr\; e^{2\pi i \tau_1 P} e^{-2\pi \tau_2 H} \\ &= q^{-\frac{c}{24}} \bar{q}^{\frac{\bar{c}}{24}}\; tr\; q^{L_0} \bar{q}^{\bar{L}_0}, \end{aligned} \tag{3.2.19}$$

where

$$L_n = \oint \frac{dz}{2\pi i} z^{n+1} T(z), \qquad \bar{L}_n = \oint \frac{d\bar{z}}{2\pi i} \bar{z}^{n+1} \bar{T}(\bar{z}) \tag{3.2.20}$$

are the Laurent series expansion of the holomorphic ($T(z)$) and anti-holomorphic ($\bar{T}(\bar{z})$) components of the energy-momentum tensor of the system. We are left with solving the trace over the operators L_0 and $\bar{L_0}$. In order to evaluate the trace we need to define the spin structure on the torus or equivalently define the boundary conditions of the fermions when transported around the non-contractible loops of the torus. When we evaluate the vacuum energy of the different configurations, we find that equation (3.2.19) represents the sector where the fermions are anti-periodic. It can be shown that the boundary conditions are changed when we do a modular transformation as defined in equations (3.1.3). We therefore need to consider the other sectors as well.

The $c = \frac{1}{2}$ representations of the Virasoro algebra, which is the algebra realised by the Laurent modes of the energy momentum tensor written in equation (3.2.20), for anti-periodic fermions can be identified with the direct sum of the highest weight states with $h = 0$ and $h = \frac{1}{2}$, where h is the conformal weight of the states. The vacuum state is the highest weight state with $h = 0$. Since we are only interested in counting the representations of the Virasoro algebra once, we need to project out half of the states. A similar argument holds for the periodic fermions.

Let us separate the periodic and the anti-periodic sector in equation (3.2.19). We include the vacuum state in the partition function which leads to the expansion

$$\begin{aligned}(q\bar{q})^{-\frac{1}{24}}\ tr\ q^{L_0}\bar{q}^{\bar{L}_0} &= (q\bar{q})^{-\frac{1}{24}}\ tr_{A\bar{A}}\ \frac{1}{2}\left(1+(-1)^F\right) q^{L_0}\bar{q}^{\bar{L}_0} \\ &+ (q\bar{q})^{-\frac{1}{24}}\ tr_{P\bar{P}}\ \frac{1}{2}\left(1\pm(-1)^F\right) q^{L_0}\bar{q}^{\bar{L}_0}. \quad (3.2.21)\end{aligned}$$

In this expression we see that there still remains the choice of the second trace in the periodic sector. We choose the sign to be positive from here on. We discuss the significance of the sign in section 4.1. We are thus left with the task to evaluate the traces. It can be shown that

$$q^{-\frac{1}{24}}\ tr_A\ q^{L_0} = q^{-\frac{1}{24}}\prod_{n=0}^{\infty}\left(1+q^{n+1/2}\right)^2 = \frac{\vartheta_3}{\eta}, \quad (3.2.22a)$$

$$q^{-\frac{1}{24}}\ tr_A\ (-1)^F q^{L_0} = q^{-\frac{1}{24}}\prod_{n=0}^{\infty}\left(1-q^{n+1/2}\right)^2 = \frac{\vartheta_4}{\eta}, \quad (3.2.22b)$$

$$2q^{-\frac{1}{24}}\ tr_P\ q^{L_0} = 2q^{\frac{1}{12}}\prod_{n=0}^{\infty}(1+q^n)^2 = \frac{\vartheta_2}{\eta}, \quad (3.2.22c)$$

$$2q^{-\frac{1}{24}}\ tr_P\ (-1)^F q^{L_0} = 2q^{\frac{1}{12}}\prod_{n=0}^{\infty}(1-q^n)^2 = \frac{\vartheta_1}{\eta}, \quad (3.2.22d)$$

where ϑ_i are the well known Jacobi theta functions [17]

$$\vartheta[^{a^I}_{b^I}] = \sum_{n\in\mathbb{Z}} q^{\frac{\left(n-\frac{a^I}{2}\right)^2}{2}} e^{2\pi i\left(v-\frac{b^I}{2}\right)\left(n-\frac{a^I}{2}\right)}, \tag{3.2.23}$$

and we define the Jacobi theta functions as

$$\vartheta[^1_1] = \vartheta_1, \qquad \vartheta[^1_0] = \vartheta_2, \qquad \vartheta[^0_0] = \vartheta_3, \qquad \vartheta[^0_1] = \vartheta_4. \tag{3.2.24}$$

These formulae should be complex conjugated for the right moving sector. When we evaluate $\frac{\vartheta_1}{\eta}$ we find that this vanishes, but we nevertheless keep its formal description as it will be important for later use. One more difficulty arises now in the evaluation of the path integral in the periodic sector.

The Fourier expansion of the periodic fermion is

$$i\psi(z) = \sum_{n\in\mathbb{Z}} \psi_n z^{-n} \tag{3.2.25}$$

and it can be shown that the commutation relation for the Fourier components of the fermion is

$$\{\psi_n, \psi_m\} = \delta_{m+n,0}. \tag{3.2.26}$$

Acting on the vacuum with the zero mode ψ_0, we find that this does not change the eigenvalue of L_0 leading to a degenerate vacuum consisting of two states. We come back to this issue in section 5.1.2.

The partition function of two holomorphic fermionic fields and two anti-holomorphic fermionic fields on the torus is [40]

$$Z = \frac{1}{2}\sum_{a,b=0,1}\left|\frac{\vartheta[^a_b]}{\eta}\right|^2. \tag{3.2.27}$$

using the shorthand notation defined in equation (3.2.24).

3.3 Bosonization and Fermionization

In section 2.2 we have shown that bosons can be interchanged with two fermions in a conformal field theory. In this section we show that this equivalence is also realised in the orbifold description of the string.

In equation (3.2.27) we found for the partition function of two holomorphic fermionic fields and two anti-holomorphic fermionic fields on the torus is [40]

$$Z = \frac{1}{2} \sum_{a,b=0,1} \left| \frac{\vartheta[{}^{a}_{b}]}{\eta} \right|^2 . \tag{3.3.1}$$

Applying a Poisson resummation on the partition function we obtain

$$\left| \frac{\vartheta[{}^{a}_{b}]}{\eta} \right|^2 = \frac{1}{\eta\bar{\eta}} \frac{1}{\sqrt{2\tau_2}} \sum_{m,n\in\mathbb{Z}} \exp\left[-\frac{\pi}{2\tau_2} \left| n - b + \tau(m-a) \right|^2 + i\pi mn \right] . \tag{3.3.2}$$

We can then relabel $n \to n + b$ and $m \to m + a$ since $a, b \in \mathbb{Z}$. When we consider now the whole partition function we find

$$\begin{aligned} &\frac{1}{2} \sum_{a,b=0,1} \left| \frac{\vartheta[{}^{a}_{b}]}{\eta} \right|^2 = \\ &\frac{1}{\eta\bar{\eta}} \sum_{a,b=0,1} \frac{1}{2\sqrt{2\tau_2}} \sum_{m,n\in\mathbb{Z}} \exp\left[-\frac{\pi}{2\tau_2} \left| n + \tau m \right|^2 + i\pi(m+a)(n+b) \right] . \end{aligned} \tag{3.3.3}$$

The summation over b gives a factor of 2 and requires $m + a \in 2\mathbb{Z}$. We therefore find that the partition function of one holomorphic fermionic field and one anti-holomorphic fermionic field on the torus is

$$Z\left(\frac{1}{\sqrt{2}}\right) = \frac{1}{\sqrt{2\tau_2}|\eta|^2} \sum_{m,n\in\mathbb{Z}} e^{-\frac{\pi}{2\tau_2}|m-n\tau|^2} . \tag{3.3.4}$$

We see that this is identical to equation (3.2.10) with the radius fixed at the maximal symmetry point $R = 1/\sqrt{2}$. Note that this value is not the self dual point under T-duality.

We show the boson fermion equivalence in the case where the boson is compactified on a complex torus and follow [46]. The complex torus can be parameterised by two complex moduli in the same way the circle is parameterised by its radius. The moduli $(T = T_1 + iT_2, U = U_1 + iU_2)$ of the complex torus are written in terms of the metric G_{ij} and the anti-symmetric tensor B_{ij}

$$G_{ij} = \frac{T_2}{U_2} \begin{pmatrix} 1 & U_1 \\ U_1 & |U|^2 \end{pmatrix} , \qquad B_{ij} = \begin{pmatrix} 0 & T_1 \\ -T_1 & 0 \end{pmatrix} . \tag{3.3.5}$$

The $\Gamma_{2,2}$ lattice from equation (3.2.16) can now be written as

$$\begin{aligned} \Gamma_{2,2}(T,U) = \sum_{\vec{m},\vec{n}\in\mathbb{Z}^2} \exp\Bigg[&-\frac{\pi\tau_2}{T_2U_2} \left| m_1U - m_2 + T(n_1 + Un_2) \right|^2 \\ &+ 2\pi i\bar{\tau}(m_1n_1 + m_2n_2) \Bigg] . \end{aligned} \tag{3.3.6}$$

Fixing the moduli at the the maximal symmetry point $(T,U) = (i,i)$ leads to

$$\Gamma_{2,2}(i,i) = \sum_{\vec{m},\vec{n}\in\mathbb{Z}^2} \exp\Big[\pi\tau_2 \left|m_1 i - m_2 + i(n_1 + i n_2)\right|^2 + 2\pi i\bar{\tau}(m_1 n_1 + m_2 n_2)\Big]. \quad (3.3.7)$$

We find that B_{ij} vanishes at this point in the moduli space and the metric G_{ij} takes the form

$$G_{ij} = \begin{pmatrix} 1 & 0 \\ 0 & 1 \end{pmatrix}, \quad (3.3.8)$$

from which it is clear that, since equation (3.3.4) holds for the partition function of one holomorphic and one anti-holomorphic fermion field, we find that

$$\frac{\Gamma_{2,2}(i,i)}{|\eta|^4} = \frac{1}{2}\sum_{a,b=0,1}\left|\frac{\vartheta[^a_b]}{\eta}\right|^4. \quad (3.3.9)$$

At the left hand side we have described a bosonic string compactified on a torus of which we have fixed the moduli at the maximal symmetry point $(T,U) = (i,i)$ in the moduli space. On the right hand side we have described a fermionic string of which the fermionic fields can propagate freely on the string. This equivalence therefore shows that at the maximal symmetry point on the torus we can exchange bosons with free fermions.

3.4 Orbifolds and Shifts

In this section we introduce the techniques for constructing orbifolds and shifts in a geometrical formulation. We start by defining the orbifold from a general manifold. We discuss the simplest example and extend this discussion to the bosonic string. We derive the bosonic string compactified to this simplest orbifold. We move on to the higher dimensional case, namely the target space of a critical string with four extended dimensions. We then introduce shifts on the target manifold. We start with the description of shifts in the one dimensional background after which we discuss shifts on the two dimensional torus representing part of the full target space of the critical string.

3.4.1 The orbifold construction

Consider a manifold $\mathcal{M}$ with a discrete group action $G : \mathcal{M} \to \mathcal{M}$. The action of the discrete group on points on the manifold is $g \in G : x \to gx$. An orbifold is now defined as the quotient space $\mathcal{M}/G$. In general an orbifold is not a manifold. An orbifold remains a manifold however when the group acts freely, i.e. when there are no fixed points under the group action. One easy example of an orbifold is $S^1/\mathbb{Z}_2$. The group elements of $\mathbb{Z}_2$ act on the points of S^1 as $g \in G = \mathbb{Z}_2 : x \to gx = -x$. This group action has two fixed points and the quotient space therefore defines an orbifold. It is easy to see that this quotient space can be represented by a line segment.

Let us now proceed to a group action on the torus. Without the introduction of the discrete group we have the following picture. Going around a non-contractible loop around the torus requires the field X not to change. We now define the discreet group $G : \mathcal{T} \to \mathcal{T}$, where $\mathcal{T}$ represents the target space. In this context it is therefore possible that the field X, when it goes around a non-contractible loop, does not go back to its original value but goes to gX, which is in the quotient space identical to X. Since modular invariance interchanges the two non-contractible loops we see that any modular invariant partition function with an orbifold as target space has four sectors. For each non-contractible loop we have two sectors: on one sector we act on the fields with the group action and on the other we do not act on the fields.

We consider the simplest example of an orbifold, namely $S^1/\mathbb{Z}_2$. The action for the free boson on the torus compactified on S^1 is described in equation (3.2.1). We see that this action is invariant under $X \to -X$ which defines an orbifold $S^1/\mathbb{Z}_2$ as target space. Similar to the derivation of the free fermionic partition function the partition function for the free boson is written as

$$Z_{orb}(R) = (q\bar{q})^{-\frac{1}{24}}\, tr_{(+)}\, \frac{1}{2}(1+g) q^{L_0} \bar{q}^{\bar{L}_0} + (q\bar{q})^{-\frac{1}{24}}\, tr_{(-)}\, \frac{1}{2}(1+g) q^{L_0} \bar{q}^{\bar{L}_0}, \quad (3.4.1)$$

where $tr_{(\pm)}$ describes the untwisted and the twisted sector respectively. The untwisted sector is defined as the sector where the field $X \to X$ around the non-contractible loop in the space direction on the torus. The twisted sector is the sector where $X \to gX = -X$ around the non-contractible loop in the space direction on the torus. We now evaluate the twisted and untwisted sector separately.

Note that the untwisted-untwisted sector is identical to the bosonic partition function as derived in section 3.2.1. We are therefore left with the untwisted-twisted sector. Since the group action g brings $X \to -X$ we find

$$(q\bar{q})^{-\frac{1}{24}}\ tr_{(+)}\ \frac{1}{2}\ g\ q^{L_0}\bar{q}^{\bar{L}_0} = \frac{1}{2}\frac{(q\bar{q})^{-\frac{1}{24}}}{\prod_{n=1}^{\infty}(1+q^n)(1+\bar{q}^n)} = \left|\frac{\eta}{\vartheta_2}\right|. \tag{3.4.2}$$

Similarly we find for the twisted sector

$$\begin{aligned}(q\bar{q})^{-\frac{1}{24}}\ tr_{(-)}\ \frac{1}{2}(1+g)q^{L_0}\bar{q}^{\bar{L}_0} = \\ \left[\frac{(q\bar{q})^{-\frac{1}{24}}}{\prod_{n=1}^{\infty}(1-q^{n-1/2})(1-\bar{q}^{n-1/2})} + \frac{(q\bar{q})^{-\frac{1}{24}}}{\prod_{n=1}^{\infty}(1+q^{n-1/2})(1+\bar{q}^{n-1/2})}\right] \\ = \left|\frac{\eta}{\vartheta_4}\right| + \left|\frac{\eta}{\vartheta_3}\right|,\end{aligned} \tag{3.4.3}$$

leading to

$$Z_{orb}(R) = \frac{1}{2}Z_{circ}(R) + \left|\frac{\eta}{\vartheta_2}\right| + \left|\frac{\eta}{\vartheta_4}\right| + \left|\frac{\eta}{\vartheta_3}\right|. \tag{3.4.4}$$

We see that the twisted sector does not depend on the modulus of the circle S^1, while the untwisted sector does. By analysing only the twisted sector we can set the radius to *any* value we like. Choosing the maximal symmetry point therefore does not change the structure of the twisted sector. We therefore move from *any* point in the moduli space to the maximal symmetry point.

We can write equation (3.4.4) as

$$Z_{orb}(R) = \frac{1}{2}\sum_{h,g=0,1}\frac{\Gamma_{1,1}\left[{}^{h}_{g}\right]}{|\eta|^2}, \tag{3.4.5}$$

where $\Gamma_{1,1}\left[{}^{0}_{0}\right] = \Gamma_{1,1}(R)$ and

$$\Gamma_{1,1}\left[{}^{h}_{g}\right] = 2\frac{|\eta|^3}{|\vartheta\left[{}^{1-h}_{1-g}\right]|}, \quad (h,g) \neq (0,0). \tag{3.4.6}$$

We fix the radius at the maximal symmetry point. If we use the identity $\vartheta_2\vartheta_3\vartheta_4 = 2\eta^3$ we find

$$Z_{orb}\left(\frac{1}{\sqrt{2}}\right) = \frac{1}{4}\left[\sum_{a,b=0,1}\left|\frac{\vartheta\left[{}^{a}_{b}\right]}{\eta}\right|^2 + 2\frac{|\vartheta_3\vartheta_4|}{|\eta|^2} + 2\frac{|\vartheta_2\vartheta_3|}{|\eta|^2} + 2\frac{|\vartheta_2\vartheta_4|}{|\eta|^2}\right]. \tag{3.4.7}$$

We see that at the maximal symmetry point the orbifold description from equation (3.4.4) is exactly equivalent to the fermionic description

written down in equation (3.2.27). By moving from any point in the moduli space to the maximal symmetry point we have not changed the structure of the twisted sector. It is fairly straight forward to rewrite this as

$$Z_{orb}\left(\frac{1}{\sqrt{2}}\right) = \frac{1}{2}\sum_{g,h=0,1}\frac{1}{2}\sum_{a,b=0,1}\left|\frac{\vartheta[^a_b]\vartheta[^{a+h}_{b+g}]}{\eta\bar{\eta}}\right|. \tag{3.4.8}$$

We consider the torus moded out by a $\mathbb{Z}_2$ symmetry. Along similar lines we find that this results in

$$Z_{orb}(T,U) = \frac{1}{2}\sum_{h,g=0,1}\frac{\Gamma_{2,2}[^h_g](T,U)}{|\eta|^4}, \tag{3.4.9}$$

with the twist parameterised by h, g. The partition function at an arbitrary point in the moduli space is similarly written as[46]

$$\Gamma_{2,2}[^h_g] = 4\frac{|\eta|^6}{|\vartheta[^{1+h}_{1+g}]\vartheta[^{1-h}_{1-g}]|}, \quad (h,g) \neq (0,0). \tag{3.4.10}$$

and $\Gamma_{2,2}[^0_0](T,U) = \Gamma_{2,2}(T,U)$ as written in equation (3.3.6). We have thus given the partition function for the bosonic string compactified on an orbifold $T^2/\mathbb{Z}_2$ for all moduli (T,U). We stress the point here that the structure of the twisted sector at *any* point in the moduli space has not changed by fixing the moduli at the maximal symmetry point similar to the one dimensional compactification. The chiral structure of the $\mathbb{Z}_2\times\mathbb{Z}_2$ orbifolds necessarily comes from the twisted sector as we show in chapter 7. By considering the chiral structure at the maximal symmetry point we have therefore considered the chiral structure of all models connected to it by a change of the moduli of the internal space.

3.4.2 The shifts

In the previous section we have constructed the string propagating on a torus. This has lead to winding and momentum modes. The winding modes represent whole loops around the compactified dimension. We can however also consider transporting the string halfway around the compactified dimension. This transportation is known as a shift, or more specific a $\mathbb{Z}_2$ shift as two subsequent shifts are identical to the identity.

From equation (2.2.6) we see that a shift around half the compactified dimension is realised by

$$X(z) \to X(z) + \pi \quad \leftrightarrow \quad \psi(z) \to -\psi(z) \tag{3.4.11}$$

and similarly for the right moving sector. Again in the case of the torus we have two non-contractible loops, which are interchanged by modular invariance. To construct a modular invariant partition function that incorporates shifts, we therefore have to consider the action of the shift on all possible directions on the string world sheet leading to four terms, each describing the shift along either of the two non-contractible loops. We consider only symmetric shifts, i.e. the shift is introduced on both the left and right moving sector simultaneously.

We first consider the bosonic string compactified to one dimension. The partition function for this system is described in (3.2.10). Adding the shift along the non-contractible loops is then realised as

$$Z(R) = \frac{1}{2} \sum_{p,q=0,1} Z^{[p]}_{[q]}(R), \tag{3.4.12}$$

where

$$Z^{[p]}_{[q]}(R) = \frac{R}{\sqrt{\tau_2}|\eta|^2} \sum_{m,n\in\mathbb{Z}} \exp\left[-\frac{\pi R^2}{\tau_2}\left|(m+\frac{q}{2}) - (n+\frac{p}{2})\tau\right|^2\right]. \tag{3.4.13}$$

The factor $\frac{p}{2}$ is necessary to avoid a relabelling of the indices. In that sense it is clear that this factor realises the $\mathbb{Z}_2$ shift. Performing a Poisson resummation we can set the partition function in the momentum representation. We obtain

$$Z^{[p]}_{[q]}(R) = \sum_{m,n\in\mathbb{Z}} (-1)^{qm} \frac{q^{\frac{P_L^2}{2}} \bar{q}^{\frac{P_R^2}{2}}}{\eta\bar{\eta}}, \tag{3.4.14}$$

where

$$P_L = \frac{1}{\sqrt{2}}\left(\frac{m}{R} + (n+\frac{p}{2})R\right), \qquad P_R = \frac{1}{\sqrt{2}}\left(\frac{m}{R} - (n+\frac{p}{2})R\right). \tag{3.4.15}$$

Fixing the radius at the maximal symmetry point and performing a Poisson resummation leads to the partition function

$$Z\left(\frac{1}{\sqrt{2}}\right) = \frac{1}{2} \sum_{p,q=0,1} \frac{1}{2} \sum_{a,b=0,1} \left|\frac{\vartheta[^{a+p}_{b+q}]}{\eta}\right|^2. \tag{3.4.16}$$

We extend this discussion to the torus. In the case of the torus we find two independent shifts since there are two non-contractible loops. We find that the full partition function is written as

$$Z(T,U) = \frac{1}{4} \sum_{p_1,q_1=0,1} \sum_{p_2,q_2=0,1} \frac{\Gamma_{2,2}\begin{bmatrix} p_1 & p_2 \\ q_1 & q_2 \end{bmatrix}(T,U)}{|\eta|^4}. \tag{3.4.17}$$

Applying these shifts, we can find the partition function for the bosonic string compactified on a torus, using equation (3.3.6), at an arbitrary point in the moduli space fairly easy. Using the momentum representation as displayed in equation (3.2.16) and equation (3.3.6), we follow along the same lines as equation (3.4.14) and find

$$\Gamma_{2,2}\begin{bmatrix} p_1 & p_2 \\ q_1 & q_2 \end{bmatrix}(T,U) = \frac{1}{2}\sum_{\vec{m},\vec{n}\in\mathbb{Z}^2}(-1)^{q_1m_1+q_2m_2} \exp\left[-\frac{\pi\tau_2}{T_2U_2}\left|m_1U - m_2 + T\left\{(n_1+\frac{p_1}{2})+U(n_2+\frac{p_2}{2})\right\}\right|^2 + 2\pi i\bar{\tau}\left\{m_1(n_1+\frac{p_1}{2})+m_2(n_2+\frac{p_2}{2})\right\}\right]. \quad (3.4.18)$$

Again we fix the moduli at the maximal symmetry point $(T,U)=(i,i)$ and we obtain

$$\Gamma_{2,2}\begin{bmatrix} p_1 & p_2 \\ q_1 & q_2 \end{bmatrix}(i,i) = \frac{1}{2}\sum_{a,b=0,1}\left|\vartheta\left[{}^{a+p_1}_{b+q_1}\right]\vartheta\left[{}^{a+p_2}_{b+q_2}\right]\right|^2. \quad (3.4.19)$$

We see that at the maximal symmetry point the bosonic partition function is *exactly* identical to the fermionic partition function. If the fermionic partition function is therefore known, we can easily move away from the maximal symmetry point to *any* point in the moduli space using the identity presented in equation (3.4.19). In the following chapters we construct from the free fermionic description the partition function at the maximal symmetry point. Using equation (3.4.19) we then move to *any* point in the moduli space. As the chiral structure does not depend on the moduli we select the maximal symmetry point to analyse the chiral structure. This structure is *completely* determined by the twisted sector and is therefore equivalent for *all* partition functions related to each other by a change of the moduli of the internal space.

Chapter 4

The Fermionic String

In this chapter we set up the free fermionic construction of the heterotic string. The partition function at an arbitrary point in the moduli space is derived. The description of the heterotic string at the self dual point under T-duality follows. We write the partition function at the self-dual point in the most general way which enables us to derive constraints on the form of the partition function. We continue to derive all the necessary and sufficient constraints for the construction of the free fermionic model of the heterotic string. Having derived the tools for the construction we end this chapter by summarising them.

4.1 The Heterotic String on a Compact Space

In this section we derive the partition function of the heterotic string at the self dual point under T-duality. We follow [54, 40] initially after which [3] proves helpful. We derive firstly the partition function at an arbitrary point in the moduli space after which we descend to the self-dual point. We write the partition function at the self-dual point in a general manner which enables us to derive constraints on the form of the partition function induced by modular invariance. We then construct the free fermionic models of the heterotic string.

We construct the partition function for the heterotic string in a $D = 4$ super symmetric extended target space and a $D = 6$ compactified internal space. We recall that a free compactified boson is from equation

(3.2.10)

$$Z(R) = \frac{R}{\sqrt{\tau_2}|\eta|^2} \sum_{m,n\in\mathbb{Z}} e^{-\frac{\pi R^2}{\tau_2}|m-n\tau|^2}. \tag{4.1.1}$$

When we take the limit $R \to \infty$ we find that since the exponent is completely suppressed apart from the $m = n = 0$, the partition function is

$$\lim_{R\to\infty} Z(R) = \lim_{R\to\infty} \frac{R}{\sqrt{\tau_2}|\eta|^2}. \tag{4.1.2}$$

Since it was expected that the partition function would diverge with the volume of the space, we remove this divergence to get the correct partition function for one boson in an extended space

$$Z_B = \frac{1}{\sqrt{\tau_2}|\eta|^2}. \tag{4.1.3}$$

We can now construct the extended sector of the heterotic string. We write the full partition function as

$$Z = Z_{ext}\, Z_{compact}, \tag{4.1.4}$$

where we focus on Z_{ext}. The extended sector consists only of extended bosons, since the super partners of the bosons are free fermions of the world sheet. We write the extended partition function in the light cone gauge fixing two bosonic coordinates

$$Z_{ext} = \left[\frac{1}{\sqrt{\tau_2}|\eta|^2}\right]^2. \tag{4.1.5}$$

We are left with describing the compactified partition function. In the case of a super symmetric target space the eight left moving free super partners of the bosonic coordinates are separated[1] from the remaining degrees of freedom. The six left and right moving bosons are compactified as are the additional 16 degrees of freedom on the right moving side. This leads to the compact partition function

$$Z_{compact} = \frac{1}{2} \sum_{a,b=0,1} c\begin{bmatrix} a \\ b \end{bmatrix} \frac{\vartheta[{}^{a}_{b}]^4}{\eta^4} \frac{\Gamma_{6,6+16}}{\eta^6\bar{\eta}^{6+16}}. \tag{4.1.6}$$

If we would take $c\left[{}^{a}_{b}\right] = 1, \forall a, b \in \{0, 1\}$ we do not find space-time super symmetry. The reason for this is that the bosonic and fermionic part of the partition function do not cancel. We can realise cancellation by using the Jacobi identity[2]

$$\vartheta_3^4 - \vartheta_4^4 - \vartheta_2^4 \pm \vartheta_1^4 = 0. \tag{4.1.7}$$

[1]The word separated will become clear later on.

The partition function of the compactified heterotic string is realised as

$$Z = \frac{1}{2\tau_2|\eta|^4}\sum_{a,b=0,1}(-1)^{a+b+\mu ab}\frac{\vartheta[^a_b]^4}{\eta^4}\frac{\Gamma_{6,22}}{\eta^6\bar{\eta}^{22}}, \tag{4.1.8}$$

where μ determines the sign of ϑ_1 in the partition function. The physical relevance of μ in this context may not be clear immediately. In deriving the partition function for the free fermions in equation (3.2.21), we made a choice by projecting out half of the anti-periodic fermionic states. This choice formally should also be done with the periodic fermions. Since the periodic fermions realise the spacetime fermions, this projects out either the *up* of the *down* states and therefore effectively sets the chirality of the super symmetry. The value of μ thus sets the chirality of the space time fermions.

The general $\Gamma_{6,6+16}$ lattice depends on 6×22 moduli: the metric G_{ij} and the antisymmetric tensor B_{ij} of the six dimensional internal space, as well as the Wilson lines Y_i^I that appear in the 2d-world–sheet action

$$\begin{aligned} S &= \frac{1}{4\pi}\int d^2\sigma\sqrt{g}g^{ab}G_{ij}\partial_a X^i\partial_b X^j + \frac{1}{4\pi}\int d^2\sigma\epsilon^{ab}B_{ij}\partial_a X^i\partial_b X^j \\ &\quad + \frac{1}{4\pi}\int d^2\sigma\sqrt{g}\sum_I \psi^I\Big[\bar{\nabla}+Y_i^I\bar{\nabla}X^i\Big]\bar{\psi}^I. \end{aligned} \tag{4.1.9}$$

Here i runs over the internal coordinates and I runs over the extra 16 right–moving degrees of freedom described by $\bar{\psi}^I$. We can evaluate the partition function for this action along the same lines as done in section 3.2.1. We find that the partition function at an arbitrary point in the moduli space is

$$\begin{aligned} \Gamma_{6,6+16} &= \frac{(\det G)^3}{\tau_2^3}\sum_{m,n}\exp\Big\{-\pi\frac{T_{ij}}{\tau_2}[m^i+n^i\tau][m^j+n^j\bar{\tau}]\Big\} \\ &\quad\times\frac{1}{2}\sum_{\gamma,\delta}\prod_{I=1}^{16}\exp\Big[-i\pi n^i\big(m^j+n^j\bar{\tau}\big)Y_i^IY_j^I\Big] \\ &\quad\times\bar{\vartheta}\begin{bmatrix}\gamma\\ \delta\end{bmatrix}\big(Y_i^I(m^i+n^i\bar{\tau})|\tau\big), \end{aligned} \tag{4.1.10}$$

where $T_{ij}=G_{ij}+B_{ij}$.

Equation (4.1.10) is the winding mode representation of the partition function. Using a Poisson resummation we can put it in the momentum representation form

$$\Gamma_{6,22} = \sum_{P,\bar{P},Q}\exp\Big\{\frac{i\pi\tau}{2}P_iG^{ij}P_j - \frac{i\pi\bar{\tau}}{2}\bar{P}_iG^{ij}\bar{P}_j - i\pi\bar{\tau}\hat{Q}^I\hat{Q}^I\Big\}, \tag{4.1.11}$$

with

$$P_i = m_i + B_{ij}n^j + \frac{1}{2}Y_i^I Y_j^I n^j + Y_i^I Q^I + G_{ij}n^j, \quad (4.1.12a)$$

$$\bar{P}_i = m_i + B_{ij}n^j + \frac{1}{2}Y_i^I Y_j^I n^j + Y_i^I Q^I - G_{ij}n^j, \quad (4.1.12b)$$

$$\hat{Q}^I = Q^I + Y_i^I n^i. \quad (4.1.12c)$$

The charge momenta Q^I are induced by the right–moving fermions $\bar{\psi}^I$ which appear explicitly in the ϑ–functions from equation (3.2.23) where the charge momentum $Q^I = (n - \frac{a^I}{2})$.

4.1.1 The fermionic partition function

In the fermionic construction we fix the moduli at the self-dual point as is shown in section 3.3. The general first order partition function for an heterotic string compactified to four dimensions where the compact dimensions are at the self-dual point under T-duality is therefore written as [5]

$$Z = \int \left[\frac{d\tau d\bar{\tau}}{\tau_2^2}\right] Z_B^2 \sum_{spinstr.} c\begin{bmatrix}\alpha\\ \beta\end{bmatrix} \prod_{f=1}^{64} Z_F\begin{bmatrix}\alpha_f\\ \beta_f\end{bmatrix}, \quad (4.1.13)$$

where we have as in equations (3.2.22)

$$Z_F\begin{bmatrix}0\\0\end{bmatrix} = \sqrt{\frac{\vartheta_3}{\eta}}, \qquad Z_F\begin{bmatrix}0\\1\end{bmatrix} = \sqrt{\frac{\vartheta_4}{\eta}}, \quad (4.1.14a)$$

$$Z_F\begin{bmatrix}1\\0\end{bmatrix} = \sqrt{\frac{\vartheta_2}{\eta}}, \qquad Z_F\begin{bmatrix}1\\1\end{bmatrix} = \sqrt{\frac{\vartheta_1}{\eta}}. \quad (4.1.14b)$$

These formulae should be complex conjugated for the right-movers.

The supercurrent is realised on the world sheet non-linearly[4]

$$T_F = \psi^\mu \partial X_\mu + i\chi^I y^I \omega^I, \quad I \in \{1, \ldots, 6\}, \quad (4.1.15)$$

where the $\{\chi^I, y^I, \omega^I\}$ are 18 real free fermions transforming as the adjoint representation of $SU(2)^6$. When we transport a right-moving free fermion around a non-contractible loop it generally transforms as

$$\bar{\phi}^a \to R(\alpha)^a{}_b \bar{\phi}^b, \quad (4.1.16)$$

where $R(\alpha)^a{}_b$ should be orthogonal and should leave the energy-momentum current unchanged. For a left-moving fermion it is somewhat more

complicated as we need to consider the super current (4.1.15) as well. We can realise the following transformation

$$\psi^\mu \rightarrow -\delta_\alpha \psi^\mu, \tag{4.1.17}$$

$$\phi^a \rightarrow L(\alpha)^a{}_b \phi^b, \tag{4.1.18}$$

where $\phi^b \neq \psi^\mu$. Since the fermions are transported along a non-contractible loop $\alpha \in \pi_1(M)$, we see that $R(\alpha)$ and $L(\alpha)$ are matrix representations of α. When the fundamental group $\pi_1(M)$ is Abelian we can diagonalise $R(\alpha)$ and $L(\alpha)$ simultaneously in some basis consisting in total of 64 fermions. We can therefore realise any configuration of boundary conditions by a set of k real fermions and l complex fermions, where $k + 2l = 64$

$$\alpha = \{\alpha(f_1^r), \ldots, \alpha(f_k^r); \alpha(f_1^c), \ldots, \alpha(f_l^c)\}\,. \tag{4.1.19}$$

In this thesis we will use a slightly different notation. We will label the fermionized left-moving internal coordinates using equations (2.2.4) and (2.2.6) as

$$\frac{1}{\sqrt{2}}\left(y^I + i\omega^I\right) = e^{iX^I} \tag{4.1.20}$$

and similarly for the right moving side. The super partners of the left-moving bosons are labelled as χ^I. The super partners of the light-cone gauge fixed bosons are labelled as $\psi^\mu_{1,2}$. The extra 16 degrees of freedom are labelled as $\bar{\psi}^{1,\ldots,5}, \bar{\eta}^{1,2,3}, \bar{\phi}^{1,\ldots,8}$ and are all complex fermions. We also write the boundary condition vector in such a way that only the periodic fermions are listed in the vector. The other fermions are considered anti-periodic.

The fermions transform under parallel transport as

$$f \rightarrow -e^{i\pi\alpha(f)}\, f, \tag{4.1.21}$$

where the minus sign is introduced by convention.

We focus on the modular properties of the partition function of equation (4.1.13). The partition function should be invariant under the modular transformations defined in equations (3.1.3). Acting with these transformations on the partition function and requiring invariance leads to two constraints on the spin-structure constants $c\binom{\alpha}{\beta}$

$$c\begin{bmatrix}\alpha\\ \beta\end{bmatrix} = e^{i\frac{\pi}{4}(\alpha\cdot\alpha + \mathbb{1}\cdot\mathbb{1})}\, c\begin{bmatrix}\alpha\\ \beta - \alpha + \mathbb{1}\end{bmatrix}, \tag{4.1.22a}$$

$$c\begin{bmatrix}\alpha\\ \beta\end{bmatrix} = e^{i\frac{\pi}{2}\alpha\cdot\beta}\, c\begin{bmatrix}\beta\\ \alpha\end{bmatrix}^*, \tag{4.1.22b}$$

where we have introduced the vector $\mathbb{1}$ where all fermions are periodic. These constraints are completely due to the transformation properties of the ϑ-functions in equation (4.1.13). Another constraint arises when we incorporate higher order loops, notably the two-loop contribution. This leads to a third constraint.

$$c\begin{bmatrix}\alpha\\ \beta\end{bmatrix}c\begin{bmatrix}\alpha'\\ \beta'\end{bmatrix} = \delta_\alpha\ \delta_{\alpha'}\ e^{-i\frac{\pi}{2}\alpha\cdot\alpha'}\ c\begin{bmatrix}\alpha\\ \beta+\alpha'\end{bmatrix}c\begin{bmatrix}\alpha'\\ \beta'+\alpha\end{bmatrix}. \tag{4.1.23}$$

We have defined the inner product of two vectors as a Lorentzian inner product

$$\alpha\cdot\beta = \left\{\frac{1}{2}\sum_{R,L}+\sum_{C,L}-\frac{1}{2}\sum_{R,R}-\sum_{C,R}\right\}\alpha(f)\beta(f), \tag{4.1.24}$$

where R and C stand for real and complex respectively. R and L stand for right and left moving fermions respectively. We have defined the space-time spin statistics index δ_α as

$$\delta_\alpha = \begin{cases}1 & \iff \alpha(\psi^\mu_{1,2}) = 0,\\ -1 & \iff \alpha(\psi^\mu_{1,2}) = 1.\end{cases} \tag{4.1.25}$$

4.2 The Free Fermionic Formulation

In this section we derive the sufficient and necessary constraints for constructing a free fermionic model. We follow [3] closely in our approach. We describe the Hilbert space in terms of basis vectors with the boundary conditions of the free fermions on the world sheet. Continuing with the derivation of the constraints on these basis vectors, we move on to show the relation of the space of boundary conditions and the Hilbert space. We end this section by deriving the charge of a state under a $U(1)$ gauge group together with the frequencies of the states in the spectrum.

4.2.1 Model building constraints

We construct from the constraints (4.1.22) – (4.1.23) the necessary constraints on the vectors α and on the spin statistics coefficients $c\left[\begin{smallmatrix}\alpha\\ \beta\end{smallmatrix}\right]$. Combining equations (4.1.22b) and (4.1.23) implies by setting $\alpha' = \alpha$

and $\beta = 0$

$$c\begin{bmatrix}\alpha\\0\end{bmatrix}^2 = \delta_\alpha c\begin{bmatrix}\alpha\\0\end{bmatrix} c\begin{bmatrix}0\\0\end{bmatrix}, \tag{4.2.1}$$

which means we can solve $c\left[\begin{smallmatrix}\alpha\\0\end{smallmatrix}\right] = \delta_\alpha$, where we have normalised $c\left[\begin{smallmatrix}0\\0\end{smallmatrix}\right] = 1$ and have discarded the option where $c\left[\begin{smallmatrix}\alpha\\0\end{smallmatrix}\right] = 0$. We define a set of vectors Ξ

$$\Xi = \left\{ \alpha \;\middle|\; c\begin{bmatrix}\alpha\\0\end{bmatrix} = \delta_\alpha \right\}. \tag{4.2.2}$$

It can be shown that this set is an Abelian additive group if we define the group action to be the standard addition of the boundary conditions for every fermion separately. If we take Ξ to be finite, which means that all boundary conditions in the vector α are rational, we see that Ξ is isomorphic to

$$\Xi = \bigoplus_{i=1}^{k} \mathbb{Z}_{N_i}, \tag{4.2.3}$$

which means that Ξ is generated by a set $\{b_1, \ldots, b_k\}$ called a set of basis vectors, such that

$$\sum_{i=1}^{k} m_i b_i = 0 \iff m_i = 0 \mod N_i \;\; \forall i, \tag{4.2.4}$$

where N_i is the smallest positive integer where $N_i b_i = 0$ or the order of $\mathbb{Z}_{N_i}$. It can be shown that the vector $\mathbb{1}$ can be realised by the first basis vector b_1. In this thesis we will take $b_1 = \mathbb{1}$ for convenience. We rewrite equation (4.1.23) for the case where $\alpha, \beta, \gamma \in \Xi$

$$c\begin{bmatrix}\alpha\\\beta+\gamma\end{bmatrix} = \delta_\alpha \, c\begin{bmatrix}\alpha\\\beta\end{bmatrix} c\begin{bmatrix}\alpha\\\gamma\end{bmatrix}. \tag{4.2.5}$$

The basis vectors b_i are necessarily constrained by modular invariance. Using equation (4.1.22a) we find that in the case of the heterotic string in four dimensions by setting $\beta = \alpha$

$$c\begin{bmatrix}\alpha\\\alpha\end{bmatrix} = -e^{\frac{i\pi}{4}\alpha\cdot\alpha} c\begin{bmatrix}\alpha\\\mathbb{1}\end{bmatrix}. \tag{4.2.6}$$

Using equation (4.2.5) we find that since β generates a finite group of order N_β we can write

$$\begin{aligned} c\begin{bmatrix}\alpha\\\beta\end{bmatrix} &= \delta_\alpha \, e^{\frac{2\pi i}{N_\beta} n} \\ &= \delta_\beta \, e^{\frac{i\pi}{2}\alpha\cdot\beta} \, e^{\frac{2\pi i}{N_\alpha} m}, \end{aligned} \tag{4.2.7}$$

where we have used equation (4.1.22b) for the second equality. Using equation (4.1.22b) and raising it to the power N_{ij}, which is the least common multiple of N_i and N_j we find using equation (4.2.5)

$$\exp\left[i\frac{\pi}{2}N_{ij}b_i\cdot b_j\right]=\left(\delta_{b_i}\delta_{b_j}\right)^{N_{ij}}. \tag{4.2.8}$$

Since the right hand side is always 1 we find that

$$N_{ij}\ b_i\cdot b_j=0 \mod 4. \tag{4.2.9}$$

If we set $i=j$ the constraint (4.2.9) holds for N_i is odd. In the case where N_i is even we find an even stronger constraint using equation (4.1.22a)

$$N_i\ b_i^2=0 \mod 8, \quad \text{when } N_i \text{ even}. \tag{4.2.10}$$

4.2.2 The spectrum

We show how to construct the spectrum of a model defined by its basis vectors b_i.

We can write equation (4.1.13) using [67]

$$Z_F\begin{bmatrix}\alpha\\ \beta\end{bmatrix}=\mathbf{Tr}_\alpha\left[q^H\exp(\pi i\beta\cdot F_\alpha)\right] \tag{4.2.11}$$

as

$$Z=\int\left[\frac{d\tau d\bar{\tau}}{\tau_2^2}\right]Z_B^2\sum_{spinstr.}c\begin{bmatrix}\alpha\\ \beta\end{bmatrix}\mathbf{Tr}_{\mathscr{H}_\alpha}\left[q^{H_\alpha}\exp(\pi i\beta\cdot F_\alpha)\right], \tag{4.2.12}$$

where H_α is the Hamiltonian in the Hilbert space sector $\mathscr{H}_\alpha$ defined by the vector $\alpha=\sum_i n_i b_i$. The inner product $\beta\cdot F_\alpha$ is similar to equation (4.1.24)

$$\beta\cdot F_\alpha=\left\{\frac{1}{2}\sum_{R,L}+\sum_{C,L}-\frac{1}{2}\sum_{R,R}-\sum_{C,R}\right\}\beta(f)F_\alpha(f), \tag{4.2.13}$$

where the fermion number operator F is

$$F(f)=\begin{cases}1,\\ -1, & \text{if fermion is complex conjugate.}\end{cases} \tag{4.2.14}$$

We write the partition function as a sum over sectors. We note that since b_i are generators of a discrete group $\mathbb{Z}_{N_i}$ and since equation (4.2.5) holds, the sum in the partition function is finite and we find

$$Z = \int \left[\frac{d\tau d\bar{\tau}}{\tau_2^2}\right] Z_B^2 \sum_{\alpha\in\Xi} \delta_\alpha \mathbf{Tr}\Bigg\{ \prod_{b_i} \Bigg(\delta_\alpha c\begin{bmatrix}\alpha\\ b_i\end{bmatrix} e^{i\pi b_i\cdot F_\alpha} + \dots \\ \dots + \left\{\delta_\alpha c\begin{bmatrix}\alpha\\ b_i\end{bmatrix} e^{i\pi b_i\cdot F_\alpha}\right\}^{N_i-1} + 1\Bigg) e^{i\pi\tau H_\alpha}\Bigg\}. \quad (4.2.15)$$

We see that only states are counted that realise a generalised GSO projection

$$e^{i\pi b_i\cdot F_\alpha}|S>_\alpha = \delta_\alpha c\begin{bmatrix}\alpha\\ b_i\end{bmatrix}^* |S>_\alpha, \quad (4.2.16)$$

which leads to the full Hilbert space of states

$$\mathscr{H} = \bigoplus_{\alpha\in\Xi} \prod_{i=1}^{k} \left\{ e^{i\pi b_i\cdot F_\alpha} = \delta_\alpha c\begin{bmatrix}\alpha\\ b_i\end{bmatrix}^* \right\} \mathscr{H}_\alpha. \quad (4.2.17)$$

The mass formula of any state in the subspace or sector $\mathscr{H}_\alpha$ of the Hilbert space $\mathscr{H}$ is given by the zero-moment Virasoro gauge conditions

$$M_L^2 = -c_L + \frac{\alpha_L\cdot\alpha_L}{8} + \text{freq.} \quad (4.2.18a)$$

$$M_R^2 = -c_R + \frac{\alpha_R\cdot\alpha_R}{8} + \text{freq.} \quad (4.2.18b)$$

where $\alpha_{L,R}$ are the boundary conditions defined by the vector $\alpha = \sum n_i b_i$ for the left and right moving fermions respectively. In the case of the heterotic string, we set in this thesis $c_L = \frac{1}{2}$ and $c_R = 1$. Naturally mass level matching is realised $M_L^2 = M_R^2$ in the spectrum.

4.2.3 U(1) charges

In this section we derive the $U(1)$ charges $Q(f)$, for the unbroken Cartan generators of the four dimensional gauge group that are in one to one correspondence with the U(1) currents f^*f for each complex fermion f. We follow [51] in our approach.

We consider a single complex free left moving fermion with boundary condition.

$$\lambda(\sigma_1 + 2\pi, t) = e^{-2\pi i\nu}\lambda(\sigma_1, t), \quad (4.2.19)$$

where ν is known as the frequency of the fermion and $t = -i\sigma_2$. $\lambda(\sigma_1, t)$ has the normal mode expansion

$$\lambda(\sigma_1, t) = \sum_{n=1}^{\infty} \left\{ b_{n+\nu-1} e^{-i(n+\nu-1)(\sigma_1+t)} + d^{\dagger}_{n-\nu} e^{i(n-\nu)(\sigma_1+t)} \right\}. \quad (4.2.20)$$

We find that the Hamiltonian for this system is given by

$$\mathscr{H}_\nu = \sum_{n=1}^{\infty} \left[(n+\nu-1) b^{\dagger}_{n+\nu-1} b_{n+\nu-1} + (n-\nu) d^{\dagger}_{n-\nu} d_{n-\nu} \right] + \frac{1}{2}\left(\nu^2 - \nu + \frac{1}{6}\right). \quad (4.2.21)$$

The last term in the Hamiltonian $\mathscr{H}_\nu$ is the vacuum energy arising from the normal ordering of the operators. When we fill the negative energy states we find the vacuum charge of the system or the $U(1)$ charge induced by the left moving complex fermion λ. Using Riemann ζ-function regularisation we find

$$\begin{aligned} Q_\nu &= \sum_{n=-\infty}^{0} (n+\nu-1)^0 = \sum_{n=0}^{\infty} (n+1-\nu)^0 = \zeta(0, 1-\nu) \\ &= -B_1(1-\nu) = \nu - \frac{1}{2}, \end{aligned} \quad (4.2.22)$$

where B_1 is the first Bernoulli polynomial. We are now ready to compute the frequency of fermions depending on their boundary conditions as defined by equation (4.1.21). We have

$$f \to -e^{i\pi\alpha(f)}\, f, \qquad f^* \to -e^{-i\pi\alpha(f)}\, f^*. \quad (4.2.23)$$

It is then easy to see that the frequency for the fermions is given by

$$\nu_f = \frac{1+\alpha(f)}{2}, \qquad \nu_{f^*} = \frac{1-\alpha(f)}{2}. \quad (4.2.24)$$

However we are able to write the frequency more concisely due to the periodicity of the phases. Using the fermion number operator F we write the fermion frequency as

$$\nu = \frac{1+\alpha(f)}{2} + F. \quad (4.2.25)$$

Using this equality we find that the $U(1)$ charge $Q_\nu(f)$, for the unbroken Cartan generators of the four dimensional gauge group that are in

one to one correspondence with the U(1) currents f^*f for each complex fermion f is

$$\begin{aligned} Q_\nu(f) &= \frac{1+\alpha(f)}{2} + F - \frac{1}{2} \\ &= \frac{1}{2}\alpha(f) + F. \end{aligned} \tag{4.2.26}$$

We have described all the necessary formulae for constructing a free fermionic heterotic string model and for calculating its spectrum and the charges of the unbroken Cartan generators generating a $U(1)$ gauge group.

4.3 The Rules Of Construction

In this section we recall the rules derived in the previous sections for the construction of an heterotic string model that is invariant under modular transformations. We separate the overview into two parts. The first part recalls the necessary conditions for the creation of the Hilbert space by means of the basis vectors as well as the constraints that apply to the GSO coefficients or spin structure constants. The second part describes the necessary tools for calculating the spectrum.

4.3.1 The foundation

In the construction of any free fermionic model, two ingredients are required. The first is a set of basis vectors that define Ξ, the space of all states. We then need to isolate all the physical states. This is done by means of the GSO projections defined in equation (4.2.16). This requires the configuration of the GSO coefficients $c\binom{\alpha}{\beta}$. These coefficients are constrained by modular invariance of the partition function. We recall the constraints for these two ingredients.

The basis vectors

The basis vectors b_i consist of a set of numbers that realise the boundary conditions of each left or right moving fermion similar to equation (4.1.19)

$$b_i = \{\alpha(\psi^\mu_{1,2}), \ldots, \alpha(\omega^6) \mid \alpha(\bar{y}^1), \ldots, \alpha(\bar{\phi}^8)\}, \tag{4.3.1}$$

where

$$f \to -e^{i\pi\alpha(f)} f. \tag{4.3.2}$$

To obtain a modular invariant model, the basis vectors are required to obey the following constraints

From equation (4.2.4) we require

$$\sum_{i=1}^{k} m_i b_i = 0 \iff m_i = 0 \mod N_i \ \forall i, \tag{4.3.3a}$$

where N_i is the smallest positive integer where $N_i b_i = 0$. From equation (4.2.9) we require

$$N_{ij}\ b_i \cdot b_j = 0 \mod 4, \tag{4.3.3b}$$

where N_{ij} is the least common multiplier of N_i and N_j. From equation (4.2.10) we require

$$N_i\ b_i \cdot b_i = 0 \mod 8, \tag{4.3.3c}$$

when N_i even. In this thesis we take the first basis vector b_1 for reasons explained in section 4.2.1 to be

$$b_1 = \mathbb{1}, \tag{4.3.3d}$$

which means that all fermions have periodic boundary conditions.

For these constraints we have used the following definition for the inner product. We have defined the inner product as in equation (4.1.24)

$$\alpha \cdot \beta = \left\{ \frac{1}{2}\sum_{R,L} + \sum_{C,L} - \frac{1}{2}\sum_{R,R} - \sum_{C,R} \right\} \alpha(f)\beta(f), \tag{4.3.4}$$

where R and C stand for real and complex respectively. R and L stand for right and left moving fermions respectively.

The coefficients

We have defined the total space of states Ξ. In this space there is only a limited number of physical states that realise a generalised GSO constraint. From equation (4.2.16) we find

$$e^{i\pi b_i \cdot F_\alpha} |S>_\alpha = \delta_\alpha c \begin{bmatrix} \alpha \\ b_i \end{bmatrix}^* |S>_\alpha, \tag{4.3.5}$$

where $|S>_\alpha$ is a state in the sector $\alpha \subset \Xi$ where $\alpha = \sum n_i b_i$ is a superposition of the basis vectors b_i. The fermion number operator F is defined as in equation (4.2.14)

$$F(f) = \begin{cases} 1 \\ -1, \text{ if fermion is complex conjugate.} \end{cases} \tag{4.3.6}$$

and the space-time spin statistics index is defined as in equation (4.1.25)

$$\delta_\alpha = \begin{cases} 1 & \iff \alpha(\psi^\mu_{1,2}) = 0, \\ -1 & \iff \alpha(\psi^\mu_{1,2}) = 1. \end{cases} \tag{4.3.7}$$

To fully define the GSO projection we need to set the GSO coefficients $c\begin{bmatrix}\alpha\\ b_i\end{bmatrix}$. These coefficients are required to obey a set of constraints

From equation (4.2.7) we have

$$\begin{aligned} c\begin{bmatrix}\alpha\\ \beta\end{bmatrix} &= \delta_\alpha \, e^{\frac{2\pi i}{N_\beta} n} \\ &= \delta_\beta \, e^{\frac{i\pi}{2}\alpha\cdot\beta} \, e^{\frac{2\pi i}{N_\alpha} m}. \end{aligned} \tag{4.3.8a}$$

From equation (4.1.22b) we require

$$c\begin{bmatrix}\alpha\\ \beta\end{bmatrix} = e^{i\frac{\pi}{2}\alpha\cdot\beta} \, c\begin{bmatrix}\beta\\ \alpha\end{bmatrix}^*. \tag{4.3.8b}$$

From equation (4.2.6) we require

$$c\begin{bmatrix}\alpha\\ \alpha\end{bmatrix} = -e^{\frac{i\pi}{4}\alpha\cdot\alpha} c\begin{bmatrix}\alpha\\ \mathbb{1}\end{bmatrix}. \tag{4.3.8c}$$

From equation (4.2.5) we require

$$c\begin{bmatrix}\alpha\\ \beta+\gamma\end{bmatrix} = \delta_\alpha \, c\begin{bmatrix}\alpha\\ \beta\end{bmatrix} c\begin{bmatrix}\alpha\\ \gamma\end{bmatrix}. \tag{4.3.8d}$$

4.3.2 The spectrum

Having defined all the basis vectors together with their GSO coefficients we are ready to construct the spectrum explicitly. Here we list the necessary formulae for analysing the complete spectrum.

From equation (4.2.18) we find that the mass of any state in the Hilbert space is for the heterotic string with a super symmetric left moving sector

$$M_L^2 = -\frac{1}{2} + \frac{\alpha_L \cdot \alpha_L}{8} + N_L, \tag{4.3.9aa}$$

$$M_R^2 = -1 + \frac{\alpha_R \cdot \alpha_R}{8} + N_R, \tag{4.3.9ab}$$

where $M_L^2 = M_R^2$. The value of the oscillators are calculated using the frequencies of the states $N_{L,R} = \sum \nu_{L,R}$. From equation (4.2.24) we find for the frequencies

$$\nu_f = \frac{1+\alpha(f)}{2}, \qquad \nu_{f^*} = \frac{1-\alpha(f)}{2}. \tag{4.3.9b}$$

When a $U(1)$ gauge group is realised by a free fermion we find that the charge under this $U(1)$ is given by equation (4.2.26)

$$Q_\nu(f) = \frac{1}{2}\alpha(f) + F. \tag{4.3.9c}$$

where as usual F is the fermion number operator and α is the boundary condition for the fermion generating the $U(1)$ gauge group.

We have discussed all the necessary tools for the construction of any heterotic free fermionic model.

Chapter 5

Realistic Models

In this chapter we discuss the construction of realistic models. We start with the simplest possible model that does not exhibit a super symmetric target space. We show that adding one additional basis vector introduces super symmetry on the background. The starting set of basis vectors for any realistic model is then discussed in detail. We isolate the spinorial representations of a $SO(10)$ gauge group. This leads us to two different advanced semi-realistic models. We derive the spectrum of a model where the gauge group is enhanced and of a model where the gauge group is not enhanced. This chapter is based in part on [13].

5.1 The $N = 4$ Models

In this section we derive the spectrum of the most simple models. We start with the description of a non super symmetric free fermionic model after which we introduce a super symmetry generator basis vector. We show that adding this vector gives rise to a super symmetric spectrum. The gauge group of the two examples is discussed. We show the mechanism for the breaking of the gauge group by adding more basis vectors.

5.1.1 The non super symmetric background

We describe the simplest possible free fermionic model. We show the massless particle content and the gauge group of the model.

From equation (4.3.3) we see that the simplest possible model is constructed using only the vector $\mathbb{1}$ as mentioned in section 4.2.1

$$\mathbb{1} = \{\psi^{1,2}, \chi^{1,\ldots,6}, y^{1,\ldots,6}, \omega^{1,\ldots,6} | \bar{y}^{1,\ldots,6}, \bar{\omega}^{1,\ldots,6}, \bar{\psi}^{1,\ldots,5}, \bar{\eta}^{1,2,3}, \bar{\phi}^{1,\ldots,8}\}. \quad (5.1.1)$$

In this vector we have used the following notation. We have written the boundary condition vector in such a way that only the periodic fermions are listed in the vector. We have labeled the fermionized left-moving internal coordinates using equations (2.2.4) and (2.2.6) as

$$\frac{1}{\sqrt{2}}\left(y^I + i\omega^I\right) = e^{iX^I} \quad (5.1.2)$$

and similarly for the right moving side. The super partners of the left-moving bosons are labeled as χ^I. The super partners of the light-cone gauge fixed bosons are labeled as $\psi^\mu_{1,2}$. The extra 16 degrees of freedom are labeled as $\bar{\psi}^{1,\ldots,5}, \bar{\eta}^{1,2,3}, \bar{\phi}^{1,\ldots,8}$ and are all complex fermions. The other fermions are considered anti-periodic. It is easy to check that this vector obeys all rules described in equations (4.3.3).

The space of states Ξ as defined in equation (4.2.2) contains two sectors. We describe the two sectors as the $\mathbb{1}$ sector and the 0 or NS sector. To fully specify the model under consideration we need to define the spin statistics or GSO coefficients. We use the latter formulation from now on. The GSO coefficients for this model are $c\left[\begin{smallmatrix}NS\\NS\end{smallmatrix}\right] \equiv c\left[\begin{smallmatrix}0\\0\end{smallmatrix}\right]$, $c\left[\begin{smallmatrix}NS\\\mathbb{1}\end{smallmatrix}\right]$, $c\left[\begin{smallmatrix}\mathbb{1}\\NS\end{smallmatrix}\right]$, $c\left[\begin{smallmatrix}\mathbb{1}\\\mathbb{1}\end{smallmatrix}\right]$. Using equations (4.3.8) we find that

$$c\begin{bmatrix}NS\\NS\end{bmatrix} = -e^{\frac{i\pi}{4}\alpha_0\cdot\alpha_0} c\begin{bmatrix}NS\\\mathbb{1}\end{bmatrix} = -c\begin{bmatrix}NS\\\mathbb{1}\end{bmatrix} = 1, \quad (5.1.3a)$$

$$c\begin{bmatrix}NS\\\mathbb{1}\end{bmatrix} = e^{i\frac{\pi}{2}\alpha_0\cdot\alpha_{\mathbb{1}}} c\begin{bmatrix}\mathbb{1}\\NS\end{bmatrix}^* = \delta_{\mathbb{1}} = -1, \quad (5.1.3b)$$

$$c\begin{bmatrix}\mathbb{1}\\NS\end{bmatrix} = \delta_{\mathbb{1}} = -1, \quad (5.1.3c)$$

$$c\begin{bmatrix}\mathbb{1}\\\mathbb{1}\end{bmatrix} \equiv -1. \quad (5.1.3d)$$

We see that the value for $c\left[\begin{smallmatrix}NS\\NS\end{smallmatrix}\right] \equiv c\left[\begin{smallmatrix}0\\0\end{smallmatrix}\right] = 1$ is consistent with equation (4.2.1) as is to be expected. It is also clear that the only sign we need to set by hand is the $c\left[\begin{smallmatrix}\mathbb{1}\\\mathbb{1}\end{smallmatrix}\right]$ coefficient. The rest is either fixed by modular invariance or fixed by definition (4.2.2). We will therefore list only the relevant GSO coefficients from now on.

The states in the spectrum have a mass described by equation (4.2.18). We find that the $\mathbb{1}$ sector does not contain massless states. The only sector which produces massless states is the NS sector. To realise mass

level matching we need to introduce oscillators. From equation (4.2.24) we find that any complex creation operator acting on the vacuum realises a frequency of

$$\nu_f = \frac{1+\alpha(f)}{2} = \frac{1}{2}, \qquad \nu_{f^*} = \frac{1-\alpha(f)}{2} = \frac{1}{2}. \tag{5.1.4}$$

The massless states are separated into four subsectors

$$S_1 : \psi^\mu_{1,2}\, \partial\bar{X}^\nu|0\rangle, \qquad S_2 : \phi^a\, \partial\bar{X}^\nu|0\rangle, \tag{5.1.5a}$$

$$S_3 : \psi^\mu_{1,2}\, \bar{\phi}^b\bar{\phi}^{b'}|0\rangle, \qquad S_4 : \phi^a\, \bar{\phi}^b\bar{\phi}^{b'}|0\rangle, \tag{5.1.5b}$$

where a runs over all the left moving free fermions apart from $\psi^\mu_{1,2}$ and b and b' run over all the right moving free fermions. We can also realise states with $M^2 = -\frac{1}{2} < 0$ which are described by

$$T_1 : \bar{\phi}^b|0\rangle, \tag{5.1.6}$$

which are known as tachyonic states. This is a well known result of non super symmetric string theories. To find the physical spectrum we need to impose the GSO projection described in equation (4.2.16). We find that all states remain in the spectrum. We have thus found in the S_1 subsector a symmetric tensor, the graviton, an anti-symmetric tensor and its trace the dilaton. The states in the S_2 subsector generate gauge bosons of a $SU(2)^6$ gauge group. Similarly the states in the S_3 subsector realise the gauge bosons of a $SO(44)$ gauge group. The states in the S_4 subsector are scalars in the adjoint representation of $SU(2)^6 \times SO(44)$. This completes the whole analysis of the heterotic string in a non super symmetric background.

5.1.2 The super symmetric background

In this section we describe a free fermionic model with a $N = 4$ super symmetric background in detail. We show the massless particle content of the model and its gauge group.

In equation (4.1.6) we have seen that separating the eight left moving free super partners of the bosonic coordinates from the rest of the compact partition function results in a super symmetric target space. We do the same in the fermionic formulation by defining the vector S in addition to the vector $\mathbb{1}$, where

$$S = \{\psi^{1,2}, \chi^{1,\ldots,6}\}. \tag{5.1.7}$$

Again it is easy to check that this vector obeys all the rules listed in equation (4.3.3). With the addition of the vector S we have introduced a bigger space of states Ξ. We find the additional sectors S, $\mathbb{1} + S$.

We finalise the specification of the whole model by setting the GSO coefficients

$$c\begin{bmatrix}\alpha\\ \beta\end{bmatrix} = \begin{matrix}\\ 1\\ S\end{matrix}\begin{matrix}\begin{matrix}1 & S\end{matrix}\\ \begin{pmatrix}-1 & -1\\ -1 & -1\end{pmatrix}\end{matrix}. \tag{5.1.8}$$

We could have chosen the coefficients differently but we will argue later on in this section that this choice does not have any physical effect.

Using equation (4.2.18) we find that in the sector $\mathbb{1} + S$ there are no massless states. We therefore focus on the new states in the S sector. In the S sector we find states of a new kind. Since the $\psi^{1,2}, \chi^{1,\dots,6}$ fermions are periodic they form a degenerate ground state. Consider the mode expansion for the free fermion[40, 67]

$$i\psi(z) = \sum \psi_n z^{-n-\frac{1}{2}}, \tag{5.1.9}$$

where the sum is over $\mathbb{Z}$ for periodic fermions and over $\mathbb{Z} + \frac{1}{2}$ for anti-periodic fermions. We find that the anti-commutator for the fermionic modes ψ_n is given by

$$\{\psi_n, \psi_m\} = \delta_{n+m,0} \tag{5.1.10}$$

We see that the zero mode ψ_0 takes a ground state into another ground state due to $\{\psi_n, \psi_0\} = 0$ for $n > 0$. We label the two states as $|\pm\rangle$, where $|+\rangle = |0\rangle$ and $|-\rangle = \psi_0|0\rangle$ leading to $F|+\rangle = 0$ and $F|-\rangle = -1$, where F is the fermion number operator as in equation (4.2.14). Since the periodic fermions contribute to the massless spectrum we find using above notation the following massless states

$$S_5 \;:\; |\pm\rangle_1|\pm\rangle_2|\pm\rangle_3|\pm\rangle_4\, \partial\bar{X}^\nu|0\rangle, \tag{5.1.11a}$$
$$S_6 \;:\; |\pm\rangle_1|\pm\rangle_2|\pm\rangle_3|\pm\rangle_4\, \bar{\phi}^b\bar{\phi}^{b'}|0\rangle, \tag{5.1.11b}$$

where we have complexified the real fermions $\psi^{1,2}$, $\chi^{1,2}$, $\chi^{3,4}$ and $\chi^{5,6}$.

Using the GSO projection from equation (4.2.16) we find that the following states remain in the spectrum

$$S_1 : \psi_\mu^{1,2}\, \partial\bar{X}^\nu|0\rangle, \qquad S_2 : \chi^a\, \partial\bar{X}^\nu|0\rangle, \tag{5.1.12a}$$
$$S_3 : \psi_\mu^{1,2}\, \bar{\phi}^b\bar{\phi}^{b'}|0\rangle, \qquad S_4 : \chi^a\, \bar{\phi}^b\bar{\phi}^{b'}|0\rangle, \tag{5.1.12b}$$

where a runs over $1, \ldots, 6$ and b and b' as in equations (5.1.5). Additionally the states

$$S_5 \quad : \quad \left[\binom{4}{1} + \binom{4}{3}\right] \partial \bar{X}^\nu |0\rangle, \tag{5.1.13a}$$

$$S_6 \quad : \quad \left[\binom{4}{1} + \binom{4}{3}\right] \bar{\phi}^b \bar{\phi}^{b'} |0\rangle, \tag{5.1.13b}$$

remain in the spectrum, where $\binom{4}{3}$ means that 3 of the 4 degenerate states are in the down state $|-\rangle$. In the second line we can separate the degeneracy induced by the spacetime spinor $\psi^\mu_{1,2}$. We separate

$$\left[\binom{4}{1} + \binom{4}{3}\right] = \binom{1}{0}\left[\binom{3}{1} + \binom{3}{3}\right] + \binom{1}{1}\left[\binom{3}{0} + \binom{3}{2}\right], \tag{5.1.14}$$

where an additional degeneracy of 4 is apparent next to the spacetime *up* and *down* spinor state.

One important feature of these super symmetric models is that the tachyonic states found in equation (5.1.6) all drop out.

If we were to set the GSO coefficients as

$$c\begin{bmatrix}\alpha\\ \beta\end{bmatrix} = \begin{array}{c} \\ 1 \\ S \end{array}\begin{array}{c} \begin{array}{cc} 1 & S \end{array} \\ \begin{pmatrix} -1 & 1 \\ 1 & 1 \end{pmatrix} \end{array}. \tag{5.1.15}$$

we find that the states in the NS sector remain the same but the states in the S sector become

$$S_5 \quad : \quad \left[\binom{4}{1} + \binom{4}{2} + \binom{4}{4}\right] \partial \bar{X}^\nu |0\rangle, \tag{5.1.16a}$$

$$S_6 \quad : \quad \left[\binom{4}{0} + \binom{4}{2} + \binom{4}{4}\right] \bar{\phi}^b \bar{\phi}^{b'} |0\rangle. \tag{5.1.16b}$$

Again we can isolate the spacetime spinor $\psi^\mu_{1,2}$, leading again to a degeneracy of 4. The configuration of *down* states is different from the configuration induced by the GSO coefficients presented in equation (5.1.8). We therefore find that $c\left[\begin{smallmatrix}\mathbb{1}\\ S\end{smallmatrix}\right]$ sets the number of down states $|-\rangle$ in the S sector. This sign choice is directly related to the value of μ from equation (4.1.8)[46, 30]

$$\mu = \frac{1}{2}\left(1 - c\begin{bmatrix}\mathbb{1}\\ S\end{bmatrix}\right). \tag{5.1.17}$$

Since the choice of chirality is a convention, we have therefore not found a physically different model with the different configuration of the GSO

coefficients. A notable result of this model is that, again, the tachyonic states from equation (5.1.6) are projected out.

The degeneracy of the space time spinors is identified as the result of an $N = 4$ super symmetric background. We therefore identify the states in the S_5 subsector as the super partners of the gravitons called gravitinos. Similarly we identify the states in the S_6 subsector as the super partners of the $SO(44)$ gauge bosons, the $SO(44)$ gauginos.

The gauge group of this model is again realised by the states in the S_2 and S_3 subsector. Since the states in the S_2 subsector do not have super partners we identify the induced gauge group not as a space time gauge group. The states in the $S_3 \subset NS$ subsector generate a $SO(44)$ space time gauge group with an $N = 4$ super symmetry where the super partners are generated by the sector $NS + S = S$. This is a general feature of free fermionic models. In a super symmetric model where the super symmetry is generated by the vector S all the super partners of a particular sector α are generated by the sector $\alpha + S$.

5.2 A $N = 1$ Model: the NAHE Set

We discuss a model that describes a $N = 1$ space time with spinorial representations of a SO(10) gauge group. This model is known in the literature to be constructed using the NAHE set. In [6] the flipped $SU(5)$ free fermionic models were analysed. In [5] an initial start was made in the construction of the set used for the flipped $SU(5)$ model. In [32] a subset of the flipped $SU(5)$ basis vector set was identified as relevant for the construction of phenomenologically interesting models. This subset was labeled the NAHE set. We start by defining the model. We then set the GSO coefficients after which we discuss some interesting properties of the model in detail.

The NAHE set consists of a set of five basis vectors. The vectors are $\mathbb{1}$, S, defined in equation (5.1.1) and equation (5.1.7), and the vectors b_1, b_2 and b_3

$$b_1 = \{\psi^{1,2}, \chi^{1,2}, y^{3,\ldots,6} \mid \bar{y}^{3,\ldots,6}, \bar{\psi}^{1,\ldots,5}, \bar{\eta}^1\}, \tag{5.2.1a}$$

$$b_2 = \{\psi^{1,2}, \chi^{3,4}, y^{1,2}, \omega^{5,6} \mid \bar{y}^{1,2}, \bar{\omega}^{5,6}, \bar{\psi}^{1,\ldots,5}, \bar{\eta}^2\}, \tag{5.2.1b}$$

$$b_3 = \{\psi^{1,2}, \chi^{3,4}, \omega^{1,\ldots,4} \mid \bar{\omega}^{1,\ldots,4}, \bar{\psi}^{1,\ldots,5}, \bar{\eta}^3\}. \tag{5.2.1c}$$

Note that these vectors b_i are labeled as such to reflect the notation of the literature best. It will be clear from the context whether b_i are gen-

eral basis vectors or the ones listed above. Since the basis vectors listed above induce a $\mathbb{Z}_2 \times \mathbb{Z}_2$ twist as will become clear later on, this notation will also be used later on for other vectors that induce the same type of twisting. The addition of these three vectors have enlarged the space of states Ξ considerably. We therefore do not list all the new sectors. We however isolate some new sectors which prove to be enlightening for further analysis of more complex models.

We set the GSO coefficients

$$c\begin{bmatrix}\alpha\\ \beta\end{bmatrix} = \begin{array}{c} \\ 1 \\ S \\ \\ b_1 \\ b_2 \\ b_3 \end{array} \begin{array}{c} \begin{array}{ccccc} 1 & S & & b_1 & b_2 & b_3 \end{array} \\ \begin{pmatrix} 1 & 1 & & -1 & -1 & -1 \\ 1 & 1 & & 1 & 1 & 1 \\ & & & & & \\ -1 & -1 & & -1 & -1 & -1 \\ -1 & -1 & & -1 & -1 & -1 \\ -1 & -1 & & -1 & -1 & -1 \end{pmatrix} \end{array}. \tag{5.2.2}$$

The space time vector bosons come from the NS sector. In this model additional vector bosons can come from the $\xi = \mathbb{1} + b_1 + b_2 + b_3$ sector. The NS sector gives rise to a $SO(6)^3 \times SO(16) \times SO(10)$. With the GSO coefficients given in equation (5.2.2) we find that the states in the ξ sector remain in the spectrum and give similar to the construction of the S sector in equation (5.1.11)

$$\xi : \left[\binom{8}{0} + \binom{8}{2} + \binom{8}{4} + \binom{8}{6} + \binom{8}{8}\right] \psi_\mu^{1,2}|0\rangle \tag{5.2.3}$$

vector bosons. This enhances the $SO(16) \to \mathbb{E}_8$ as the ξ sector contains 128 states, the spinorial representation of $SO(16)$ and the NS sector contains 120 states, the vectorial representation of $SO(16)$. We therefore find the gauge group $SO(6)^3 \times SO(10) \times \mathbb{E}_8$.

The additional basis vectors b_i induce additional GSO projections on the states in the S sector. We find that b_1 reduces the number of states in the $S_5 \subset S$ sector to

$$S_5 : \left[\binom{2}{1}\right]\left[\binom{2}{0} + \binom{2}{2}\right]\ \partial\bar{X}^\nu|0\rangle. \tag{5.2.4}$$

The b_2 vector reduces the number of states in the $S_5 \subset S$ sector to

$$S_5 : \left[\binom{1}{1}\binom{1}{0}\binom{1}{0}\binom{1}{0} + \binom{1}{0}\binom{1}{1}\binom{1}{1}\binom{1}{1}\right]\ \partial\bar{X}^\nu|0\rangle. \tag{5.2.5}$$

The b_3 vector does not reduce the number of states any further. We find that there is a degeneracy of 1 of the space time spinorial *up* and

down state. We have therefore reduced the number of space time super symmetries to $N = 1$.

The NAHE set divides the 44 right-moving and 20 left-moving real internal fermions in the following way: $\bar{\psi}^{1,\cdots,5}$ are complex and produce the observable $SO(10)$ symmetry; $\bar{\phi}^{1,\cdots,8}$ are complex and produce the hidden $\mathbb{E}_8$ gauge group; $\{\bar{\eta}^1, \bar{y}^{3,\cdots,6}\}$, $\{\bar{\eta}^2, \bar{y}^{1,2}, \bar{\omega}^{5,6}\}$, $\{\bar{\eta}^3, \bar{\omega}^{1,\cdots,4}\}$ give rise to the three horizontal $SO(6)$ symmetries. The left-moving $\{y, \omega\}$ states are also divided into the sets $\{y^{3,\cdots,6}\}$, $\{y^{1,2}, \omega^{5,6}\}$, $\{\omega^{1,\cdots,4}\}$. The left-moving $\chi^{12}, \chi^{34}, \chi^{56}$ states carry the super symmetry charges. Each sector b_1, b_2 and b_3 carries periodic boundary conditions under $(\psi^\mu|\bar{\psi}^{1,\cdots,5})$ and one of the three groups: $(\chi_{12}, \{y^{3,\cdots,6}|\bar{y}^{3,\cdots 6}\}, \bar{\eta}^1)$, $(\chi_{34}, \{y^{1,2}, \omega^{5,6}|\bar{y}^{1,2}$-$\bar{\omega}^{5,6}\}, \bar{\eta}^2)$, $(\chi_{56}, \{\omega^{1,\cdots,4}|\bar{\omega}^{1,\cdots 4}\}, \bar{\eta}^3)$.

There are three sectors of special interest in this model. They are the sectors b_1, b_2 and b_3. We will focus on only one as the other two can be dealt with similarly. In the sector b_1 we find massless states as is easily verified using equation (4.2.18). Similar to the sector S we get a degenerate vacuum. One complication arises here. In the case of the S vector we could pair two left, or right moving fermions to create a complex fermion. Although at the level of the NAHE set this is possible as well for the internal fermions $y^i, \omega^i, \bar{y}^i, \bar{\omega}^i$, adding more vectors generally disallows this type of pairing.

Periodic free fermions have a conformal weight $h = \frac{1}{16}$[40]. Fields with conformal weight $(h, \bar{h}) = (\frac{1}{16}, \frac{1}{16})$ realise an order operator σ in a two-dimensional Ising model[63]. Since in this case the real fermions have periodic boundary conditions we can pair a real left moving fermion with a real right-moving fermion to construct an order operator σ

$$\sigma^a = \phi^a(z)\bar{\phi}^a(\bar{z}), \tag{5.2.6}$$

leading to a degenerate vacuum. We find that the unprojected lowest mass states induced by the sector b_1 can be written as

$$|S\rangle = |\psi_\mu^{1,2}\rangle_\pm \, |\chi^{1,2}\rangle_\pm \prod_{l=3}^{6} |\sigma^l\rangle_\pm \, |\bar{\eta}^1\rangle_\pm \prod_{m=1}^{5} |\bar{\psi}^m\rangle_\pm |0\rangle, \tag{5.2.7}$$

where we have used the following pairing

$$\psi_\mu^{1,2} = \frac{1}{\sqrt{2}}\left(\psi_\mu^1 + i\psi_\mu^2\right), \tag{5.2.8a}$$

$$\chi^{2k-1,2k} = \frac{1}{\sqrt{2}}\left(\chi^{2k-1} + i\chi^{2k}\right), \tag{5.2.8b}$$

$$\sigma^l = y^l\bar{y}^l, \tag{5.2.8c}$$

where the other fermions are already complex by construction. We impose the GSO projection as defined in equation (4.2.16). We use the combinatorics notation as employed in equation (5.1.13). Projecting using the basis vector $\mathbb{1}$ gives

$$\left[\binom{12}{0}+\binom{12}{2}+\binom{12}{4}+\binom{12}{6}+\binom{12}{8}+\binom{12}{10}+\binom{12}{12}\right]=2^{11} \quad (5.2.9)$$

states in the b_1 sector. Projecting with the basis vector S gives

$$\left[\binom{2}{0}+\binom{2}{2}\right]\left[\binom{10}{0}+\binom{10}{2}+\binom{10}{4}+\binom{10}{6}+\binom{10}{8}+\binom{10}{10}\right]=2^{10} \quad (5.2.10)$$

states in the b_1 sector. Projecting with the basis vector b_1 does not reduce the number of states. Projecting with the vector b_2 reduces the number of states to

$$\begin{aligned}&\binom{1}{0}\binom{1}{0}\left[\binom{5}{0}+\binom{5}{2}+\binom{5}{4}\right]\left[\binom{5}{0}+\binom{5}{2}+\binom{5}{4}\right]+\\ &\quad\binom{1}{1}\binom{1}{1}\left[\binom{5}{1}+\binom{5}{3}+\binom{5}{5}\right]\left[\binom{5}{1}+\binom{5}{3}+\binom{5}{5}\right]=2^9. \quad (5.2.11)\end{aligned}$$

Note that the sign of $c\binom{b_1}{b_2}$ determines the number of *up* and *down* states in the vacuum. Projecting with the last basis vector b_3 does not reduce the number of states any further. We find that the b_1 sector produces spinorial **16** representations of $SO(10)$. There is a degeneracy of 16 for the *up* and *down* state of the space time spinor $\psi_\mu^{1,2}$. This degeneracy is interpreted as 16 families of the spinorial **16** of $SO(10)$. Since the number of *up* and *down* states in the vacuum is determined by the sign of $c\binom{b_1}{b_2}$, we find that this sign determines the chirality of the **16**, i.e. determines whether we find a $\overline{\mathbf{16}}$ or **16** of $SO(10)$. A similar method can be followed for the sectors b_2 and b_3. We therefore find 16 spinorial **16** of $SO(10)$ coming from each b_i giving a total of 48 generations.

We have thus found a model with a $SO(6)^3 \times SO(10) \times \mathbb{E}_8$ gauge group and $N = 1$ space time super symmetry. The next step in the construction of a realistic model is to break the $SO(10)$ gauge group and simultaneously reduce the number of families to three. This is usually done using three more basis vectors called α, β and γ. In section 5.3 we discuss such models in detail and derive their complete spectra.

5.3 Two Advanced Models

In this section we discuss two advanced semi realistic models. We first recall the setup of the NAHE set after which we break the unification $SO(10)$ to standard model like gauge groups. We then discuss one model in which the gauge group is not enhanced and one in which the gauge group is enhanced.

A model in the free fermionic formulation [5, 51] is constructed by choosing a consistent set of boundary condition basis vectors as explained in section 4.3. The basis vectors, b_k, span a finite additive group $\Xi = \sum_k n_k b_k$ where $n_k = 0, \cdots, N_{z_k} - 1$. The physical massless states in the Hilbert space of a given sector $\alpha \subset \Xi$, are obtained by acting on the vacuum with bosonic and fermionic operators and by applying the generalised GSO projections. The $U(1)$ charges, $Q(f)$, for the unbroken Cartan generators of the four dimensional gauge group are in one to one correspondence with the $U(1)$ currents f^*f for each complex fermion f, and are from equation (4.2.26)

$$Q(f) = \frac{1}{2}\alpha(f) + F_\alpha(f), \tag{5.3.1}$$

where $\alpha(f)$ is the boundary condition of the world–sheet fermion f in the sector α, and $F_\alpha(f)$ is the fermion number operator from equation (4.2.14). For each periodic complex fermion f there are two degenerate vacua $|+\rangle, |-\rangle$, annihilated by the zero modes f_0 and ${f_0}^*$ and with fermion numbers $F(f) = 0, -1$, respectively as explained in section 5.2.

The realistic models in the free fermionic formulation are generated by a basis of boundary condition vectors for all world–sheet fermions [7, 60, 33, 19, 8, 58, 21, 23]. The basis is constructed in two stages. The first stage consists of the NAHE set [7, 60, 32, 26, 21], which is a set of five boundary condition basis vectors, $\{\mathbb{1}, S, b_1, b_2, b_3\}$ as explained in section 5.2. The gauge group at the level of the NAHE set is $SO(10) \times SO(6)^3 \times \mathbb{E}_8$ with $N = 1$ space–time super symmetry. The vector S is the super symmetry generator and the super partners of the states from a given sector α are obtained from the sector $S + \alpha$ as explained in section 5.1.2. The space–time vector bosons that generate the gauge group arise from the Neveu–Schwarz (NS) sector and from the sector $\zeta \equiv \mathbb{1} + b_1 + b_2 + b_3$. The NS sector produces the generators of $SO(10) \times SO(6)^3 \times SO(16)$. The sector ζ produces the spinorial **128** of $SO(16)$ and completes the hidden gauge group to $\mathbb{E}_8$. The vectors b_1, b_2 and b_3 produce 48 spinorial **16**'s of $SO(10)$, sixteen from each sector b_1, b_2 and b_3. The vacuum of these sectors contains eight periodic world sheet fermions,

five of which produce the charges under the $SO(10)$ group, while the remaining three periodic fermions generate charges with respect to the flavour symmetries. Each of the sectors b_1, b_2 and b_3 is charged with respect to a different set of flavour quantum numbers, $SO(6)_{1,2,3}$.

The second stage of the basis construction consist of adding three additional basis vectors to the NAHE set. Three additional vectors are needed to reduce the number of generations to three, one from each sector b_1, b_2 and b_3. One specific example is given in table 5.3.1. The choice of boundary conditions to the set of real internal fermions $\{y,\omega|\bar{y},\bar{\omega}\}^{1,\cdots,6}$ determines the low energy properties, such as the number of generations.

The $SO(10)$ gauge group is broken to one of its subgroups $SU(5)\times U(1)$, $SO(6)\times SO(4)$ or $SU(3)\times SU(2)\times U(1)^2$ by the assignment of boundary conditions to the set $\bar{\psi}^{1\cdots5}_{\frac{1}{2}}$:

$$1.\ b\{\bar{\psi}^{1\cdots5}_{\frac{1}{2}}\} = \{\frac{1}{2}\frac{1}{2}\frac{1}{2}\frac{1}{2}\frac{1}{2}\frac{1}{2}\} \Rightarrow SU(5)\times U(1), \quad (5.3.2a)$$

$$2.\ b\{\bar{\psi}^{1\cdots5}_{\frac{1}{2}}\} = \{11100\} \Rightarrow SO(6)\times SO(4). \quad (5.3.2b)$$

To break the $SO(10)$ symmetry to $SU(3)_C\times SU(2)_L\times U(1)_C\times U(1)_L$ both steps, 1 and 2, are used, in two separate basis vectors. The breaking pattern $SO(10)\to SU(3)_C\times SU(2)_L\times SU(2)_R\times U(1)_{B-L}$ is achieved by the following assignment in two separate basis vectors

$$1.\ b\{\bar{\psi}^{1\cdots5}_{\frac{1}{2}}\} = \{11100\} \Rightarrow SO(6)\times SO(4), \quad (5.3.3a)$$

$$2.\ b\{\bar{\psi}^{1\cdots5}_{\frac{1}{2}}\} = \{\frac{1}{2}\frac{1}{2}\frac{1}{2}00\} \Rightarrow SU(3)_C\times U(1)_C\times SU(2)_L\times SU(2)_R. \quad (5.3.3b)$$

Similarly, the breaking pattern $SO(10)\to SU(4)_C\times SU(2)_L\times U(1)_R$ is achieved by the following assignment in two separate basis vectors

$$1.\ b\{\bar{\psi}^{1\cdots5}_{\frac{1}{2}}\} = \{11100\} \Rightarrow SO(6)\times SO(4), \quad (5.3.4a)$$

$$2.\ b\{\bar{\psi}^{1\cdots5}_{\frac{1}{2}}\} = \{000\frac{1}{2}\frac{1}{2}\} \Rightarrow SU(4)_C\times SU(2)_L\times U(1)_R. \quad (5.3.4b)$$

We comment here that a recurring feature of some of the three generation free fermionic heterotic string models is the emergence of a combination of the basis vectors which extend the NAHE set,

$$X = n_\alpha\alpha + n_\beta\beta + n_\gamma\gamma, \quad (5.3.5)$$

for which $X_L \cdot X_L = 0$ and $X_R \cdot X_R \neq 0$. Such a combination may produce additional space–time vector bosons, depending on the choice of GSO phases. These additional space–time vector bosons enhance the four dimensional gauge group. This situation is similar to the presence of the combination of the NAHE set basis vectors $\mathbb{1} + b_1 + b_2 + b_3$, which enhances the hidden gauge group, at the level of the NAHE set, from $SO(16)$ to $\mathbb{E}_8$. In the free fermionic models this type of gauge symmetry enhancement in the observable sector is, in general, family universal and is intimately related to the $\mathbb{Z}_2 \times \mathbb{Z}_2$ orbifold structure which underlies the realistic free fermionic models. This will become clear later on in chapters 6 and 7. Such enhanced symmetries were shown to forbid proton decay mediating operators to all orders of nonrenormalizable terms [23]. Below we discuss examples of models with and without gauge enhancement.

The SU421 symmetry breaking pattern induced by the boundary condition assignment given in equation (5.3.4) has an important distinction from the previous symmetry breaking patterns. As in the previous cases, since it involves a breaking of an $SO(2n)$ group to $SU(n) \times U(1)$ it contains 1/2 boundary conditions. As discussed above the observable and hidden non–Abelian gauge groups arise from the sets of complex world–sheet fermions $\{\bar{\psi}^{1,\cdots,5}\bar{\eta}^{1,\cdots,3}\}$ and $\{\bar{\phi}^{1,\cdots,8}\}$, respectively. The breaking pattern (5.3.4) entails an assignment of $1/2$ boundary condition to two complex fermions in the observable set, whereas the symmetry breaking patterns in equations (5.3.2) and (5.3.3) involve three such assignments. On the other hand, the modular invariance rules [5, 51] for the product $b_j \cdot \gamma$, where b_j are the NAHE set basis vectors and γ is the basis vector that contains the $1/2$ boundary conditions, enforces that no other complex fermion from the observable set has $1/2$ boundary conditions as explained in section 4.3.1. Additionally, the constraint on the product $\gamma \cdot \gamma$ imposes that either 8 or 12 complex fermions have $1/2$ boundary conditions. Since, as we saw, only two can have such boundary conditions from the observable set, it implies that six and only six from the hidden set must have $1/2$ boundary conditions. This is in contrast to the other cases that allow assignment of twelve $1/2$ boundary conditions in the basis vector γ. The consequence of having only eight $1/2$ boundary conditions in the basis vector γ is the appearance of additional sectors that may lead to enhancement of the four dimensional gauge group.

	ψ^μ	χ^{12}	χ^{34}	χ^{56}	$\bar{\psi}^{1,\ldots,5}$	$\bar{\eta}^1$	$\bar{\eta}^2$	$\bar{\eta}^3$	$\bar{\phi}^{1,\ldots,8}$
α	0	0	0	0	1 1 1 0 0	0	0	0	1 1 1 1 0 0 0 0
β	0	0	0	0	1 1 1 0 0	0	0	0	1 1 1 1 0 0 0 0
γ	0	0	0	0	0 0 0 $\frac{1}{2}$ $\frac{1}{2}$	0	0	0	$\frac{1}{2}$ $\frac{1}{2}$ $\frac{1}{2}$ $\frac{1}{2}$ $\frac{1}{2}$ $\frac{1}{2}$ 0 0

	y^3y^6	$y^4\bar{y}^4$	$y^5\bar{y}^5$	$\bar{y}^3\bar{y}^6$	$y^1\omega^5$	$y^2\bar{y}^2$	$\omega^6\bar{\omega}^6$	$\bar{y}^1\bar{\omega}^5$	$\omega^2\omega^4$	$\omega^1\bar{\omega}^1$	$\omega^3\bar{\omega}^3$	$\bar{\omega}^2\bar{\omega}^4$
α	1	1	1	0	1	1	1	0	1	1	1	0
β	0	1	0	1	0	1	0	1	1	0	0	0
γ	0	0	1	1	1	0	0	0	0	1	0	0

Table 5.3.1: Additional basis vectors giving rise to a $SU(4)\times SU(2)\times U(1)$ gauge group without enhancement.

5.3.1 A model without enhanced symmetry

As our first example of a SU421 free fermionic heterotic string model we consider the model defined in table 5.3.1 and equation (5.3.6), specified below in addition to the NAHE set explained in section 5.2. Also given in table 5.3.1 are the pairings of left– and right–moving real fermions from the set $\{y,\omega|\bar{y},\bar{\omega}\}$. These fermions are paired to form either complex, left– or right–moving fermions, or Ising model operators, which combine a real left–moving fermion with a real right–moving fermion.

The generalised GSO coefficients for the model with basis vectors given in table 5.3.1 are

$$\begin{array}{c} \\ \mathbb{1} \\ S \\ \\ b_1 \\ b_2 \\ b_3 \\ \\ \alpha \\ \beta \\ \gamma \end{array} \begin{array}{c} \begin{array}{cccccccc} \mathbb{1} & S & b_1 & b_2 & b_3 & \alpha & \beta & \gamma \end{array} \\ \left(\begin{array}{cccccccc} 1 & 1 & -1 & -1 & -1 & 1 & 1 & 1 \\ 1 & 1 & 1 & 1 & 1 & -1 & -1 & -1 \\ & & & & & & & \\ -1 & -1 & -1 & -1 & -1 & -1 & -1 & 1 \\ -1 & -1 & -1 & -1 & -1 & 1 & 1 & 1 \\ -1 & -1 & -1 & -1 & -1 & -1 & 1 & i \\ & & & & & & & \\ 1 & -1 & 1 & -1 & 1 & 1 & 1 & i \\ 1 & -1 & -1 & 1 & -1 & -1 & -1 & i \\ 1 & -1 & -1 & 1 & -1 & -1 & 1 & i \end{array}\right) \end{array}. \qquad (5.3.6)$$

In matrix (5.3.6) only the entries above the diagonal are independent and those below and on the diagonal are fixed by the modular invariance constraints. Blank lines are inserted to emphasise the division of the free phases between the different sectors of the realistic free fermionic

models. Thus, the first two lines involve only the GSO phases of $c\binom{\{\mathbb{1},S\}}{a_i}$. The set $\{\mathbb{1},S\}$ generates the $N=4$ model with S being the space–time super symmetry generator and therefore the phases $c\binom{S}{a_i}$ are those that control the space–time super symmetry in the super string models. Similarly, in the free fermionic models, sectors with periodic and anti–periodic boundary conditions, of the form of b_i, produce the chiral generations. The phases $c\binom{b_i}{b_j}$ determine the chirality of the states from these sectors similar to equation (5.1.17).

In the free fermionic models the basis vectors b_i are those that respect the $SO(10)$ symmetry while the vectors denoted by Greek letters are those that break the $SO(10)$ symmetry. As the Standard Model matter states arise from sectors which preserve the $SO(10)$ symmetry, the phases that fix the Standard Model charges are, in general, the phases $c\binom{b_i}{a_i}$. The phases associated with the basis vectors $\{\alpha,\beta,\gamma\}$ are associated with exotic physics, beyond the Standard Model. These phases, therefore, also affect the final four dimensional gauge symmetry.

The final gauge group of the model defined in table 5.3.1 and matrix (5.3.6) arises as follows. In the observable sector the NS boundary conditions produce gauge group generators for

$$SU(4)_C \times SU(2)_L \times U(1)_R \times U(1)_{1,2} \times SU(2)_3 \times U(1)_{4,5} \times SU(2)_6. \quad (5.3.7)$$

Here the flavour $SU(2)_3 \times SU(2)_6$ symmetries are generated by $\{\bar{\eta}^3\bar{\zeta}^3\}$ where $\bar{\zeta}^3 = \frac{1}{\sqrt{2}}(\bar{w}^2 + i\bar{w}^4)$. In previous free fermionic models this group factor breaks to $U(1)^2$, but this is an artifact of the specific model considered in table 5.3.1, and is not a generic feature of SU421 models. Thus, the $SO(10)$ symmetry is broken to $SU(4)\times SU(2)_L \times U(1)_R$, as discussed above, where,

$$U(1)_R = \mathrm{Tr}\, U(2)_L \;\Rightarrow\; Q_R = \sum_{i=4}^{5} Q(\bar{\psi}^i). \quad (5.3.8)$$

The flavour $SO(6)^3$ symmetries are broken to $U(1)_{1,2}\times SU(2)_3 \times U(1)_{4,5} \times SU(2)_6$, where $Q_{1,2} = Q(\bar{\eta}_{1,2})$, $Q_4 = Q(\bar{y}^3\bar{y}^5)$ and $Q_5 = Q(\bar{y}^1\bar{\omega}^5)$. In the hidden sector the NS boundary conditions produce the generators of

$$SU(4)_H \times SU(2)_{H_1} \times SU(2)_{H_2} \times SU(2)_{H_3} \times U(1)_{7,8} \quad (5.3.9)$$

where $SU(2)_{H_1} \times SU(2)_{H_2}$ and $SU(2)_{H_3}$ arise from the complex world–sheet fermions $\{\bar{\phi}^7\bar{\phi}^8\}$ and $\{\bar{\phi}^5\bar{\phi}^6\}$, respectively; and $U(1)_7$ and $U(1)_8$

correspond to the combinations of world–sheet charges

$$Q_7 = \sum_{i=5}^{6} Q(\bar{\phi}^i), \tag{5.3.10}$$

$$Q_8 = \sum_{i=1}^{4} Q(\bar{\phi}^i). \tag{5.3.11}$$

As we discussed in section 5.3 the SU421 models contain additional sectors that may produce space–time vector bosons and enhance the four dimensional gauge group. In the model of table 5.3.1 these are the sectors 2γ, $\zeta_1 \equiv \mathbb{1}+b_1+b_2+b_3$ and $\zeta_2 \equiv \mathbb{1}+b_1+b_2+b_3+2\gamma$. However, due to the choice of one–loop phases in equation (5.3.6) all the additional vector bosons from these sectors are projected out by the GSO projections and there is therefore no gauge enhancement from these sectors in this model.

In addition to the graviton, dilaton, antisymmetric sector and spin–1 gauge bosons, the NS sector gives two pairs of colour triplets, transforming as (6,1,0) under $SU(4)_C \times SU(2)_L \times U(1)_R$; three quadruplets of $SO(10)$ singlets with $U(1)_{1,2,3}$ charges; and three singlets of the entire four dimensional gauge group. The states from the sectors b_j $(j = 1, 2, 3)$ produce the three light twisted generations. These states and their decomposition under the entire gauge group are shown in appendix A.1. The remaining massless states and their quantum numbers also appear in appendix A.1.

5.3.2 A model with enhanced symmetry

We next turn to our second example defined by table 5.3.2 and matrix (5.3.12).

The generalised GSO coefficients for the model described by table 5.3.2

	ψ^μ	χ^{12}	χ^{34}	χ^{56}	$\bar{\psi}^{1,\ldots,5}$	$\bar{\eta}^1$	$\bar{\eta}^2$	$\bar{\eta}^3$	$\bar{\phi}^{1,\ldots,8}$
α	0	0	0	0	1 1 1 0 0	0	0	0	1 1 1 1 0 0 0 0
β	0	0	0	0	1 1 1 0 0	0	0	0	1 1 1 1 0 0 0 0
γ	0	0	0	0	0 0 0 $\frac{1}{2}$ $\frac{1}{2}$	0	0	0	$\frac{1}{2}$ $\frac{1}{2}$ $\frac{1}{2}$ $\frac{1}{2}$ $\frac{1}{2}$ $\frac{1}{2}$ 0 0

	y^3y^6	$y^4\bar{y}^4$	$y^5\bar{y}^5$	$\bar{y}^3\bar{y}^6$	$y^1\omega^5$	$y^2\bar{y}^2$	$\omega^6\bar{\omega}^6$	$\bar{y}^1\bar{\omega}^5$	$\omega^2\omega^4$	$\omega^1\bar{\omega}^1$	$\omega^3\bar{\omega}^3$	$\bar{\omega}^2\bar{\omega}^4$
α	0	0	1	1	1	0	0	0	0	1	0	1
β	1	0	0	0	0	0	1	1	0	0	1	1
γ	0	1	0	1	0	1	0	1	1	0	0	1

Table 5.3.2: Additional basis vectors giving rise to a $SU(4)\times SU(2)\times U(1)$ gauge group with enhancement.

are

$$\begin{array}{c} \\ \mathbb{1} \\ S \\ \\ b_1 \\ b_2 \\ b_3 \\ \\ \alpha \\ \beta \\ \gamma \end{array} \begin{array}{c} \begin{array}{cccccccc} \mathbb{1} & S & b_1 & b_2 & b_3 & \alpha & \beta & \gamma \end{array} \\ \begin{pmatrix} 1 & 1 & -1 & -1 & -1 & 1 & 1 & 1 \\ 1 & 1 & 1 & 1 & 1 & -1 & -1 & -1 \\ \\ -1 & -1 & -1 & -1 & -1 & 1 & -1 & -1 \\ -1 & -1 & -1 & -1 & -1 & -1 & -1 & -1 \\ -1 & -1 & -1 & -1 & -1 & 1 & 1 & i \\ \\ 1 & -1 & 1 & 1 & 1 & -1 & 1 & -1 \\ 1 & -1 & 1 & -1 & 1 & 1 & -1 & 1 \\ -1 & -1 & 1 & 1 & -1 & -1 & 1 & -1 \end{pmatrix} \end{array} . \qquad (5.3.12)$$

The total gauge group of the model defined by table 5.3.2 and matrix (5.3.12) arises as follows. In the observable sector the NS boundary conditions produce the generators of $SU(4)_C \times SU(2)_L \times U(1)_R \in SO(10) \times U(1)_{1,2,3} \times U(1)_{4,5,6}$, while in the hidden sector the NS boundary conditions produce the generators of

$$SU(4)_H \times SU(2)_{H_1} \times SU(2)_{H_2} \times SU(2)_{H_3} \times U(1)_7 \times U(1)_8 \,. \qquad (5.3.13)$$

$U(1)_7$ and $U(1)_8$ correspond to the combinations of the world–sheet charges given in equations (5.3.10) and (5.3.11), respectively and where $Q_{1,2,3} = Q(\bar{\eta}_{1,2,3})$, $Q_4 = Q(\bar{y}^3\bar{y}^5)$, $Q_5 = Q(\bar{y}^1\bar{\omega}^5)$ and $Q_6 = Q(\bar{\omega}^2\bar{\omega}^4)$.

The model with enhancement contains two combinations of non–NAHE basis vectors with $X_L \cdot X_L = 0$, which therefore may give rise to additional space–time vector bosons. The first is the sector 2γ. The second arises from the vector combination given by $\zeta + 2\gamma$, where $\zeta \equiv \mathbb{1}+b_1+b_2+b_3$. Both sectors arise from the NAHE set basis vectors plus 2γ

and are therefore independent of the assignment of periodic boundary conditions in the basis vectors α, β.Both are therefore generic for the pattern of symmetry breaking $SO(10) \to SU(4)_C \times SU(2)_L \times U(1)_R$, in NAHE based models.

In the model without enhancement the additional space–time vector bosons from both sectors are projected out and therefore there is no gauge enhancement. In the model with enhancement all the space–time vector bosons from the sector 2γ are projected out by the GSO projections and therefore give no gauge enhancement from this sector. The sector $\zeta + 2\gamma$ may, or may not, give rise to additional space–time vector bosons, depending on the choice of GSO phase

$$c\begin{bmatrix}\gamma\\ b_3\end{bmatrix} = \pm 1, \tag{5.3.14}$$

where with the $+1$ choice all the additional vector bosons are projected out, whereas the -1 choice gives rise to additional space–time gauge bosons which are charged with respect to the $SU(2)_L \times SU(2)_{H_1}$ groups. This enhances the $SU(2)_L \times SU(2)_{H_1}$ group to $SO(5)$. Thus, in this case, the full massless spectrum transforms under the final gauge group, $SU(4)_C \times SO(5) \times U(1)_R \times U(1)_{1,2,3} \times U(1)_{4,5,6} \times SU(4)_H \times SU(2)_{H_2} \times SU(2)_{H_3} \times U(1)_{7,8}$.

In addition to the graviton, dilaton, antisymmetric sector and spin–1 gauge bosons, the NS sector gives rise to three quadruplets of $SO(10)$ singlets with $U(1)_{1,2,3}$ charges; and three singlets of the entire four dimensional gauge group. The states from the sectors $b_j \oplus \zeta + 2\gamma$ $(j = 1, 2, 3)$ produce the three light generations. The states from these sectors and their decomposition under the entire gauge group are shown in appendix A.2.

5.4 Overview of the Realistic Models

In the previous section we have shown how to construct realistic and semi-realistic models. We have given details of two specific models. In this section we give a recapitulation of the general properties of realistic and semi-realistic models. We describe properties which have been dealt with in detail in the previous sections. We show that the realistic models are $\mathbb{Z}_2 \times \mathbb{Z}_2$ orbifolds with symmetric shifts. This section therefore provides a bridge between specific models and the classification of the chiral $\mathbb{Z}_2 \times \mathbb{Z}_2$ heterotic string models.

The notation and details of the construction of these models are given in chapter 4 and [7, 60, 33, 19, 8, 58, 21, 20, 18, 22, 11, 12, 32, 26, 14, 10]. In the free fermionic formulation of the heterotic string in four dimensions all the world-sheet degrees of freedom required to cancel the conformal anomaly are represented in terms of free world–sheet fermions [5, 51]. In the light-cone gauge the world-sheet field content consists of two transverse left- and right-moving space-time coordinate bosons, $X^{\mu}_{1,2}$ and $\bar{X}^{\mu}_{1,2}$, and their left-moving fermionic super partners $\psi^{\mu}_{1,2}$, and additional 62 purely internal Majorana-Weyl fermions, of which 18 are left-moving, and 44 are right-moving. In the super symmetric sector the world-sheet super symmetry is realised non-linearly and the world-sheet supercurrent [4] is from equation (4.1.15) given by

$$T_F = \psi^{\mu}\partial X_{\mu} + i\chi^I y^I \omega^I, \ (I = 1, \cdots, 6). \tag{5.4.1}$$

The $\{\chi^I, y^I, \omega^I\}$ $(I = 1, \cdots, 6)$ are 18 real free fermions transforming as the adjoint representation of $\mathrm{SU}(2)^6$. Under parallel transport around a non-contractible loop on the toroidal world-sheet the fermionic fields pick up a phase as is shown in equation (4.1.21). Each set of specified phases for all world-sheet fermions, around all the non-contractible loops is called the spin structure of the model. Such spin structures are usually given in the form of 64 dimensional boundary condition vectors, with each element of the vector specifying the phase of the corresponding world-sheet fermion. The basis vectors are constrained by string consistency requirements and completely determine the vacuum structure of the model. The physical spectrum is obtained by applying the generalised GSO projections [5, 51].

The boundary condition basis vectors defining a typical realistic free fermionic heterotic string model is constructed in two stages. The first stage consists of the NAHE set, which is a set of five boundary condition basis vectors, $\{1, S, b_1, b_2, b_3\}$ [34, 35, 37, 38, 56, 57, 32, 26] and is explained in detail in section 5.2. The gauge group induced by the NAHE set is $SO(10) \times SO(6)^3 \times \mathbb{E}_8$ with $N = 1$ super symmetry. The space-time vector bosons that generate the gauge group arise from the Neveu–Schwarz sector and from the sector $\xi_2 \equiv 1 + b_1 + b_2 + b_3$. The Neveu-Schwarz sector produces the generators of $SO(10) \times SO(6)^3 \times SO(16)$. The ξ_2-sector produces the spinorial **128** of SO(16) and completes the hidden gauge group to $\mathbb{E}_8$.

The second stage of the construction consists of adding to the NAHE set three (or four) additional basis vectors. These additional vectors reduce the number of generations to three, one from each of the sectors b_1, b_2 and b_3, and simultaneously break the four dimensional gauge group. The assignment of boundary conditions to $\{\bar{\psi}^{1,\cdots,5}\}$ breaks SO(10) to one

of its subgroups $\mathrm{SU}(5)\times\mathrm{U}(1)$ [7, 60], $\mathrm{SO}(6)\times\mathrm{SO}(4)$ [8, 58], $\mathrm{SU}(3)\times\mathrm{SU}(2)\times\mathrm{U}(1)^2$ [33, 19, 21, 20, 18, 22, 11, 12], $\mathrm{SU}(3)\times\mathrm{SU}(2)^2\times\mathrm{U}(1)$ [14, 10] or $\mathrm{SU}(4)\times\mathrm{SU}(2)\times\mathrm{U}(1)$ [13]. Similarly, the hidden $\mathbb{E}_8$ symmetry is broken to one of its subgroups, and the flavour $\mathrm{SO}(6)^3$ symmetries are broken to $U(1)^n$, with $3\leq n\leq 9$. For details and phenomenological studies of these three generation string models we refer interested readers to the original literature and review articles [62, 59, 25, 27, 28].

The correspondence of the free fermionic models with the orbifold construction is illustrated by extending the NAHE set, $\{1,S,b_1,b_2,b_3\}$, by at least one additional boundary condition basis vector [24, 16]

$$\xi_1=(0,\cdots,0|\underbrace{1,\cdots,1}_{\bar\psi^{1,\cdots,5},\bar\eta^{1,2,3}},0,\cdots,0)\,. \tag{5.4.2}$$

With a suitable choice of the GSO projection coefficients the model possesses an $\mathrm{SO}(4)^3\times\mathbb{E}_6\times\mathrm{U}(1)^2\times\mathbb{E}_8$ gauge group and $N=1$ space-time super symmetry. The matter fields include 24 generations in the 27 representation of $\mathbb{E}_6$, eight from each of the sectors $b_1\oplus b_1+\xi_1$, $b_2\oplus b_2+\xi_1$ and $b_3\oplus b_3+\xi_1$. Three additional 27 and $\overline{27}$ pairs are obtained from the Neveu-Schwarz $\oplus\,\xi_1$ sector.

To construct the model in the orbifold formulation one starts with the compactification on a torus with nontrivial background fields [64, 65]. The subset of basis vectors

$$\{1,S,\xi_1,\xi_2\} \tag{5.4.3}$$

generates a toroidally-compactified model with $N=4$ space-time super symmetry and $\mathrm{SO}(12)\times\mathbb{E}_8\times\mathbb{E}_8$ gauge group. The same model is obtained in the geometric (bosonic) language by tuning the background fields to the values corresponding to the SO(12) lattice.

Adding the two basis vectors b_1 and b_2 to the set (5.4.3) corresponds to the $\mathbb{Z}_2\times\mathbb{Z}_2$ orbifold model with standard embedding. Starting from the $N=4$ model with $\mathrm{SO}(12)\times\mathbb{E}_8\times\mathbb{E}_8$ symmetry [64, 65], and applying the $\mathbb{Z}_2\times\mathbb{Z}_2$ twist on the internal coordinates, reproduces the spectrum of the free-fermion model with the six-dimensional basis set $\{1,S,\xi_1,\xi_2,b_1,b_2\}$. The Euler characteristic of this model is 48 with $h_{11}=27$ and $h_{21}=3$.

It is noted that the effect of the additional basis vector ξ_1 of equation (5.4.2), is to separate the gauge degrees of freedom, spanned by the world-sheet fermions $\{\bar\psi^{1,\cdots,5},\bar\eta^1,\bar\eta^2,\bar\eta^3,\bar\phi^{1,\cdots,8}\}$, from the internal compactified degrees of freedom $\{y,\omega|\bar y,\bar\omega\}^{1,\cdots,6}$. In the realistic free fermionic

models this is achieved by the vector 2γ [16], with

$$2\gamma = (0,\cdots,0| \underbrace{1,\cdots,1}_{\bar{\psi}^{1,\cdots,5},\bar{\eta}^{1,2,3}\bar{\phi}^{1,\cdots,4}},0,\cdots,0)\ , \tag{5.4.4}$$

which breaks the $\mathbb{E}_8\times\mathbb{E}_8$ symmetry to $SO(16)\times SO(16)$. The $\mathbb{Z}_2\times\mathbb{Z}_2$ twist induced by b_1 and b_2 breaks the gauge symmetry to $SO(4)^3\times SO(10)\times U(1)^3\times SO(16)$. The orbifold still yields a model with 24 generations, eight from each twisted sector, but now the generations are in the chiral **16** representation of SO(10), rather than in the **27** of $\mathbb{E}_6$. The same model can be realized with the set $\{1,S,\xi_1,\xi_2,b_1,b_2\}$, by projecting out the $16\oplus\overline{16}$ from the ξ_1-sector taking

$$c\begin{bmatrix}\xi_1\\ \xi_2\end{bmatrix}\to -c\begin{bmatrix}\xi_1\\ \xi_2\end{bmatrix}. \tag{5.4.5}$$

This choice also projects out the massless vector bosons in the 128 of SO(16) in the hidden-sector $\mathbb{E}_8$ gauge group, thereby breaking the $\mathbb{E}_6\times\mathbb{E}_8$ symmetry to $SO(10)\times U(1)\times SO(16)$. We can define two $N=4$ models generated by the set (5.4.3), Z_+ and Z_-, depending on the sign in equation (5.4.5). The first, say Z_+, produces the $\mathbb{E}_8\times\mathbb{E}_8$ model, whereas the second, say Z_-, produces the $\mathrm{SO}(16)\times\mathrm{SO}(16)$ model. However, the $\mathbb{Z}_2\times\mathbb{Z}_2$ twist acts identically in the two models, and their physical characteristics differ only due to the discrete torsion equation (5.4.5).

This analysis confirms that the $\mathbb{Z}_2\times\mathbb{Z}_2$ orbifold on the $SO(12)$ lattice is at the core of the realistic free fermionic models. To illustrate how the chiral generations are generated in the free fermionic models we consider the $\mathbb{E}_6$ model which is produced by the extended NAHE–set $\{1,S,\xi_1,\xi_2,b_1,b_2\}$.

The chirality of the states from a twisted sector b_j is determined by the free phase $c\begin{bmatrix}b_j\\ b_i\end{bmatrix}$. Since we have a freedom in the choice of the sign of this free phase, we can get from the sector (b_i) either the **27** or the $\overline{\mathbf{27}}$. Which of those we obtain in the physical spectrum depends on the sign of the free phase. The free phases $c\begin{bmatrix}b_j\\ b_i\end{bmatrix}$ also fix the total number of chiral generations. Since there are two b_i projections for each sector b_j, $i\neq j$ we can use one projections to project out the states with one chirality and the other projection to project out the states with the other chirality. Thus, the total number of generations with this set of basis vectors is given by

$$8\left(\frac{c\begin{bmatrix}b_1\\ b_2\end{bmatrix}+c\begin{bmatrix}b_1\\ b_3\end{bmatrix}}{2}\right)+8\left(\frac{c\begin{bmatrix}b_2\\ b_1\end{bmatrix}+c\begin{bmatrix}b_2\\ b_3\end{bmatrix}}{2}\right)+8\left(\frac{c\begin{bmatrix}b_3\\ b_1\end{bmatrix}+c\begin{bmatrix}b_3\\ b_1\end{bmatrix}}{2}\right).$$

	ψ^μ	χ^{12}	χ^{34}	χ^{56}	$\bar{\psi}^{1,\ldots,5}$	$\bar{\eta}^1$	$\bar{\eta}^2$	$\bar{\eta}^3$	$\bar{\phi}^{1,\ldots,8}$
α	0	0	0	0	1 1 1 0 0	0	0	0	1 1 1 1 0 0 0 0
β	0	0	0	0	1 1 1 0 0	0	0	0	1 1 1 1 0 0 0 0
γ	0	0	0	0	$\frac{1}{2}\ \frac{1}{2}\ \frac{1}{2}\ \frac{1}{2}\ \frac{1}{2}$	$\frac{1}{2}$	$\frac{1}{2}$	$\frac{1}{2}$	$\frac{1}{2}$ 0 1 1 $\frac{1}{2}\ \frac{1}{2}\ \frac{1}{2}$ 0

	y^3y^6	$y^4\bar{y}^4$	$y^5\bar{y}^5$	$\bar{y}^3\bar{y}^6$	$y^1\omega^5$	$y^2\bar{y}^2$	$\omega^6\bar{\omega}^6$	$\bar{y}^1\bar{\omega}^5$	$\omega^2\omega^4$	$\omega^1\bar{\omega}^1$	$\omega^3\bar{\omega}^3$	$\bar{\omega}^2\bar{\omega}^4$
α	1	0	0	0	0	0	1	1	0	0	1	1
β	0	0	1	1	1	0	0	0	0	1	0	1
γ	0	1	0	1	0	1	0	1	1	0	0	0

Table 5.4.1: Model for the illustration of the reduction to three generations.

Since the modular invariance rules fix $c\binom{b_j}{b_i} = c\binom{b_i}{b_j}$ we get that the total number of generations is either 24 or 8. Thus, to reduce the number of generation further it is necessary to introduce additional basis vectors.

To illustrate the reduction to three generations in the realistic free fermionic models we consider the model in table 5.4.1. Here the vector ξ_1 (5.4.2) is replaced by the vector 2γ (5.4.4). At the level of the NAHE set we have 48 generations. One half of the generations is projected by the vector 2γ. Each of the three vectors in table 5.4.1 acts non trivially on the degenerate vacuum of the sectors b_1, b_2 and b_3 and reduces the number of generations in each step by a half. Thus, we obtain one generation from each sector b_1, b_2 and b_3.

The geometrical interpretation of the basis vectors beyond the NAHE set is facilitated by taking combinations of the basis vectors in 5.4.1, which entails choosing another set to generate the same vacuum. The combinations $\alpha+\beta$, $\alpha+\gamma$, $\alpha+\beta+\gamma$ produce the boundary conditions under the set of internal real fermions as is displayed in table 5.4.2. It is noted that the two combinations $\alpha+\beta$ and $\beta+\gamma$ are fully symmetric between the left and right movers, whereas the third, $\alpha+\beta+\gamma$, is asymmetric. The action of the first two combinations on the compactified bosonic coordinates translates therefore to symmetric shifts. Thus, we see that reduction of the number of generations is obtained by further action of symmetric shifts as described in chapter 3.

Due to the presence of the third combination, the situation is more complicated. The third combination in table 5.4.2 is asymmetric between the left and right movers and therefore does not have an obvious geometrical interpretation. In subsequent chapters we perform a complete

	y^3y^6	$y^4\bar{y}^4$	$y^5\bar{y}^5$	$\bar{y}^3\bar{y}^6$	$y^1\omega^5$	$y^2\bar{y}^2$	$\omega^6\bar{\omega}^6$	$\bar{y}^1\bar{\omega}^5$
$\alpha+\beta$	1	0	1	1	1	0	1	1
$\beta+\gamma$	0	1	1	0	1	1	0	1
$\alpha+\beta+\gamma$	1	1	1	0	1	1	1	0

	$\omega^2\omega^4$	$\omega^1\bar{\omega}^1$	$\omega^3\bar{\omega}^3$	$\bar{\omega}^2\bar{\omega}^4$
$\alpha+\beta$	0	1	1	0
$\beta+\gamma$	1	1	0	1
$\alpha+\beta+\gamma$	1	1	1	0

Table 5.4.2: A redefinition of the model listed in table 5.4.1

classification of all the possible NAHE–based $\mathbb{Z}_2 \times \mathbb{Z}_2$ orbifold models with symmetric shifts on the complex tori, which reveals that three generations are not obtained in this manner. Three generations are obtained in the free fermionic models by the inclusion of the asymmetric shift in (5.4.2). This outcome has profound implications on the type of geometries that may be related to the realistic string vacua, as well as on the issue of moduli stabilisation.

Part II

Classification of the Chiral $\mathbb{Z}_2 \times \mathbb{Z}_2$ Heterotic String Models

Chapter 6

The Classification in the Orbifold Formulation

In this chapter we set up the partition function of the heterotic string using the geometrical description. We start by describing the $N = 4$ heterotic string. We break the number of super symmetries using a $\mathbb{Z}_2 \times \mathbb{Z}_2$ twist. This leads to four subclasses of $\mathbb{Z}_2 \times \mathbb{Z}_2$ heterotic string models. We isolate the different subclasses and show their partition functions. This chapter is based on parts of [29, 30, 31].

6.1 $N = 1$ Heterotic Orbifold Constructions

In this section we revise the $\mathbb{Z}_2 \times \mathbb{Z}_2$ heterotic orbifold construction and relate this to the free fermionic construction. We isolate the individual conformal blocks that will facilitate the classification of the models and set up a procedure to analyse all possible $N = 1$ heterotic $\mathbb{Z}_2 \times \mathbb{Z}_2$ models. We start by describing the procedure to descend from $N = 4$ to $N = 1$ super symmetric heterotic vacua.

6.1.1 The $N = 4$ orbifold models

The partition function for any heterotic model via the fermionic construction is from equation (4.1.13)

$$Z = \frac{1}{\tau_2}\frac{1}{\eta^{12}\bar{\eta}^{24}}\sum_{a,b\in\Xi} c\binom{a}{b}\frac{1}{2^M}\prod_{i=1}^{20}\vartheta\binom{a_i}{b_i}^{\frac{1}{2}}\prod_{j=1}^{44}\bar{\vartheta}\binom{a_j}{b_j}^{\frac{1}{2}}. \tag{6.1.1}$$

In the above equation M is the number of basis vectors and the parameters in the ϑ–functions represent the action of the vectors. In order to obtain a super symmetric model we need at least two basis vectors $\{1, S\}$ as explained in section 5.1.2

$$\begin{aligned} 1 &= \{\psi^{1,2}, \chi^{1,\dots,6}, y^{1,\dots,6}, \omega^{1,\dots,6}| \\ &\quad \bar{y}^{1,\dots,6}, \bar{\omega}^{1,\dots,6}, \bar{\psi}^{1,\dots,5}, \bar{\eta}^{1,2,3}, \bar{\phi}^{1,\dots,8}\}, \qquad (6.1.2)\\ S &= \{\psi^{1,2}, \chi^{1,\dots,6}\}. \qquad (6.1.3) \end{aligned}$$

The super symmetric GSO projection is induced by the set S for any choice of the GSO coefficient

$$c\begin{bmatrix} S \\ 1 \end{bmatrix} = \pm 1. \tag{6.1.4}$$

The corresponding partition function has a factorised left–moving contribution coming from the sector S. We find from equation (4.1.8)

$$Z_{1,S} = \frac{1}{\tau_2|\eta|^4}\frac{1}{2}\sum_{a,b=0}^{1}(-1)^{a+b+\mu ab}\frac{\vartheta\binom{a}{b}^4}{\eta^4}\frac{\Gamma_{6,6+16}[SO(44)]}{\eta^6\bar{\eta}^{22}}, \tag{6.1.5}$$

where

$$\frac{\Gamma_{6,6+16}[SO(44)]}{\eta^6\bar{\eta}^{22}} = \frac{1}{2}\sum_{c,d}\frac{\vartheta\binom{c}{d}^6\bar{\vartheta}\binom{c}{d}^{22}}{\eta^6\bar{\eta}^{22}}, \tag{6.1.6}$$

and as in equation (5.1.17)

$$\mu = \frac{1}{2}\left(1 - c\begin{bmatrix} \mathbb{1} \\ S \end{bmatrix}\right) \tag{6.1.7}$$

defines the chirality of $N = 4$ super symmetry. Therefore, the role of the boundary condition vector S is to factorise the left–moving contribution [53],

$$Z^L_{N=4} = \frac{1}{2}\sum_{a,b=0}^{1}(-1)^{a+b+\mu ab}\vartheta\binom{a}{b}(v)\vartheta\binom{a}{b}^3(0) \sim v^4, \tag{6.1.8}$$

which is zero with the multiplicity of $N = 4$ super symmetry.

The above partition function gives rise to a $SO(44)$ right–moving gauge group and is the maximally symmetric point in the moduli space of the Narain $\Gamma_{6,6+16}$ lattice. The general $\Gamma_{6,6+16}$ lattice depends on 6×22 moduli, the metric G_{ij} and the antisymmetric tensor B_{ij} of the six dimensional internal space, as well as the Wilson lines Y_i^I that appear in the 2d-world–sheet as in equation (4.1.9)

$$\begin{aligned} S &= \frac{1}{4\pi}\int d^2\sigma\sqrt{g}g^{ab}G_{ij}\partial_a X^i\partial_b X^j + \frac{1}{4\pi}\int d^2\sigma\epsilon^{ab}B_{ij}\partial_a X^i\partial_b X^j \\ &\quad + \frac{1}{4\pi}\int d^2\sigma\sqrt{g}\sum_I \psi^I\Big[\bar{\nabla} + Y_i^I\bar{\nabla}X^i\Big]\bar{\psi}^I. \end{aligned} \tag{6.1.9}$$

Here i runs over the internal coordinates and I runs over the extra 16 right–moving degrees of freedom described by $\bar{\psi}^I$.

The compactified sector of the partition function is given by $\Gamma_{6,6+16}$

$$\begin{aligned} \Gamma_{6,6+16} &= \frac{(\det G)^3}{\tau_2^3}\sum_{m,n}\exp\Big\{-\pi\frac{T_{ij}}{\tau_2}[m^i + n^i\tau][m^j + n^j\bar{\tau}]\Big\} \\ &\quad \times\frac{1}{2}\sum_{\gamma,\delta}\prod_{I=1}^{16}\exp\Big[-i\pi n^i\big(m^j + n^j\bar{\tau}\big)Y_i^I Y_j^I\Big] \\ &\quad \times\bar{\vartheta}\begin{bmatrix}\gamma\\ \delta\end{bmatrix}\big(Y_i^I(m^i + n^i\bar{\tau})|\tau\big), \end{aligned} \tag{6.1.10}$$

where $T_{ij} = G_{ij} + B_{ij}$.

Equation (6.1.10) is the winding mode representation of the partition function. Using a Poisson resummation we can put it in the momentum representation form:

$$\Gamma_{6,22} = \sum_{P,\bar{P},Q}\exp\left\{\frac{i\pi\tau}{2}P_iG^{ij}P_j - \frac{i\pi\bar{\tau}}{2}\bar{P}_iG^{ij}\bar{P}_j - i\pi\bar{\tau}\hat{Q}^I\hat{Q}^I\right\}, \tag{6.1.11}$$

with

$$P_i = m_i + B_{ij}n^j + \frac{1}{2}Y_i^IY_j^In^j + Y_i^IQ^I + G_{ij}n^j, \tag{6.1.12a}$$

$$\bar{P}_i = m_i + B_{ij}n^j + \frac{1}{2}Y_i^IY_j^In^j + Y_i^IQ^I - G_{ij}n^j, \tag{6.1.12b}$$

$$\hat{Q}^I = Q^I + Y_i^In^i. \tag{6.1.12c}$$

The charge momenta $Q^I = n - \frac{a^I}{2}$ are induced by the right–moving fermions $\bar{\psi}^I$ which appear explicitly in the ϑ–functions from equation (3.2.23).

For generic G_{ij}, B_{ij} and for vanishing values for Wilson lines, $Y_i^I = 0$ one obtains an $N = 4$ model with a gauge group $U(1)^6 \times SO(32)$. The $U(1)^6$ can be extended to $SO(12)$ by fixing the moduli of the internal manifold [24, 16].

The $N = 4$ fermionic construction based on $\{1, S\}$ (6.1.5) has an extended gauge group, $SO(44)$. From the lattice construction point of view, a $N = 4$ model with a gauge group $G \subset SO(44)$ can be generated by switching on Wilson lines and fine tune the moduli of the internal manifold. Moving from the $SO(44)$ to $U(1)^6 \times SO(32)$ heterotic point as well as to the $U(1)^6 \times \mathbb{E}_8 \times \mathbb{E}_8$ point can be realized continuously [55]. The partition function at the $U(1)^6 \times \mathbb{E}_8 \times \mathbb{E}_8$ point takes a simple factorised form

$$\begin{aligned}\Gamma_{6,6+16} &= \frac{(\det G)^3}{\tau_2^3} \sum_{m,n} \exp\left\{ -\pi \frac{T_{ij}}{\tau_2} [m^i + n^i\tau][m^j + n^j\bar{\tau}] \right\} \\ &\quad \times \frac{1}{2} \sum_{\gamma,\delta} \bar{\vartheta} \begin{bmatrix} \gamma \\ \delta \end{bmatrix}^8 \times \frac{1}{2} \sum_{h,g} \bar{\vartheta} \begin{bmatrix} h \\ g \end{bmatrix}^8 . \end{aligned} \tag{6.1.13}$$

6.1.2 The $N = 1$ orbifold models

To break the number of super symmetries down from $N = 4$ to $N = 1$ in the fermionic formulation using a $\mathbb{Z}_2 \times \mathbb{Z}_2$ twist, we introduce the vectors b_1 and b_2.

$$b_1 = \{\chi^{3,4}, \chi^{5,6}, \; y^{3,4}, y^{5,6} \mid \dots\}, \tag{6.1.14}$$

$$b_2 = \{\chi^{1,2}, \chi^{5,6}, y^{1,2}, \; y^{5,6} \mid \dots\}. \tag{6.1.15}$$

The b_1 twists the second and third complex planes (3,4) and (5,6) while b_2 twists the first and third (1,2) and (5,6) ones. Thus, b_1, b_2 separate the internal lattice into the three complex planes: (1,2), (3,4) and (5,6). Note that these basis vectors are linear combinations of the vectors defined in equation (5.2.1).

The action of the b_i–twists fully determines the fermionic content for the left–moving sector. The dots $\dots$ in b_1, b_2 stand for the n_1, n_2 right–moving fermions. To generate a modular invariant model we can distinguish four options n_i are either 8, 16, 24 or 32 real right-moving fermions in the basis vector b_i.

Defining the basis vectors with 8 real right–moving fermions leads to massless states in the spectrum in vectorial representations of the gauge

groups; 16 real right–moving fermions give rise to spinorial representations on each plane. Adding either 24 or 32 right–moving fermions would produce massive states in the spectrum. We discard the last two options. We thus need to introduce 16 real fermions (8 complex) in the vectors b_1, b_2 for the existence of spinorial representations on the first and second plane.

A suitable choice having section 4.3 in mind, is for instance,

$$b_1 = \{\chi^{3,4}, \chi^{5,6}, y^{3,4}, y^{5,6} \,|\bar{y}^{3,4}, \bar{y}^{5,6}, \; \bar{\eta}^1, \bar{\psi}^{1,\ldots,5}\}, \tag{6.1.16}$$

$$b_2 = \{\chi^{1,2}, \chi^{5,6}, y^{1,2}, y^{5,6} \,|\bar{y}^{1,2}, \bar{y}^{5,6}, \; \bar{\eta}^2, \bar{\psi}^{1,\ldots,5}\}. \tag{6.1.17}$$

The $N = 1$ partition function based on $\{1, S, b_1, b_2\}$ is

$$\begin{aligned} Z_{N=1} &= \frac{1}{\tau_2 |\eta|^4} \frac{1}{2} \sum_{\alpha,\beta} e^{i\pi(a+b+\mu ab)} \\ &\quad \frac{1}{4} \sum_{h_1,h_2,g_1,g_2} \frac{\vartheta\left[{a \atop b}\right]}{\eta} \frac{\vartheta\left[{a+h_2 \atop b+g_2}\right]}{\eta} \frac{\vartheta\left[{a+h_1 \atop b+g_1}\right]}{\eta} \frac{\vartheta\left[{a-h_1-h_2 \atop b-g_1-g_2}\right]}{\eta} \\ &\quad \times \frac{1}{2} \sum_{\gamma,\delta} \frac{\Gamma_{6,6}\begin{bmatrix}\gamma,h_1,h_2\\ \delta,g_1,g_2\end{bmatrix}}{\eta^6 \bar{\eta}^6} \times \frac{Z_\eta\begin{bmatrix}\gamma,h_1,h_2\\ \delta,g_1,g_2\end{bmatrix}}{\bar{\eta}^7} \\ &\quad \times \frac{Z_{18}\left[{\gamma \atop \delta}\right]}{\bar{\eta}^9} \; e^{i\pi\varphi_L}, \end{aligned} \tag{6.1.18a}$$

$$\Gamma_{6,6}\begin{bmatrix}\gamma,h_1,h_2\\ \delta,g_1,g_2\end{bmatrix} = \left|\vartheta\left[{\gamma \atop \delta}\right]\vartheta\left[{\gamma+h_2 \atop \delta+g_2}\right]\right|^2 \left|\vartheta\left[{\gamma \atop \delta}\right]\vartheta\left[{\gamma+h_1 \atop \delta+g_1}\right]\right|^2 \left|\vartheta\left[{\gamma \atop \delta}\right]\vartheta\left[{\gamma-h_1-h_2 \atop \delta-g_1-g_2}\right]\right|^2 \tag{6.1.18b}$$

$$Z_\eta\begin{bmatrix}\gamma,h_1,h_2\\ \delta,g_1,g_2\end{bmatrix} = \bar{\vartheta}\left[{\gamma+h_2 \atop \delta+g_2}\right]\bar{\vartheta}\left[{\gamma+h_1 \atop \delta+h_2}\right] \bar{\vartheta}\left[{\gamma-h_1-h_2 \atop \delta-g_1-g_2}\right]^5, \tag{6.1.18c}$$

$$Z_{18}\left[{\gamma \atop \delta}\right] = \bar{\vartheta}\left[{\gamma \atop \delta}\right]^9, \tag{6.1.18d}$$

In equation (6.1.18b) the internal manifold is twisted and thereby separated explicitly into three planes. The above model is the minimal $\mathbb{Z}_2 \times \mathbb{Z}_2$ with $N = 1$ super symmetry and massless spinorial representations in the same $SO(10)$ group coming from the first and/or from the second plane. The number of families depends on the choice of the phase φ_L. The freedom of this phase arises from the different possible choices of the modular invariant GSO coefficients $c\left[{v_i \atop v_j}\right]$. The maximal number of the families for this model is 32. Introducing internal shifts, associated in part to φ_L, can reduce this number as we will discuss below.

We could have chosen the boundary conditions for different right-moving fermions. This would lead to spinorial representations on each plane, but the group to which they would belong would differ in each plane. As we require spinors in the same group we have discarded this option.

Choosing an overlap with more than 6 complex fermions in the right-moving sector between the vectors b_1 and b_2 leads to a $SO(14)$ gauge group and is discussed in detail in section 7.4.1.

In order to have spinors in the spectrum on *all* three planes we need to separate at least an $SO(16)$ (or $\mathbb{E}_8$) from the $\Gamma_{6,22}$ lattice . We therefore introduce the additional vector

$$z = \{\bar{\phi}^{1,\dots,8}\} \tag{6.1.19}$$

to the set. It is easy to see that this vector is consistent with the rules written down in section 4.3.1. With this vector the partition function for the gauge sector (6.1.18d) modifies to

$$Z_{18}\begin{bmatrix}\gamma\\ \delta\end{bmatrix} = \frac{1}{2}\sum_{h_z,g_z} \bar{\vartheta}\begin{bmatrix}\gamma\\ \delta\end{bmatrix}\bar{\vartheta}\begin{bmatrix}\gamma+h_z\\ \delta+g_z\end{bmatrix}^8. \tag{6.1.20}$$

We can further separate out the internal $\Gamma_{6,6}$ lattice by introducing the additional vector

$$e = \{y_{1,\dots,6}, \omega_{1,\dots,6}|\bar{y}_{1,\dots,6}, \bar{\omega}_{1,\dots,6}\}, \tag{6.1.21}$$

which modifies the $\Gamma_{6,6}$ lattice in (6.1.18b) to

$$\Gamma_{6,6}\begin{bmatrix}\gamma,h_1,h_2\\ \delta,g_1,g_2\end{bmatrix} = \frac{1}{2}\sum_{h_e,g_e} \left|\vartheta\begin{bmatrix}\gamma+h_e\\ \delta+g_e\end{bmatrix}\vartheta\begin{bmatrix}\gamma+h_e+h_2\\ \delta+g_e+g_2\end{bmatrix}\right|^2 \left|\vartheta\begin{bmatrix}\gamma+h_e\\ \delta+g_e\end{bmatrix}\vartheta\begin{bmatrix}\gamma+h_e+h_1\\ \delta+g_e+g_1\end{bmatrix}\right|^2 \left|\vartheta\begin{bmatrix}\gamma+h_e\\ \delta+g_e\end{bmatrix}\vartheta\begin{bmatrix}\gamma+h_e-h_1-h_2\\ \delta+g_e-g_1-g_2\end{bmatrix}\right|^2. \tag{6.1.22}$$

In the above $\{1, S, b_1, b_2, e, z\}$ construction the gauge group of the observable sector becomes either $SO(10)\times U(1)^3$ or $\mathbb{E}_6\times U(1)^2$ and the hidden sector necessarily is $SO(16)$ or $\mathbb{E}_8$ depending on the generalised GSO coefficients, (the choice of the phase φ_L), while the gauge group from the $\Gamma_{6,6}$ lattice becomes $G_L = SO(6)\times U(1)^3$.

So far the construction of the $N = 1$ models is generic. The only requirement we are imposing is the presence of *spinors on all three planes*. We denote this subclass of models the S^3 models. In a $N = 1$ model the spinors could be replaced by vectorial representations of the observable gauge group. This replacement gives rise to three additional classes of models which we denote by S^2V, SV^2 and V^3. The condition of spinorial representations arising from each one of the $\mathbb{Z}_2\times\mathbb{Z}_2$ orbifold planes together with the complete separation of the internal manifold is synonymous to having a well defined hidden gauge group. In subsequent sections we discuss these four classes of models. We define two subclasses of the S^2V models. When we separate one $SO(8)$ we find that

spinorial representations of a second $SO(10)$ are present in the spectrum. We also find in this subclass of models massless states on the third plane. Part of the massless states form vectorial representations of the observable $SO(10)$. Note that when we separate a second $SO(8)$ from the hidden sector we end up in the S^3 subclass of $\mathbb{Z}_2 \times \mathbb{Z}_2$ heterotic orbifold models as is discussed in [30, 29]. We refer to the class where no $SO(8)$ gauge group is separated from the hidden sector as the simple S^2V models. The models that have a $SO(8)$ gauge group separated are referred to as the extended S^2V models.

6.2 The S^3 Orbifold Models

In the class of $\mathbb{Z}_2 \times \mathbb{Z}_2$ orbifold models, the internal manifold is broken into three planes. The hidden gauge group is necessarily $\mathbb{E}_8$ or $SO(16)$ broken to any subgroup by Wilson lines (at the $N = 4$ level). In order to classify all possible S^3 models, it is necessary to consider all possible basis vectors consistent with the rules from section 4.3.1. Namely:

$$z_1 = \{\bar{\phi}^{1,\dots,4}\}, \tag{6.2.1}$$

$$z_2 = \{\bar{\phi}^{5,\dots,8}\}, \tag{6.2.2}$$

$$e_i = \{y_i, \omega_i | \bar{y}_i, \bar{\omega}_i\}, \quad i \in \{1,2,3,4,5,6\}. \tag{6.2.3}$$

The z_1, z_2 vectors allow for a breaking of hidden $\mathbb{E}_8$ or $SO(16)$ to $SO(8) \times SO(8)$ depending on the modular coefficients. As we discuss below this splitting of the hidden gauge group has important consequences in the classification of the S^3 class of models by the number of generations. The introduction of e_i vectors is necessary in order to obtain all possible internal shifts which also induces all possible modification to the number of generations.

The partition function for the $N = 1$, S^3 model based on $\{1, S, e_i, z_1, z_2,$-

$b_1, b_2\}$ is

$$
\begin{aligned}
Z_{N=1} &= \frac{1}{\tau_2|\eta|^4}\frac{1}{2}\sum_{\alpha,\beta} e^{i\pi(a+b+\mu ab)} \\
&\quad \frac{1}{4}\sum_{h_1,h_2,g_1,g_2} \frac{\vartheta\left[\begin{smallmatrix}a\\b\end{smallmatrix}\right]}{\eta}\,\frac{\vartheta\left[\begin{smallmatrix}a+h_1\\b+g_1\end{smallmatrix}\right]}{\eta}\,\frac{\vartheta\left[\begin{smallmatrix}a+h_2\\b+g_2\end{smallmatrix}\right]}{\eta}\,\frac{\vartheta\left[\begin{smallmatrix}a-h_1-h_2\\b-g_1-g_2\end{smallmatrix}\right]}{\eta} \\
&\quad \times\sum_{p_i,q_i} \frac{\Gamma_{2,2}\left[\begin{smallmatrix}h_1|p_1,p_2\\g_1|q_1,q_2\end{smallmatrix}\right]}{\eta^2\bar\eta^2}\,\frac{\Gamma_{2,2}\left[\begin{smallmatrix}h_2|p_3,p_4\\g_2|q_3,q_4\end{smallmatrix}\right]}{\eta^2\bar\eta^2}\,\frac{\Gamma_{2,2}\left[\begin{smallmatrix}-h_1-h_2|p_5,p_6\\-g_1-g_2|q_5,q_6\end{smallmatrix}\right]}{\eta^2\bar\eta^2} \\
&\quad \times\frac{1}{8}\sum_{\gamma,\gamma',\xi,\delta,\delta',\zeta} \frac{Z_\eta\left[\begin{smallmatrix}\gamma,h_1,h_2\\\delta,g_1,g_2\end{smallmatrix}\right]}{\bar\eta^7}\times\frac{Z_2\left[\begin{smallmatrix}\gamma\\\delta\end{smallmatrix}\right]}{\bar\eta} \\
&\quad \times\frac{Z_{16}\left[\begin{smallmatrix}\gamma',\xi\\\delta',\zeta\end{smallmatrix}\right]}{\bar\eta^8}\,e^{i\pi\varphi_L}, \qquad (6.2.4a)
\end{aligned}
$$

$$
Z_\eta\left[\begin{smallmatrix}\gamma,h_1,h_2\\\delta,g_1,g_2\end{smallmatrix}\right] = \bar\vartheta\left[\begin{smallmatrix}\gamma+h_2\\\delta+g_2\end{smallmatrix}\right]\bar\vartheta\left[\begin{smallmatrix}\gamma+h_1\\\delta+h_2\end{smallmatrix}\right]\,\bar\vartheta\left[\begin{smallmatrix}\gamma-h_1-h_2\\\delta-g_1-g_2\end{smallmatrix}\right]^5, \qquad (6.2.4b)
$$

$$
Z_2\left[\begin{smallmatrix}\gamma\\\delta\end{smallmatrix}\right] = \bar\vartheta\left[\begin{smallmatrix}\gamma\\\delta\end{smallmatrix}\right], \qquad (6.2.4c)
$$

$$
Z_{16}\left[\begin{smallmatrix}\gamma',\xi\\\delta',\zeta\end{smallmatrix}\right] = \bar\vartheta\left[\begin{smallmatrix}\gamma'\\\delta'\end{smallmatrix}\right]^4\bar\vartheta\left[\begin{smallmatrix}\gamma'+\xi\\\delta'+\zeta\end{smallmatrix}\right]^4. \qquad (6.2.4d)
$$

The $\Gamma_{6,6}$ lattice of $N=4$ is twisted by h_i, g_i, thus in the $N=1$ case separated into three (2,2) planes. The contribution of each of these planes in $N=1$ partition function is written in terms of twists h_i, g_i and shifts p_i, q_i on the $\Gamma_{2,2}$ lattice. The expressions of those lattices at the maximal symmetry point is [30] like equations (3.4.9) and (3.4.19)

$$
\Gamma_{2,2}\left[\begin{smallmatrix}h|p_i,p_j\\g|q_i,q_j\end{smallmatrix}\right]|_{f.p} = \frac{1}{4}\sum_{a_i,b_i,a_j,b_j} e^{i\pi\phi_1+i\pi\phi_2}\left|\vartheta\left[\begin{smallmatrix}a_i\\b_i\end{smallmatrix}\right]\vartheta\left[\begin{smallmatrix}a_i+h\\b_i+g\end{smallmatrix}\right]\vartheta\left[\begin{smallmatrix}a_j\\b_j\end{smallmatrix}\right]\vartheta\left[\begin{smallmatrix}a_j+h\\b_j+g\end{smallmatrix}\right]\right|, \qquad (6.2.5)
$$

where the phases

$$
\phi_i = a_iq_i + b_ip_i + q_ip_i, \qquad \phi_j = a_jq_j + b_jp_j + q_jp_j, \qquad (6.2.6)
$$

define the two shifts of the $\Gamma_{2,2}$ lattice. At the generic point of the moduli space the shifted $\Gamma_{2,2}$ lattice depends on the moduli (T,U), keeping however identical modular transformation properties as those of the fermionic point.

For non-zero twist, $(h,g)\neq(0,0)$, $\Gamma_{2,2}$ is independent of the moduli T,U and thus it is identical to that of (6.2.5) constructed at the fermionic point[46, 45]. Thus for non– zero twist, $(h,g)\neq(0,0)$,

$$
\Gamma_{2,2}\left[\begin{smallmatrix}h|p_i,p_j\\g|q_i,q_j\end{smallmatrix}\right]_{(T,U)}|_{(h,g)\neq(0,0)} = \Gamma_{2,2}\left[\begin{smallmatrix}h|p_i,p_j\\g|q_i,q_j\end{smallmatrix}\right]|_{f.p}. \qquad (6.2.7)
$$

For zero twist, $(h,g) = (0,0)$, the momentum and winding modes are moduli dependent and are shifted by q_i, q_j and p_i, p_j, we find from equation (3.4.18)

$$\Gamma_{2,2}\begin{bmatrix}0|p_i,p_j\\0|q_i,q_j\end{bmatrix}_{(T,U)} = \sum_{\vec{m},\vec{n}\in Z} e^{i\pi\{m_1q_i+m_2q_j\}} \exp\left\{2\pi i\bar{\tau}\left[m_1\left(n_1+\frac{p_i}{2}\right)+m_2\left(n_2+\frac{p_j}{2}\right)\right] - \frac{\pi\tau_2}{T_2U_2}\left|m_1U-m_2+T(n_1+\frac{p_i}{2})+TU(n_2+\frac{p_j}{2})\right|^2\right\}. \quad (6.2.8)$$

The phase φ_L is determined by the chirality of the super symmetry as well as by the other modular coefficients similar to equation (5.1.17)

$$\varphi_L(a,b) = \frac{1}{2}\sum_{i,j}\left(1-c\begin{bmatrix}v_i\\v_j\end{bmatrix}\right)\alpha_i\beta_j, \quad (6.2.9)$$

where α_i and β_j are the upper– and lower– arguments in ϑ–functions corresponding to the boundary conditions in the two directions of the world sheet torus and which are associated to the basis vectors v_i and v_j of the fermionic construction. The only freedom which remains in the general S^3 $N=1$ model is therefore the choice of the generalised GSO projection coefficients $c\begin{bmatrix}v_i\\v_j\end{bmatrix} = \pm 1$. The space of models is classified according to that choice which determines at the end the phase φ_L. We have in total 55 independent choices for $c\begin{bmatrix}v_i\\v_j\end{bmatrix}$ that can take the values ± 1. Thus, the total number of models in this restricted class of $N=1$ models is 2^{55}. We classify all these models according to the values of the GSO coefficients.

The NAHE model is an example of a model of the general S^3, $N=1$ deformed fermionic $N=1$ model. More precisely we can write the NAHE set basis vectors as a linear combination of basis vectors $\{1, S, e_i, z_1, z_2,$- $b_1, b_2\}$ which define the general S^3 $N=1$ model as mentioned in section 6.1.2

$$b_1^{\text{NAHE}} = S + b_1, \quad (6.2.10)$$
$$b_2^{\text{NAHE}} = S + b_2 + e_5 + e_6, \quad (6.2.11)$$
$$b_3^{\text{NAHE}} = 1 + b_1 + b_2 + e_5 + e_6 + z_1 + z_2. \quad (6.2.12)$$

We see that the NAHE set is included in these models as mentioned in section 6.1.2.

6.3 The Simple S^2V Orbifold Models

In this section we present the $N = 1$ $\mathbb{Z}_2 \times \mathbb{Z}_2$ heterotic string orbifold models that exhibit spinorial representations on the first two planes. We write down the partition functions of the simple S^2V models.

Without separating a $SO(8)$ from the $N = 1$ partition function we introduce the free shifts on the internal manifold. In the fermionic language this is accomplished by means of the vectors e_i

$$e_i = \{y^i, \omega^i | \bar{y}^i, \bar{\omega}^i\}, \quad i \in \{1, 2, 3, 4, 5, 6\}. \tag{6.3.1}$$

The partition function for this subclass of models generated using the basis set $\{1, S, b_1, b_2, e_i\}$ is

$$\begin{aligned} Z_{N=1} &= \frac{1}{\tau_2 |\eta|^4} \frac{1}{2} \sum_{a,b} e^{i\pi(a+b+\mu ab)} \\ &\quad \frac{1}{4} \sum_{h_1,h_2,g_1,g_2} \frac{\vartheta\left[\begin{smallmatrix} a \\ b \end{smallmatrix}\right]}{\eta} \frac{\vartheta\left[\begin{smallmatrix} a+h_2 \\ b+g_2 \end{smallmatrix}\right]}{\eta} \frac{\vartheta\left[\begin{smallmatrix} a+h_1 \\ b+g_1 \end{smallmatrix}\right]}{\eta} \frac{\vartheta\left[\begin{smallmatrix} a-h_1-h_2 \\ b-g_1-g_2 \end{smallmatrix}\right]}{\eta} \\ &\quad \times \sum_{p_i,q_i} \frac{\Gamma_{2,2}\left[\begin{smallmatrix} h_1 | p_1,p_2 \\ g_1 | q_1,q_2 \end{smallmatrix}\right]}{\eta^2 \bar{\eta}^2} \frac{\Gamma_{2,2}\left[\begin{smallmatrix} h_2 | p_3,p_4 \\ g_2 | q_3,q_4 \end{smallmatrix}\right]}{\eta^2 \bar{\eta}^2} \frac{\Gamma_{2,2}\left[\begin{smallmatrix} -h_1-h_2 | p_5,p_6 \\ -g_1-g_2 | q_5,q_6 \end{smallmatrix}\right]}{\eta^2 \bar{\eta}^2} \\ &\quad \times \frac{1}{2} \sum_{\gamma,\delta} \frac{Z_\eta\left[\begin{smallmatrix} \gamma, h_1, h_2 \\ \delta, g_1, g_2 \end{smallmatrix}\right]}{\bar{\eta}^7} \times \frac{Z_{18}\left[\begin{smallmatrix} \gamma \\ \delta \end{smallmatrix}\right]}{\bar{\eta}^9} \, e^{i\pi\varphi_L}, \end{aligned} \tag{6.3.2a}$$

$$Z_\eta\left[\begin{smallmatrix} \gamma, h_1, h_2 \\ \delta, g_1, g_2 \end{smallmatrix}\right] = \bar{\vartheta}[{}^{\gamma+h_2}_{\delta+g_2}] \bar{\vartheta}[{}^{\gamma+h_1}_{\delta+h_2}] \, \bar{\vartheta}[{}^{\gamma-h_1-h_2}_{\delta-g_1-g_2}]^5, \tag{6.3.2b}$$

$$Z_{18}\left[\begin{smallmatrix} \gamma \\ \delta \end{smallmatrix}\right] = \bar{\vartheta}[{}^{\gamma}_{\delta}]^9. \tag{6.3.2c}$$

The $\Gamma_{6,6}$ lattice of $N = 4$ is twisted by h_i, g_i, thus in the $N = 1$ case separated into three (2,2) planes. The contribution of each of these planes in the $N = 1$ partition function is written in terms of twists h_i, g_i and shifts p_i, q_i on the $\Gamma_{2,2}$ lattice. The expressions of those lattices at the self dual point (free fermionic point) is similar to equation (6.2.5)

$$\Gamma_{2,2}\left[\begin{smallmatrix} h | p_i,p_j \\ g | q_i,q_j \end{smallmatrix}\right] |_{f.p} = \frac{1}{4} \sum_{a_i,b_i,a_j,b_j} e^{i\pi\phi_1 + i\pi\phi_2} \left| \vartheta[{}^{a_i}_{b_i}] \vartheta[{}^{a_i+h}_{b_i+g}] \vartheta[{}^{a_j}_{b_j}] \vartheta[{}^{a_j+h}_{b_j+g}] \right|, \tag{6.3.3}$$

where the phases

$$\phi_i = a_i q_i + b_i p_i + q_i p_i, \qquad \phi_j = a_j q_j + b_j p_j + q_j p_j, \tag{6.3.4}$$

define the two shifts of the $\Gamma_{2,2}$ lattice. At the generic point of the moduli space the shifted $\Gamma_{2,2}$ lattice depends on the moduli (T, U), keeping however identical modular transformation properties as those at the fermionic point.

6.4 The Extended S^2V Orbifold Models

In this section we present the $N = 1$ $\mathbb{Z}_2 \times \mathbb{Z}_2$ heterotic string orbifold models that exhibit spinorial representations on the first two planes with a broken hidden gauge group. We write down the partition functions of the extended S^2V models.

Separating a $SO(8)$ from the hidden gauge group and introducing the free shifts on the internal manifold is realised in the fermionic language by the vectors

$$e_i = \{y^i, \omega^i | \bar{y}^i, \bar{\omega}^i\}, \quad i \in \{1,2,3,4,5,6\}, \tag{6.4.1}$$

$$z_2 = \{\bar{\phi}^{5,\ldots,8}\}. \tag{6.4.2}$$

The partition function for this subclass of models generated by the basis set $\{1, S, b_1, b_2, e_i, z_2\}$ is similar to equations (6.3.2). The difference lies in equation (6.3.2c) and reads for this subclass of models

$$Z_{18}\begin{bmatrix}\gamma,\xi\\ \delta,\zeta\end{bmatrix} = \frac{1}{2}\sum_{\xi,\zeta}\bar{\vartheta}[^{\gamma}_{\delta}]^5\bar{\vartheta}[^{\xi}_{\zeta}]^4. \tag{6.4.3}$$

We note that in this subclass of the $\mathbb{Z}_2 \times \mathbb{Z}_2$ orbifolds the hidden $SO(18)$ identified as $Z_{18} = Z_{10}Z_8$ is broken to a $SO(10) \times SO(8)$ by means of the z_2 vector. In this subclass of models we find that a priori spinorial representations of this second $SO(10)$ can appear in the massless spectrum. We will expand on this issue further in section 7.3.2.

Chapter 7

The Classification in the Fermionic Formulation

In this chapter we use the direct translation of the geometrical description of the heterotic super string in a free fermionic description to classify the four subclasses of the $\mathbb{Z}_2 \times \mathbb{Z}_2$ heterotic string models. We use the methods and techniques developed in chapter 5. We discuss each of the subclasses S^3, S^2V, SV^2 and V^3 of models in detail. We give their basis set for the free fermionic formulation. The gauge group and the observable matter spectrum is derived. This formulations allows for the classification of the chiral $\mathbb{Z}_2 \times \mathbb{Z}_2$ heterotic string models. This chapter is based on parts of [29, 30, 31].

7.1 The S^3 Free Fermionic Models

A model in the free fermionic formulation of the heterotic super string is determined by a set of basis vectors, associated with the phases picked up by the fermions when parallelly transported along non-trivial loops and a set of coefficients associated with GSO projections as described in section 4.3. The free fermions in the light-cone gauge in the traditional notation are: $\psi^\mu, \chi^i, y^i, \omega^i, i = 1, \ldots, 6$ (left movers) and $\bar{y}^i, \bar{\omega}^i, i = 1, \ldots, 6$, $\psi^A, A = 1, \ldots, 5$, $\bar{\phi}^\alpha, \alpha = 1, 8$ (right movers). The chiral $\mathbb{Z}_2 \times \mathbb{Z}_2$ fermionic models under consideration with spinorial representations on each plane are generated by a set of 12 basis vectors

$$B = \{v_1, v_2, \ldots, v_{12}\}, \tag{7.1.1}$$

where

$$\begin{aligned}
v_1 = 1 &= \{\psi^\mu,\ \chi^{1,\dots,6}, y^{1,\dots,6}, \omega^{1,\dots,6} | \bar{y}^{1,\dots,6}, \bar{\omega}^{1,\dots,6}, \bar{\eta}^{1,2,3}, \bar{\psi}^{1,\dots,5}, \bar{\phi}^{1,\dots,8}\},\\
v_2 = S &= \{\psi^\mu, \chi^{1,\dots,6}\},\\
v_{2+i} = e_i &= \{y^i, \omega^i | \bar{y}^i, \bar{\omega}^i\},\ i = 1,\dots,6,\\
v_9 = b_1 &= \{\chi^{34}, \chi^{56}, y^{34}, y^{56} | \bar{y}^{34}, \bar{y}^{56}, \bar{\eta}^1, \bar{\psi}^{1,\dots,5}\},\\
v_{10} = b_2 &= \{\chi^{12}, \chi^{56}, y^{12}, y^{56} | \bar{y}^{12}, \bar{y}^{56}, \bar{\eta}^2, \bar{\psi}^{1,\dots,5}\},\\
v_{11} = z_1 &= \{\bar{\phi}^{1,\dots,4}\},\\
v_{12} = z_2 &= \{\bar{\phi}^{5,\dots,8}\}.
\end{aligned} \tag{7.1.2}$$

The vectors $1, S$ generate a $N = 4$ super symmetric model as explained in section 5.1.2. The vectors $e_i, i = 1,\dots,6$ give rise to all possible symmetric shifts of internal fermions $(y^i, \omega^i, \bar{y}^i, \bar{\omega}^i)$ while b_1 and b_2 stand for the $\mathbb{Z}_2 \times \mathbb{Z}_2$ orbifold twists. The remaining fermions not affected by the action of the previous vectors are $\bar{\phi}^i, i = 1,\dots,8$ which normally give rise to the hidden sector gauge group. The vectors z_1, z_2 divide these eight fermions in two sets of four which in the $\mathbb{Z}_2 \times \mathbb{Z}_2$ case is the maximum consistent partition function [5, 51]. This is the most general basis, with symmetric shifts for the internal fermions, that is compatible with Kac–Moody level one $SO(10)$ embedding.

The associated projection coefficients are denoted by $c\binom{v_i}{v_j}, i, j = 1,\dots,12$ and can take the values ± 1. They are related by modular invariance $c\binom{v_i}{v_j} = \exp\{i\frac{\pi}{2} v_i \cdot v_j\} c\binom{v_j}{v_i}$ and $c\binom{v_i}{v_i} = \exp\{i\frac{\pi}{4} v_i \cdot v_i\} c\binom{v_j}{1}$ leaving 2^{66} independent coefficients. Out of them, the requirement of $N = 1$ super symmetric spectrum fixes (up to a phase convention) all $c\binom{S}{v_i}, i = 1,\dots,12$. Moreover, without loss of generality we can set $c\binom{1}{1} = -1$, and leave the rest 55 coefficients free. For more details we refer to chapter 4. Therefore, a simple counting gives 2^{55} (that is approximately $10^{16.6}$) distinct models in the class under consideration. In the following we study this class of models by deriving analytic formulas for the gauge group and the spectrum and then using these formulas for the classification.

7.1.1 The gauge group

We describe the gauge configuration of the models defined by the basis vectors $\{1, S, e_i, z_1, z_2, b_1, b_2\}$. For this purpose we start with a simplification and separate out the internal manifold using equation (6.1.21). As the twisting vectors b_1 and b_2 are used to break the $SO(16) \to SO(10) \times U(1)^3$ we will firstly describe the configuration without these vectors.

$c\binom{z_1}{z_2}$	$c\binom{e}{z_1}$	$c\binom{e}{z_2}$	Gauge group G
+	+	+	$\mathbb{E}_8 \times SO(28)$
+	-	+	$SO(24) \times SO(20)$
+	+	-	$SO(24) \times SO(20)$
+	-	-	$SO(32) \times SO(12)$
-	+	+	$SO(16) \times SO(16) \times SO(12)$
-	-	+	$SO(16) \times SO(16) \times SO(12)$
-	+	-	$SO(16) \times SO(16) \times SO(12)$
-	-	-	$\mathbb{E}_8 \times \mathbb{E}_8 \times SO(12)$

Table 7.1.1: The configuration of the gauge group of the $N = 4$ theory. We have separated a priori the internal and the hidden and observable gauge group using the vectors e and z_i. Introducing the other vectors e_i and b_i only induce breaking of these groups.

The gauge group induced by the vectors $\{1, S, e, z_1, z_2\}$ without enhancements is.

$$G = SO(16) \times SO(8)_1 \times SO(8)_2 \times SO(12), \tag{7.1.3}$$

where the internal manifold is described by $SO(12)$ and the hidden sector by $SO(8)\times SO(8)$ and the observable by $SO(16)$. By choosing the GSO coefficients the SO(16) can enhance either to $\mathbb{E}_8$ or mix with the other sectors producing either $SO(24)$ or $SO(32)$. Similarly the $SO(8) \times SO(8)$ can enhance either to $SO(16)$ or $\mathbb{E}_8$ or mix with the observable or internal manifold gauge group. This leads to enhancements of the form $SO(20)$ or $SO(24)$. The exact form depends only on the three GSO coefficients $c\binom{e}{z_1}$, $c\binom{e}{z_2}$, $c\binom{z_1}{z_2}$. We have shown the results in table 7.1.1.

Proceeding to the complete model $\{1, S, e_i, z_1, z_2, b_1, b_2\}$ we break these gauge groups to their subgroups. Imposing the shifts e_i we can break the internal gauge group down to its Cartan generators by a suitable choice of the coefficients. By a suitable choice we can break $SO(20) \rightarrow SO(8) \times U(1)^6$.

When we also include the twists we break $SO(16) \rightarrow SO(10)\times U(1)^3$ and $\mathbb{E}_8 \rightarrow \mathbb{E}_6 \times U(1)^2$. Similarly we can break $SO(24) \rightarrow SO(10) \times U(1)^3 \times SO(8)$ and $SO(32) \rightarrow SO(10) \times U(1)^3 \times SO(8) \times SO(8)$. Enhancements can subsequently occur of the form $SO(8) \times U(1) \subset SO(32) \rightarrow SO(10)$ or $SO(8) \times SO(8) \times U(1) \subset SO(32) \rightarrow SO(18)$. We find possible enhancements of the form $SO(10) \times SO(8) \subset SO(32) \rightarrow SO(18)$.

In table 7.1.1 we notice that the coefficient $c\binom{z_1}{z_2}$ distinguishes between the $SO(32)$ models and the $\mathbb{E}_8 \times \mathbb{E}_8$ models. Since we require complete

separation of the gauge group into a well defined observable and hidden gauge group, we set the coefficient $c\binom{z_1}{z_2} = -1$ in the classification.

Gauge bosons arise from the following four sectors at the $N = 1$ level.

$$G = \{0, z_1, z_2, z_1 + z_2, x\}, \tag{7.1.4}$$

where

$$x = 1 + S + \sum_{i=1}^{6} e_i + \sum_{k=1}^{2} z_k = \{\bar{\eta}^{123}, \bar{\psi}^{12345}\} \, . \tag{7.1.5}$$

The 0 sector gauge bosons give rise to the gauge group at the $N = 1$ level

$$SO(10) \times U(1)^3 \times SO(8) \times SO(8). \tag{7.1.6}$$

The x gauge bosons when present lead to enhancements of the traditionally called observable sector (the sector that includes $SO(10)$) while the $z_1 + z_2$ sector can enhance the hidden sector ($SO(8) \times SO(8)$). However, the z_1, z_2 sectors accept oscillators that can also give rise to mixed type gauge bosons and completely reorganise the gauge group. The appearance of mixed states is in general controlled by the phase $c\binom{z_1}{z_2}$. The choice $c\binom{z_1}{z_2} = +1$ allows for mixed gauge bosons and leads to the gauge groups presented in Table 7.1.2.

The choice $c\binom{z_1}{z_2} = -1$ eliminates all mixed gauge bosons and there are a few possible enhancements: $SO(10) \times U(1) \to \mathbb{E}_6$ and/or $SO(8)^2 \to \{SO(16), \mathbb{E}_8\}$. The x sector gauge bosons survive only when the GSO coefficients are such that

$$c\begin{bmatrix} x \\ z_k \end{bmatrix} = c\begin{bmatrix} x \\ e_i \end{bmatrix} = 1, \tag{7.1.7}$$

and the states in the sector x remain. We can rewrite this as

$$\sum_{j=1, i\neq j}^{6} (e_i \, | e_j \,) + \sum_{k=1}^{2} (e_i \, | z_k \,) = 0 \quad \mod 2 \, , \; i = 1, \ldots, 6, \tag{7.1.8}$$

$$\sum_{j=1}^{6} (e_j \, | z_k \,) = 0 \quad \mod 2 \, , \; k = 1, 2, \tag{7.1.9}$$

where we have introduced the notation

$$c\begin{bmatrix} v_i \\ v_j \end{bmatrix} = e^{i\pi(v_i | v_j \,)} \; , \; (v_i \, | v_j \,) = 0, 1, \tag{7.1.10}$$

and one of the constraints in (7.1.8) and (7.1.9) can be dropped because of linear independence with the rest.

$c\begin{bmatrix}z_1\\z_2\end{bmatrix}$	$c\begin{bmatrix}b_1\\z_1\end{bmatrix}$	$c\begin{bmatrix}b_2\\z_1\end{bmatrix}$	$c\begin{bmatrix}b_1\\z_2\end{bmatrix}$	$c\begin{bmatrix}b_2\\z_2\end{bmatrix}$	$c\begin{bmatrix}e_1\\z_1\end{bmatrix}$	$c\begin{bmatrix}e_2\\z_2\end{bmatrix}$	$c\begin{bmatrix}e_1\\e_2\end{bmatrix}$	Gauge group
+	+	+	+	+	+	+	+	$SO(10)\times SO(18)\times U(1)^2$
+	+	+	+	+	−	−	+	$SO(10)\times SO(9)^2\times U(1)^3$
+	+	+	+	+	−	+	+	$SO(10)^2\times SO(9)\times U(1)^2$
+	+	+	+	−	+	+	+	$SO(10)^3\times U(1)$
+	−	−	+	−	+	+	+	$SO(26)\times U(1)^3$
−	+	+	+	+	+	+	+	$E_6\times U(1)^2\times E_8$
−	−	+	−	+	+	+	+	$E_6\times U(1)^2\times SO(16)$
−	−	+	+	−	+	+	+	$E_6\times U(1)^2\times SO(8)\times SO(8)$
−	+	+	+	+	+	+	−	$SO(10)\times U(1)^3\times E_8$
−	+	+	+	+	−	−	−	$SO(10)\times U(1)^3\times SO(16)$

Table 7.1.2: Typical enhanced gauge groups and associated projection coefficients for a generic model generated by the basis (7.1.2) (coefficients not included equal to +1 except those fixed by space-time super symmetry and conventions).

As far as the $SO(8) \times SO(8)$ is concerned, we have using a similar line of thought as before, the following possibilities

$$\text{(i)} \quad (e_i \,|z_1\,) = (b_a \,|z_1\,) = 0 \;\forall\; i = 1, \ldots, 6,\; a = 1, 2, \tag{7.1.11a}$$

$$\text{(ii)} \quad (e_i \,|z_2\,) = (b_a \,|z_2\,) = 0 \;\forall\; i = 1, \ldots, 6,\; a = 1, 2, \tag{7.1.11b}$$

$$\text{(iii)} \quad (e_i \,|z_1 + z_2\,) = (b_a \,|z_1 + z_2\,) = 0 \;\forall\; i = 1, \ldots, 6,\; a = 1, 2, \tag{7.1.11c}$$

Depending on which of the above equations are true the enhancement is

$$\text{both (i) and (ii)} \Longrightarrow \mathbb{E}_8, \tag{7.1.12a}$$

$$\text{one of (i) or (ii) or (iii)} \Longrightarrow SO(16), \tag{7.1.12b}$$

$$\text{none of (i) or (ii) or (iii)} \Longrightarrow SO(8) \times SO(8). \tag{7.1.12c}$$

In the following we will restrict to the case $c\binom{z_1}{z_2} = -1$ as this is the more promising phenomenologically.

7.1.2 Observable matter spectrum

The untwisted sector matter is common to all models and consists of six vectorials of $SO(10)$ and 12 non-Abelian gauge group singlets. In models where the gauge group enhances to $\mathbb{E}_6$ extra matter comes from the x sector giving rise to six $\mathbb{E}_6$ fundamental reps **(27)**.

Chiral twisted matter arises from several sectors. In section 5.2 we saw that twisted matter comes from the sector $S + b_1$. From equation (5.2.7) we find that the states in the sector $S + b_1$ are

$$|S\rangle_{S+b_1} = |\psi_\mu^{1,2}\rangle_\pm \; |\chi^{1,2}\rangle_\pm \prod_{l=3}^{6} |\sigma_y^l\rangle_\pm \; |\bar{\eta}^1\rangle_\pm \prod_{m=1}^{5} |\bar{\psi}^m\rangle_\pm |0\rangle, \tag{7.1.13}$$

where we have used the following pairing

$$\psi_\mu^{1,2} = \frac{1}{\sqrt{2}} \left(\psi_\mu^1 + i\psi_\mu^2\right), \tag{7.1.14a}$$

$$\chi^{2k-1,2k} = \frac{1}{\sqrt{2}} \left(\chi^{2k-1} + i\chi^{2k}\right), \tag{7.1.14b}$$

$$\sigma_y^l = y^l \bar{y}^l, \tag{7.1.14c}$$

where the other fermions are already complex by construction.

The vector $S + b_1 + e_3$ is

$$S + b_1 + e_3 = \{\psi_\mu^{1,2}, \chi^{12}, \omega^3, y^4, y^{56} \mid \bar{\omega}^3, \bar{y}^4, \bar{y}^{56}, \bar{\eta}^1, \bar{\psi}^{1,\ldots,5}\}. \tag{7.1.15}$$

The states in this sector are

$$|S\rangle_{S+b_1+e_3} = |\psi_\mu^{1,2}\rangle_\pm \, |\chi^{1,2}\rangle_\pm |\sigma_\omega^3\rangle_\pm \prod_{l=4}^{6} |\sigma_y^l\rangle_\pm \, |\bar{\eta}^1\rangle_\pm \prod_{m=1}^{5} |\bar{\psi}^m\rangle_\pm |0\rangle, \quad (7.1.16)$$

where we have used the following pairing

$$\psi_\mu^{1,2} = \frac{1}{\sqrt{2}}\left(\psi_\mu^1 + i\psi_\mu^2\right), \quad (7.1.17a)$$

$$\chi^{2k-1,2k} = \frac{1}{\sqrt{2}}\left(\chi^{2k-1} + i\chi^{2k}\right), \quad (7.1.17b)$$

$$\sigma_y^l = y^l \bar{y}^l, \quad (7.1.17c)$$

$$\sigma_\omega^m = \omega^m \bar{\omega}^m, \quad (7.1.17d)$$

where the other fermions are already complex by construction. It is then clear that by adding the basis vector e_i, where $i \in \{3, \ldots, 6\}$, to the vector b_1 gives rise to new massless chiral twisted matter.

We therefore find that the chiral twisted matter arises from the following sectors

$$B_{pqrs}^{(1)} = S + b_1 + p\, e_3 + q\, e_4 + r\, e_5 + s\, e_6 + (x), \quad (7.1.18a)$$

$$B_{pqrs}^{(2)} = S + b_2 + p\, e_1 + q\, e_2 + r\, e_5 + s\, e_6 + (x), \quad (7.1.18b)$$

$$B_{pqrs}^{(3)} = S + b_3 + p\, e_1 + q\, e_2 + r\, e_3 + s\, e_4 + (x), \quad (7.1.18c)$$

where $b_3 = b_1 + b_2 + x$. These are 48 sectors (16 sectors per orbifold plane) and we choose to label them using the plane number i (upper index) and the integers $p, q, r, s = \{0, 1\}$ (lower index) corresponding to the coefficients of the appropriate shift vectors. Note that for a particular orbifold plane i only four shift vectors can be added to the twist vector b_i (the ones that have non empty intersection) the other two give rise to massive states. Each of the above sectors (7.1.18) can produce a single spinorial of $SO(10)$ (or fundamental of $\mathbb{E}_6$ in the case of enhancement). Since the $\mathbb{E}_6$ model spectrum is in one to one correspondence with the $SO(10)$ spectrum in the following we use the name spinorial meaning the **16** of $SO(10)$ and in the case of enhancement the **27** of $\mathbb{E}_6$.

One of the advantages of our formulation is that it allows to extract generic formulas regarding the number and the chirality of each spinorial. This is important because it allows an algebraic treatment of the entire class of models without deriving each model explicitly.

We now concentrate on one sector. We take for convenience the sector $S+b_1$ thereby setting $p, q, r, s = 0$ in equation (7.1.18a). The $S+b_1$ sector

is described in equation (7.1.13). The projection induced by $\mathbb{1}$ sets the overall sign to be equal to $+1$ as explained in equation (5.2.9). The GSO constraints of the e_i vectors are

$$GSO_{e_i} \equiv \delta_{S+b_1} c\begin{bmatrix} S+b_1 \\ e_i \end{bmatrix} = -c\begin{bmatrix} S+b_1 \\ e_i \end{bmatrix} = -c\begin{bmatrix} e_i \\ S+b_1 \end{bmatrix}. \tag{7.1.19}$$

If we set the coefficients for the e_1 or e_2 to -1 we project out the sector $S+b_1$. We have therefore obtained a constraint for the sector to survive. The number of families from this sector depends on the projector

$$P^{(1)}_{0000} \propto \frac{1-c\left[\begin{smallmatrix} e_1 \\ S+b_1 \end{smallmatrix}\right]}{2}\frac{1-c\left[\begin{smallmatrix} e_2 \\ S+b_1 \end{smallmatrix}\right]}{2}. \tag{7.1.20}$$

Imposing the b_1 projection reveals no results of interest for the number of generations. The GSO projection induced by the b_1 vector is

$$GSO_{b_1} = -c\begin{bmatrix} S+b_1 \\ b_1 \end{bmatrix} = -c\begin{bmatrix} b_1 \\ S+b_1 \end{bmatrix} = -1. \tag{7.1.21}$$

This result induces a constraint not relevant for this calculation. The GSO projection induced by the b_2 vector is

$$GSO_{b_2} = -c\begin{bmatrix} S+b_1 \\ b_2 \end{bmatrix} = -c\begin{bmatrix} b_2 \\ S+b_1 \end{bmatrix}. \tag{7.1.22}$$

This induces a constraint on the chirality of the $\bar{\psi}^{1,\ldots,5}$

$$\mathrm{Ch}(\chi^{12})\mathrm{Ch}(y^5\bar{y}^5)\mathrm{Ch}(y^6\bar{y}^6)\mathrm{Ch}(\bar{\psi}^{1,\ldots,5}) = -c\begin{bmatrix} b_2 \\ S+b_1 \end{bmatrix}. \tag{7.1.23}$$

The chirality of the internal fermions is set by the coefficients $c\left[\begin{smallmatrix} e_i \\ S+b_1 \end{smallmatrix}\right]$. We only consider the states where the spacetime spinor is in the *up* state by convention. Due to the GSO projection of the S vector we can solve the chirality of the $\chi^{1,2}$ state. The chirality of the $\bar{\psi}^{1,\ldots,5}$ is

$$\mathrm{Ch}(\bar{\psi}^{1,\ldots,5}) = c\begin{bmatrix} b_2+e_5+e_6 \\ S+b_1 \end{bmatrix}. \tag{7.1.24}$$

The GSO projection of the last vector z completes the projector $P^{(1)}_{0000}$

$$P^{(1)}_{0000} \propto \frac{1-c\left[\begin{smallmatrix} z_1 \\ S+b_1 \end{smallmatrix}\right]}{2}\frac{1-c\left[\begin{smallmatrix} z_2 \\ S+b_1 \end{smallmatrix}\right]}{2}. \tag{7.1.25}$$

The chirality of the $\bar{\psi}^{1,\ldots,5}$ contributes to the total number of generations per plane. In the $S+b_1$ sector the number of generations therefore is

$$\begin{aligned}\mathrm{Ch}(\bar{\psi}^{1,\ldots,5}) = c\begin{bmatrix} b_2+e_5+e_6 \\ S+b_2 \end{bmatrix} &\times \frac{1-c\left[\begin{smallmatrix} e_1 \\ S+b_1 \end{smallmatrix}\right]}{2}\frac{1-c\left[\begin{smallmatrix} e_2 \\ S+b_1 \end{smallmatrix}\right]}{2} \\ &\times \frac{1-c\left[\begin{smallmatrix} z_1 \\ S+b_1 \end{smallmatrix}\right]}{2}\frac{1-c\left[\begin{smallmatrix} z_2 \\ S+b_1 \end{smallmatrix}\right]}{2} \equiv X^{(1)}_{0000}P^{(1)}_{0000},\end{aligned} \tag{7.1.26}$$

where we have identified a chirality operator $X^{(1)}_{pqrs}$ and a projector operator $P^{(1)}_{pqrs}$. Similarly we can derive these formulae for the other planes and sectors as well.

The number of surviving spinorials per sector (7.1.18) is given by

$$P^{(1)}_{pqrs} = \frac{1}{16}\prod_{i=1,2}\left(1-c\begin{bmatrix} e_i \\ B^{(1)}_{pqrs}\end{bmatrix}\right)\prod_{m=1,2}\left(1-c\begin{bmatrix} z_m \\ B^{(1)}_{pqrs}\end{bmatrix}\right) \quad (7.1.27a)$$

$$P^{(2)}_{pqrs} = \frac{1}{16}\prod_{i=3,4}\left(1-c\begin{bmatrix} e_i \\ B^{(2)}_{pqrs}\end{bmatrix}\right)\prod_{m=1,2}\left(1-c\begin{bmatrix} z_m \\ B^{(2)}_{pqrs}\end{bmatrix}\right) \quad (7.1.27b)$$

$$P^{(3)}_{pqrs} = \frac{1}{16}\prod_{i=5,6}\left(1-c\begin{bmatrix} e_i \\ B^{(3)}_{pqrs}\end{bmatrix}\right)\prod_{m=1,2}\left(1-c\begin{bmatrix} z_m \\ B^{(3)}_{pqrs}\end{bmatrix}\right) \quad (7.1.27c)$$

where P^i_{pqrs} is a projector that takes values $\{0,1\}$. The chirality of the surviving spinorials is given by

$$X^{(1)}_{pqrs} = c\begin{bmatrix} b_2+(1-r)e_5+(1-s)e_6 \\ B^{(1)}_{pqrs}\end{bmatrix}, \quad (7.1.28a)$$

$$X^{(2)}_{pqrs} = c\begin{bmatrix} b_1+(1-r)e_5+(1-s)e_6 \\ B^{(2)}_{pqrs}\end{bmatrix}, \quad (7.1.28b)$$

$$X^{(3)}_{pqrs} = c\begin{bmatrix} b_1+(1-r)e_3+(1-s)e_4 \\ B^{(3)}_{pqrs}\end{bmatrix}, \quad (7.1.28c)$$

where $X^i_{pqrs}=+$ corresponds to a **16** of $SO(10)$(or **27** in the case of $\mathbb{E}_6$) and $X^i_{pqrs}=-$ corresponds to a $\overline{\mathbf{16}}$ (or $\overline{\mathbf{27}}$) and we have chosen the space-time chirality $C(\psi^\mu)=+1$. The net number of spinorials and thus the net number of families is given by

$$N_F = \sum_{i=1}^{3}\sum_{p,q,r,s=0}^{1} X^{(i)}_{pqrs}P^{(i)}_{pqrs}. \quad (7.1.29)$$

Similar formulas can be easily derived for the number of vectorials and the number of singlets and can be extended to the $U(1)$ charges but in this work we restrict to the spinorial calculation.

Formulas (7.1.27) allow us to identify the mechanism of spinorial reduction, or in other words the fixed point reduction, in the fermionic language. For a particular sector ($B^{(i)}_{pqrs}$) of the orbifold plane i there exist two shift vectors (e_{2i-1}, e_{2i}) and the two z vectors (z_1, z_2) that have no common elements with $B^{(i)}_{pqrs}$. Setting the relative projection coefficients (7.1.27) to -1 each of the above four vectors acts as a projector that cuts

the number of fixed points in the associated sector by a factor of two. Since four such projectors are available for each sector the number of fixed points can be reduced from 16 to 1 per plane.

The projector action (7.1.27) can be expanded and written in a simpler form

$$\Delta^{(i)} W^{(i)} = Y^{(i)}, \tag{7.1.30}$$

where

$$\begin{aligned}
\Delta^{(1)} &= \begin{bmatrix} (e_1\,|e_3\,) & (e_1\,|e_4\,) & (e_1\,|e_5\,) & (e_1\,|e_6\,) \\ (e_2\,|e_3\,) & (e_2\,|e_4\,) & (e_2\,|e_5\,) & (e_2\,|e_6\,) \\ (z_1\,|e_3\,) & (z_1\,|e_4\,) & (z_1\,|e_5\,) & (z_1\,|e_6\,) \\ (z_2\,|e_3\,) & (z_2\,|e_4\,) & (z_2\,|e_5\,) & (z_2\,|e_6\,) \end{bmatrix}, \\
\Delta^{(2)} &= \begin{bmatrix} (e_3\,|e_1\,) & (e_3\,|e_2\,) & (e_3\,|e_5\,) & (e_3\,|e_6\,) \\ (e_4\,|e_1\,) & (e_4\,|e_2\,) & (e_4\,|e_5\,) & (e_4\,|e_6\,) \\ (z_1\,|e_1\,) & (z_1\,|e_2\,) & (z_1\,|e_5\,) & (z_1\,|e_6\,) \\ (z_2\,|e_1\,) & (z_2\,|e_2\,) & (z_2\,|e_5\,) & (z_2\,|e_6\,) \end{bmatrix}, \\
\Delta^{(3)} &= \begin{bmatrix} (e_5\,|e_1\,) & (e_5\,|e_2\,) & (e_5\,|e_3\,) & (e_5\,|e_4\,) \\ (e_6\,|e_1\,) & (e_6\,|e_2\,) & (e_6\,|e_3\,) & (e_6\,|e_4\,) \\ (z_1\,|e_1\,) & (z_1\,|e_2\,) & (z_1\,|e_3\,) & (z_1\,|e_4\,) \\ (z_2\,|e_1\,) & (z_2\,|e_2\,) & (z_2\,|e_3\,) & (z_2\,|e_4\,) \end{bmatrix},
\end{aligned} \tag{7.1.31a}$$

and

$$Y^{(1)} = \begin{bmatrix} (e_1\,|b_1\,) \\ (e_2\,|b_1\,) \\ (z_1\,|b_1\,) \\ (z_2\,|b_1\,) \end{bmatrix}, \quad Y^{(2)} = \begin{bmatrix} (e_3\,|b_2\,) \\ (e_4\,|b_2\,) \\ (z_1\,|b_2\,) \\ (z_2\,|b_2\,) \end{bmatrix}, \quad Y^{(3)} = \begin{bmatrix} (e_5\,|b_3\,) \\ (e_6\,|b_3\,) \\ (z_1\,|b_3\,) \\ (z_2\,|b_3\,) \end{bmatrix}, \tag{7.1.31b}$$

and

$$W^i = \begin{bmatrix} p_i \\ q_i \\ r_i \\ s_i \end{bmatrix}, \tag{7.1.31c}$$

where

$$c\begin{bmatrix} \alpha \\ \beta \end{bmatrix} = e^{i\pi(\alpha|\beta\,)}. \tag{7.1.32}$$

Note that we have fixed $(\alpha\,|1\,) = 1 = (\alpha\,|S\,)$. They form three systems of equations of the form $\Delta^i\, W^i = Y^i$ (one for each orbifold plane). Each system contains 4 unknowns p_i, q_i, r_i, s_i which correspond to the labels of surviving spinorials in the plane i. We call the set of solutions of each system Ξ_i. The net number of families (7.1.29) can be written as

$$N_F = \sum_{i=1}^{3} \sum_{p,q,r,s \in \Xi_i} X^{(i)}_{pqrs}. \tag{7.1.33}$$

The chiralities (7.1.28) can be further expanded in the exponential form defined in equation (7.1.32)

$$\begin{aligned}\chi^{(1)}_{pqrs} &= 1 + (b_1\,|b_2\,) + (1-r)\,(e_5\,|b_1\,) + (1-s)\,(e_6\,|b_1\,) + p\,(e_3\,|b_2\,)\\ &\quad +q\,(e_4\,|b_2\,) + r\,(e_5\,|b_2\,) + s\,(e_6\,|b_2\,) + p(1-r)\,(e_3\,|e_5\,)\\ &\quad +p(1-s)\,(e_3\,|e_6\,) + q(1-r)\,(e_4\,|e_5\,) + q(1-s)\,(e_4\,|e_6\,)\\ &\quad +(r+s)\,(e_5\,|e_6\,) \mod 2, \end{aligned} \tag{7.1.34a}$$

$$\begin{aligned}\chi^{(2)}_{pqrs} &= 1 + (b_1\,|b_2\,) + (1-r)\,(e_5\,|b_2\,) + (1-s)\,(e_6\,|b_2\,) + p\,(e_1\,|b_1\,)\\ &\quad +q\,(e_2\,|b_1\,) + r\,(e_5\,|b_1\,) + s\,(e_6\,|b_1\,) + p(1-r)\,(e_1\,|e_5\,)\\ &\quad +q(1-r)\,(e_2\,|e_5\,) + p(1-s)\,(e_1\,|e_6\,) + q(1-s)\,(e_2\,|e_6\,)\\ &\quad +(r+s)\,(e_5\,|e_6\,) \mod 2, \end{aligned} \tag{7.1.34b}$$

$$\begin{aligned}\chi^{(3)}_{pqrs} &= 1 + (b_1\,|b_2\,) + (1-p)\,(e_1\,|b_1\,) + (1-q)\,(e_2\,|b_1\,) + (e_5+e_6\,|b_1\,)\\ &\quad +(1-r)\,(e_3\,|b_2\,) + (1-s)\,(e_4\,|b_2\,)\\ &\quad +(1-r)(1-p)\,(e_3\,|e_1\,) + (1-r)(1-q)\,(e_3\,|e_2\,)\\ &\quad +(1-r)\,(e_3\,|e_5\,) + (1-r)\,(e_3\,|e_6\,) + (1-s)\,(e_4\,|e_6\,)\\ &\quad +(1-r)\,(e_3\,|z_1+z_2\,) + (1-s)\,(e_4\,|z_1+z_2\,)\\ &\quad +(b_1\,|z_1+z_2\,) \mod 2. \end{aligned} \tag{7.1.34c}$$

We remark here that the projection coefficient $c\begin{bmatrix} b_1 \\ b_2 \end{bmatrix}$ simply fixes the overall chirality and that our equations depend only on

$$(e_i\,|e_j\,),\ (e_i\,|b_k\,), (e_i\,|z_n\,),\ (z_n\,|b_k\,), i=1,\ldots,6, k=1,2, n=1,2 \tag{7.1.35}$$

However, the following six parameters do not appear in the expressions $(e_1\,|e_2\,)$, $(e_3\,|e_4\,)$, $(e_3\,|b_1\,)$, $(e_4\,|b_1\,)$, $(e_1\,|b_2\,)$, $(e_2\,|b_2\,)$ and thus in a generic model the chiral content depends on 37 discrete parameters.

7.2 The Simple S^2V Free Fermionic Models

The subclass of models under consideration is generated by a set of 10 basis vectors.

$$V_1 = \{v_1, \ldots, v_{10}\}, \tag{7.2.1}$$

where

$$\begin{aligned} v_1 = 1 &= \{\psi^\mu,\ \chi^{1,\ldots,6}, y^{1,\ldots,6}, \omega^{1,\ldots,6} | \bar{y}^{1,\ldots,6}, \bar{\omega}^{1,\ldots,6}, \bar{\eta}^{1,2,3}, \bar{\psi}^{1,\ldots,5}, \bar{\phi}^{1,\ldots,8}\},\\ v_2 = S &= \{\psi^\mu, \chi^{1,\ldots,6}\},\\ v_{2+i} = e_i &= \{y^i, \omega^i | \bar{y}^i, \bar{\omega}^i\},\ i=1,\ldots,6,\\ v_9 = b_1 &= \{\chi^{34}, \chi^{56}, y^{34}, y^{56} | \bar{y}^{34}, \bar{y}^{56}, \bar{\eta}^1, \bar{\psi}^{1,\ldots,5}\},\\ v_{10} = b_2 &= \{\chi^{12}, \chi^{56}, y^{12}, y^{56} | \bar{y}^{12}, \bar{y}^{56}, \bar{\eta}^2, \bar{\psi}^{1,\ldots,5}\}. \end{aligned} \tag{7.2.2}$$

The vectors $1, S$ generate a $N = 4$ super symmetric model. The vectors e_i, $i = 1, \ldots, 6$ give rise to all possible symmetric shifts of internal fermions $(y^i, \omega^i, \bar{y}^i, \bar{\omega}^i)$ while b_1 and b_2 stand for the $\mathbb{Z}_2 \times \mathbb{Z}_2$ orbifold twists. This is the most general basis, with symmetric shifts for the internal fermions, that is compatible with Kac–Moody level one $SO(10)$ gauge group. The associated projection coefficients are denoted by $c\binom{v_i}{v_j}, i, j = 1, \ldots, 10$ and can take the values ± 1. They are related by modular invariance $c\binom{v_i}{v_j} = \exp\{i\frac{\pi}{2} v_i \cdot v_j\} c\binom{v_j}{v_i}$ and $c\binom{v_i}{v_i} = \exp\{i\frac{\pi}{4} v_i \cdot v_i\} c\binom{v_j}{1}$ leaving 2^{45} independent coefficients. Out of them, the requirement of $N = 1$ super symmetric spectrum fixes (up to a phase convention) all $c\binom{S}{v_i}, i = 1, \ldots, 10$. Moreover, without loss of generality we can set $c\binom{1}{1} = -1$, and leave the remaining 36 coefficients free. Therefore, a simple counting gives 2^{36} (that is approximately $10^{10.8}$) distinct models in the subclass under consideration.

7.2.1 The gauge group

The gauge group in this subclass of models at the $N = 4$ level is not enhanced. The group induced by the vectors $\{1, S, e\}$, where e is defined as in equation (6.1.21) is

$$G = SO(12) \times SO(32). \tag{7.2.3}$$

We find that no other sector induces gauge bosons and the gauge group cannot be enhanced. The internal gauge group $SO(12)$ can be broken to its Cartan generators by means of a suitable choice of the GSO coefficients induced by the e_i i.e. the vectors e_i can break $SO(12) \to U(1)^6$. The $SO(32)$ is broken to $SO(10) \times U(1)^2 \times SO(18)$ by means of the vectors b_i at the $N = 1$ level. We do not get find enhancements in this subclass at the $N = 1$ level.

7.2.2 Observable matter spectrum

The untwisted sector is common to all models in this subclass. The differences between the models become apparent in the twisted sector. Therefore, we focus on the twisted sector.

The sectors that give rise to massless chiral matter are

$$B^{(1)}_{pqrs} = S + b_1 + p\, e_3 + q\, e_4 + r\, e_5 + s\, e_6, \tag{7.2.4a}$$

$$B^{(2)}_{pqrs} = S + b_2 + p\, e_1 + q\, e_2 + r\, e_5 + s\, e_6. \tag{7.2.4b}$$

These give 16 different sectors on each of the first two orbifold planes. The upper index i represents the plane and the lower index $p,q,r,s = \{0,1\}$ represents the sector on the plane i.

Due to the GSO projections we can derive the projectors for the different sectors as a function of the GSO coefficients. They are

$$P^{(1)}_{pqrs} = \frac{1}{4}\prod_{i=1,2}\left(1-c\begin{bmatrix} e_i \\ B^{(1)}_{pqrs}\end{bmatrix}\right), \tag{7.2.5a}$$

$$P^{(2)}_{pqrs} = \frac{1}{4}\prod_{i=3,4}\left(1-c\begin{bmatrix} e_i \\ B^{(1)}_{pqrs}\end{bmatrix}\right), \tag{7.2.5b}$$

where $P^{(i)}_{pqrs}$ is a projector that takes values $\{0,1\}$. The chirality of the surviving spinorials is given by

$$X^{(1)}_{pqrs} = c\begin{bmatrix} b_2+(1-r)e_5+(1-s)e_6 \\ B^{(1)}_{pqrs}\end{bmatrix}, \tag{7.2.6a}$$

$$X^{(2)}_{pqrs} = c\begin{bmatrix} b_1+(1-r)e_3+(1-s)e_4 \\ B^{(2)}_{pqrs}\end{bmatrix}, \tag{7.2.6b}$$

where $X^i_{pqrs} = +$ corresponds to a **16** of $SO(10)$ and $X^i_{pqrs} = -$ corresponds to a $\overline{\mathbf{16}}$ and we have chosen the space-time chirality $C(\psi^\mu) = +1$. The net number of spinorials and thus the net number of families is given by

$$N_F = \sum_{i=1}^{2}\sum_{p,q,r,s=0}^{1} X^{(i)}_{pqrs}P^{(i)}_{pqrs}. \tag{7.2.7}$$

Similar formulas can be easily derived for the number of vectorials and the number of singlets and can be extended to the $U(1)$ charges but in this work we restrict to the spinorial calculation.

Formulas (7.2.5) allow us to identify the mechanism of spinorial reduction, or in other words the fixed point reduction, in the fermionic language. For a particular sector ($B^{(i)}_{pqrs}$) of the orbifold plane i there exist two shift vectors (e_{2i-1}, e_{2i}). Setting the relative projection coefficients (7.2.5) to -1 each of the above two vectors acts as a projector that cuts the number of fixed points in the associated sector by a factor of two. Since two such projectors are available for each sector the number of fixed points can be reduced from 16 to 4 per plane.

Note that contrary to section 7.1, it is of no use to put these formulas in a simpler form using the matrix formulation developed therein. The

reason being that in these cases we have two projectors for the simple $SO(8)$ models, while we still have 2^4 different sectors on each plane. We are therefore always left with two free coefficients. This is the exact origin of the fact that in these models we cannot reduce the number of generations down to one per plane.

We remark here that the projection coefficient $c\binom{b_1}{b_2}$ simply fixes the overall chirality and that our equations depend only on

$$(e_i\,|e_j\,)\,,\ (e_i\,|b_A\,)\,. \tag{7.2.8}$$

7.3 The Extended S^2V Free Fermionic Models

The S^2V $SO(8)$ subclass of models is generated by a set of 11 basis vectors.

$$V_1 = \{v_1, \ldots, v_{11}\}, \tag{7.3.1}$$

where

$$\begin{aligned}
v_1 = 1 &= \{\psi^\mu,\ \chi^{1,\ldots,6}, y^{1,\ldots,6}, \omega^{1,\ldots,6} | \bar{y}^{1,\ldots,6}, \bar{\omega}^{1,\ldots,6}, \bar{\eta}^{1,2,3}, \bar{\psi}^{1,\ldots,5}, \bar{\phi}^{1,\ldots,8}\},\\
v_2 = S &= \{\psi^\mu, \chi^{1,\ldots,6}\},\\
v_{2+i} = e_i &= \{y^i, \omega^i | \bar{y}^i, \bar{\omega}^i\},\ i = 1, \ldots, 6,\\
v_9 = b_1 &= \{\chi^{34}, \chi^{56}, y^{34}, y^{56} | \bar{y}^{34}, \bar{y}^{56}, \bar{\eta}^1, \bar{\psi}^{1,\ldots,5}\},\\
v_{10} = b_2 &= \{\chi^{12}, \chi^{56}, y^{12}, y^{56} | \bar{y}^{12}, \bar{y}^{56}, \bar{\eta}^2, \bar{\psi}^{1,\ldots,5}\},\\
v_{11} = z_2 &= \{\bar{\phi}^{5,\ldots,8}\}.
\end{aligned} \tag{7.3.2}$$

The remaining fermions not affected by the action of the previous vectors are $\bar{\eta}^3, \bar{\phi}^i, i = 1, \ldots, 8$ which normally give rise to the hidden sector gauge group. The vector z_2 divide these nine fermions in two sets, one giving rise to the additional $SO(10)$ and the other giving rise to a hidden $SO(8)$.

The associated projection coefficients are denoted by $c\binom{v_i}{v_j}, i, j = 1, \ldots, 11$ and can take the values ± 1. Due to modular invariance they give rise to 2^{55} independent coefficients. Out of them, the requirement of $N = 1$ super symmetric spectrum fixes (up to a phase convention) all $c\binom{S}{v_i}, i = 1, \ldots, 11$. Moreover, without loss of generality we can set $c\binom{1}{1} = -1$, and leave the remaining 45 coefficients free. Therefore, a simple counting gives 2^{45} (that is approximately $10^{13.5}$) distinct models in the class under consideration.

$c\binom{e}{z_2}$	Group G
-1	$SO(20) \times SO(24)$
1	$SO(12) \times SO(32)$

Table 7.3.1: The configuration of the gauge group of the $N = 4$ theory. We have separated a priori the internal gauge group using the vectors e and z_2. Introducing the other vectors e_i and b_i only induce breaking of these groups.

In the following we study this class of models by deriving analytic formulas for the gauge group and the spectrum and then using these formulas for the classification. It is easy to see that the third twisted plane has massless states since $b_3 = b_1 + b_2$ gives rise to vectorial representations of the observable $SO(10)$.

7.3.1 The gauge group

The gauge group in this subclass of models at the $N = 4$ level, induced by the vectors $\{1, S, e, z_2\}$ without enhancements is

$$G = SO(12) \times SO(24) \times SO(8). \tag{7.3.3}$$

Enhancements can occur due to the z_2 sector. Both the SO(12) and the SO(24) can be enhanced by a suitable choice of the GSO coefficient $c\binom{e}{z_2}$. The enhancements are listed in table 7.3.1

The internal gauge group $SO(12)$ can be reduced to its Cartan generators $U(1)^6$. The $SO(24)$ is broken to $SO(10)^2 \times U(1)^2$. We therefore find the gauge group at the $N = 1$ level

$$SO(10) \times U(1)^2 \times SO(10) \times SO(8). \tag{7.3.4}$$

In this subclass we always get enhancement. We have argued that the hidden sector gets enhanced when $c\binom{e}{z_2} = 1$. This is the configuration where the internal sector is completely separated from the gauge sector. At the $N = 1$ level we can get enhancement of $SO(8) \times U(1) \to SO(10)$. We discuss this case in more detail below. In a similar fashion we can get enhancement of $SO(8) \times SO(10) \to SO(18)$. Matter states under this enhanced gauge group are not realised. The enhancement in the adjoint representation is only found when $-c\binom{b_1}{z_2} = -c\binom{b_1}{z_2} = c\binom{e_3}{z_2} = c\binom{e_4}{z_2} = 1$. This enhancement is only realised at the $N = 1$ level as is explained in section 9.1.

7.3.2 Observable matter spectrum

The untwisted sector is common to all models in this subclass. The differences between the models become apparent in the twisted sector. Therefore, we focus on the twisted sector.

The sectors that give rise to massless chiral states are split up into two types. The first type gives spinorial representations of the first $SO(10)$ and the second type gives spinorial representations of the second $SO(10)$. Due to the sector z_2 we can get enhancement of the $SO(8) \times U(1) \to SO(10)$. This sector can give rise to spinorial representations as well and we label this as the type 3 spinorials. The sectors that give chiral matter of the first type are

$$B^{(1)}_{pqrs} = S + b_1 + p\,e_3 + q\,e_4 + r\,e_5 + s\,e_6, \tag{7.3.5a}$$
$$B^{(2)}_{pqrs} = S + b_2 + p\,e_1 + q\,e_2 + r\,e_5 + s\,e_6, \tag{7.3.5b}$$

and the sectors giving chiral matter of the second type are

$$\bar{B}^{(1)}_{pqrs} = S + b_1 + x + p\,e_3 + q\,e_4 + r\,e_5 + s\,e_6, \tag{7.3.6a}$$
$$\bar{B}^{(2)}_{pqrs} = S + b_2 + x + p\,e_1 + q\,e_2 + r\,e_5 + s\,e_6, \tag{7.3.6b}$$

where

$$x = 1 + S + \sum_{i=1}^{6} e_i + z_2. \tag{7.3.7}$$

These give 16 different sectors on the first two orbifold planes for each type. The upper index i represents the plane and the lower index p, q,-$r, s = \{0, 1\}$ represents the sector on the plane i. The sectors giving rise to chiral states of the second type are represented by $\bar{B}$.

The spinorial $SO(8) \times U(1) \to SO(10)$ enhancement can occur in this subclass of models due to the sectors

$$B^{(3)}_{pqrs} = S + b_1 + b_2 + z_2 + p\,e_1 + q\,e_2 + r\,e_3 + s\,e_4 \tag{7.3.8}$$

and the sector

$$V^{(3)}_{pqrs} = S + b_1 + b_2 + p\,e_1 + q\,e_2 + r\,e_3 + s\,e_4. \tag{7.3.9}$$

Vectorials of the $SO(8)$ are only realised when $c\binom{b_3}{z_2} = -1$. The sector $V^{(3)}_{pqrs}$ then gives rise to the 8_v and the sector $B^{(3)}_{pqrs}$ gives 8_s to complete the 16 or $\overline{16}$, depending on the GSO coefficients. In order to find the chirality of the spinorial representation of $SO(10)$ we look at which

$U(1) \subset SO(10)\times U(1)^2\times SO(10)\times SO(8)$ is used. We therefore focus on the vectorial bilinear realisation of the enhancement. This enhancement is realised by the NS sector and the z_2 sector giving $45 = 28 + 1 + 8^+ + 8^-$. When $-c\binom{b_1}{z_2} = c\binom{b_2}{z_2} = c\binom{e_5}{z_2} = c\binom{e_6}{z_2} = 1$ the state

$$\psi^\mu_{1,2}\ \bar{\eta}^1\ \left[\bar{\phi}^{5,\ldots,8}\right]\ |0> \tag{7.3.10}$$

survives and the enhancement is realised with the $U(1)$ induced by $\bar{\eta}^1$. When $c\binom{b_1}{z_2} = -c\binom{b_2}{z_2} = c\binom{e_1}{z_2} = c\binom{e_2}{z_2} = 1$ the state

$$\psi^\mu_{1,2}\ \bar{\eta}^2\ \left[\bar{\phi}^{5,\ldots,8}\right]\ |0> \tag{7.3.11}$$

survives and the enhancement is realised with the $U(1)$ induced by $\bar{\eta}^2$. Depending now on the charge of state under the correct $U(1)$ we get either a 16 or $\overline{16}$ of the $SO(10)$ by $16 = 8_s(1) + 8_v(-1)$ or $\overline{16} = 8_s(-1) + 8_v(1)$. We have therefore listed the sign of the $U(1)$ charge of the correct state to describe the chirality of the type three $SO(10)$. Note that this $SO(10)$ is realised on the third plane.

Since the enhancement is only present when $c\binom{b_3}{z_2} = -1$, we can conclude that the enhancement only takes place at the $N = 1$ level of the model. Models that are liftable to an $N = 4$ theory therefore do not exhibit this type of enhancement. For completeness we do give our results for the spinorial representations of the third $SO(10)$, that is found on the third plane. When enhancement does not occur we do find spinorial representations of a $SO(8)$ gauge group. The chirality of these spinors is determined by $c\binom{z_2}{B^{(3)}_{pqrs}}$. Again only two projectors can be realised leading to a reduction of the number of generations under the $SO(8)$ of $16 \to 4$. Since we focus in this classification on the generations of an observable $SO(10)$ we do not consider these states here.

Due to the GSO projections we can derive the projectors for the different sectors as a function of the GSO coefficients. They are for the first type

$$P^{(1)}_{pqrs} = \frac{1}{8}\prod_{i=1,2}\left(1 - c\binom{e_i}{B^{(1)}_{pqrs}}\right)\left(1 - c\binom{z_2}{B^{(1)}_{pqrs}}\right), \tag{7.3.12a}$$

$$P^{(2)}_{pqrs} = \frac{1}{8}\prod_{i=3,4}\left(1 - c\binom{e_i}{B^{(1)}_{pqrs}}\right)\left(1 - c\binom{z_2}{B^{(2)}_{pqrs}}\right), \tag{7.3.12b}$$

and for the second type

$$\bar{P}^{(1)}_{pqrs} = \frac{1}{8}\prod_{i=1,2}\left(1 - c\binom{e_i}{\bar{B}^{(1)}_{pqrs}}\right)\left(1 - c\binom{z_2}{\bar{B}^{(1)}_{pqrs}}\right), \tag{7.3.13a}$$

$$\bar{P}^{(2)}_{pqrs} = \frac{1}{8}\prod_{i=3,4}\left(1 - c\binom{e_i}{\bar{B}^{(2)}_{pqrs}}\right)\left(1 - c\binom{z_2}{\bar{B}^{(2)}_{pqrs}}\right), \tag{7.3.13b}$$

and for the third type

$$P^{(3)}_{pqrs} = \frac{1}{4}\prod_{i=5,6}\left(1 - c\begin{bmatrix} e_i \\ B^{(3)}_{pqrs}\end{bmatrix}\right). \tag{7.3.14}$$

Again we have represented the projectors for the second type as $\bar{P}$. $P^{(i)}_{pqrs}$, or $\bar{P}^{(i)}_{pqrs}$ for the second type chiral states, is a projector that takes values $\{0,1\}$. The chirality of the surviving spinorials of the first type is given by

$$X^{(1)}_{pqrs} = c\begin{bmatrix} b_2 + (1-r)e_5 + (1-s)e_6 \\ B^{(1)}_{pqrs}\end{bmatrix}, \tag{7.3.15a}$$

$$X^{(2)}_{pqrs} = c\begin{bmatrix} b_1 + (1-r)e_3 + (1-s)e_4 \\ B^{(2)}_{pqrs}\end{bmatrix}, \tag{7.3.15b}$$

while for the second type they are

$$\bar{X}^{(1)}_{pqrs} = c\begin{bmatrix} b_2 + e_3 + e_4 + r\ e_5 + s\ e_6 \\ \bar{B}^{(1)}_{pqrs}\end{bmatrix}, \tag{7.3.16a}$$

$$\bar{X}^{(2)}_{pqrs} = c\begin{bmatrix} b_1 + e_1 + e_2 + r\ e_5 + s\ e_6 \\ \bar{B}^{(2)}_{pqrs}\end{bmatrix}, \tag{7.3.16b}$$

and for the third type they are when $-c\left[\begin{smallmatrix} b_1 \\ z_2\end{smallmatrix}\right] = c\left[\begin{smallmatrix} b_2 \\ z_2\end{smallmatrix}\right] = 1$

$$X^{(3)}_{pqrs} = c\begin{bmatrix} (1-r)e_3 + (1-s)e_4 + b_1 \\ B^{(3)}_{pqrs}\end{bmatrix}, \tag{7.3.17a}$$

and when $c\left[\begin{smallmatrix} b_1 \\ z_2\end{smallmatrix}\right] = -c\left[\begin{smallmatrix} b_2 \\ z_2\end{smallmatrix}\right] = 1$

$$X^{(3)}_{pqrs} = c\begin{bmatrix} (1-p)e_1 + (1-q)e_2 + b_2 \\ B^{(3)}_{pqrs}\end{bmatrix}, \tag{7.3.17b}$$

where $X^i_{pqrs} = +1$ ($\bar{X}^i_{pqrs} = +1$) corresponds to a **16** of the first (second) $SO(10)$ and $X^i_{pqrs} = -1$ ($\bar{X}^i_{pqrs} = -1$) corresponds to a $\overline{\mathbf{16}}$ and we have chosen the space-time chirality $C(\psi^\mu) = +1$. The net number of spinorials of the first type and therefore the net number of families is given by

$$N_F = \sum_{i=1}^{2}\sum_{p,q,r,s=0}^{1} X^{(i)}_{pqrs}P^{(i)}_{pqrs}, \tag{7.3.18}$$

while for the second type

$$\bar{N}_F = \sum_{i=1}^{2}\sum_{p,q,r,s=0}^{1} \bar{X}^{(i)}_{pqrs}\bar{P}^{(i)}_{pqrs}, \tag{7.3.19}$$

and for the third type

$$N_F = \sum_{p,q,r,s=0}^{1} X^{(i)}_{pqrs} P^{(i)}_{pqrs}. \tag{7.3.20}$$

Similar formulas can be easily derived for the number of vectorials and the number of singlets and can be extended to the $U(1)$ charges but in this work we restrict to the spinorial calculation.

Formulas (7.3.12) – (7.3.13) allow us to identify the mechanism of spinorial reduction, or in other words the fixed point reduction, in the fermionic language. For a particular sector ($B^{(i)}_{pqrs}$) of the orbifold plane i there exist two shift vectors (e_{2i-1}, e_{2i}) and one z vector z_2. Setting the relative projection coefficients (7.3.12) – (7.3.13) to -1 each of the above three vectors acts as a projector that cuts the number of fixed points in the associated sector by a factor of two. Since three such projectors are available for each sector the number of fixed points can be reduced from 16 to 2 per plane. This argumentation holds for the spinorial representations of both the $SO(10)$'s.

Note that contrary to section 7.1, it is of no use to put these formulas in a simpler form using the matrix formulation developed therein. The reason being that in these cases we have three projectors for the extended $SO(8)$ models, while we still have 2^4 different sectors on each plane. We are therefore always left with one free coefficients. This is the exact origin of the fact that in these models we cannot reduce the number of generations down to one per plane.

We remark here that the projection coefficient $c\binom{b_1}{b_2}$ simply fixes the overall chirality and that our equations depend only on

$$(e_i\,|e_j\,)\,,\ (e_i\,|b_A\,)\,,(e_i\,|z_2\,)\,,\ (z_2\,|b_A\,)\,,\ i=1,\ldots,6,\ A=1,2. \tag{7.3.21}$$

7.4 The SV^2 and V^3 Free Fermionic Models

In this section we discuss the remaining models. We start by describing the SV^2 models and continue with the V^3 models. We show that these models do not give rise to phenomenologically interesting models. As a result we do not derive the projectors and chirality operators of these models as we have done in sections 7.1, 7.2 and 7.3.

Again we start from the $N = 4$ partition function written down in equation (6.1.5). Reducing the number of super symmetries from $N = 4$ to $N = 1$ is realised using a $\mathbb{Z}_2 \times \mathbb{Z}_2$ twist. This is the origin of the four different subclasses of models.

Below we show that the SV^2 and V^3 subclasses do not contain realistic models.

7.4.1 The SV^2 free fermionic models

Intuitively one may think that the SV^2 models are realised using the two twisting vectors b_1 and b_2 in the fermionic construction.

$$b_1 = \{\chi^{3,4}, \chi^{5,6}, y^{3,4}, y^{5,6} \,|\bar{y}^{3,4}, \bar{y}^{5,6}, \; \bar{\eta}^1, \bar{\psi}^{1,\ldots,5}\}, \tag{7.4.1}$$

$$b_2 = \{\chi^{1,2}, \chi^{5,6}, y^{1,2}, y^{5,6} \,|\bar{y}^{1,2}, \bar{y}^{5,6}, \; \bar{\eta}^1, \bar{\eta}^3\}. \tag{7.4.2}$$

Indeed we find that this gives spinorial representations on the first twisted plane and vectorial representations on the second plane. The third plane, however, gives rise to spinorial representations as well. In defining the second twisting vector as equation (7.4.2), we have merely redefined the S^2V models.

Let us therefore consider all possible options. We fix the basis vector b_1 and consider different configurations of the vector b_2. We can relax the constraint of vectorial representations on the second and third plane. We require only that there are no spinorials on the second and third plane of the observable $SO(10)$. This leads to four possible b_2 vectors. Due to modular invariance we can either choose 8 real fermions or 16 real fermions on the right moving side. Choosing the latter gives us three options. In the latter case we can either choose, due to modular invariance, that the overlap of the fermions of the b_1 and b_2 vector on the right moving side are 4, 8 or 12 real fermions. We have labeled the different options in table 7.4.1.

We now discuss the different options in more detail.

A One possible vector to describe this subclass of models defined in table 7.4.1 is given by

$$b_2 = \{\chi^{1,2} \; \chi^{5,6} \; y^{1,2} \; y^{5,6} \mid \bar{y}^{1,2} \; \bar{y}^{5,6} \; \bar{\eta}^1 \; \bar{\eta}^3 \bar{\phi}^{1,\ldots,4}\}. \tag{7.4.3}$$

At the level of the 10 basis vectors $\{1, S, b_1, b_2, e_i\}$ it is easy to show

Subclass	# right-moving real fermions	# overlapping real fermions
A	16	4
B	16	8
C	16	12
D	8	4

Table 7.4.1: The a priori different possible options for the realisation of the SV^2 models.

that the gauge group induced by the gauge fermions is

$$G = SO(10)^3 \times U(1). \tag{7.4.4}$$

One $SO(10)$ gauge group is realised on each of the three planes. On the first two planes there are spinorial representations of their respective $SO(10)$ gauge group. At this level we can only realise two projector operators which leads to a total reduction of the number of generations to 4 on each of the two planes. Adding z_2 as defined in equation (7.3.2) we obtain the gauge group described in equation (7.3.4). It is easy to see that this addition of the vector z_2 realises an equivalent description of the extended S^2V models. We therefore conclude that adding z_1 results in the S^3 models. The only models relevant for this subclass are those that do not have a separated $SO(8)$ gauge group and we have seen that this model can only realise $4, 8, 16$ generations on each plane of their respective $SO(10)$ gauge groups.

B One possible vector to describe this subclass of models defined in table 7.4.1 is given by

$$b_2 = \{\chi^{1,2}\ \chi^{5,6}\ y^{1,2}\ y^{5,6} \mid \bar{y}^{1,2}\ \bar{y}^{5,6}\ \bar{\psi}^{1,2,3}\bar{\phi}^{1,2,3}\}. \tag{7.4.5}$$

At the level of the 10 vectors $\{1, S, b_1, b_2, e_i\}$ it is easy to show that the gauge group induced by the gauge fermions is

$$G = SO(6)^3 \times SO(14). \tag{7.4.6}$$

We are not able to generate an $SO(10)$ unification group in this subclass of models. Adding z_2 breaks $SO(14) \to SO(8) \times SO(6)$ but allows for enhancements to appear. However enhancements to an $SO(10)$ gauge group are never realised. We can now add the alternative vector $\tilde{z}_1$

$$\tilde{z}_1 = \{\bar{\eta}^{2,3}\bar{\phi}^{1,2}\}. \tag{7.4.7}$$

This breaks $SO(6) \times SO(6) \rightarrow SU(2) \times SU(2) \times U(1) \times SU(2) \times SU(2) \times U(1)$. The addition of this last vector does not realise an enhancement to an observable $SO(10)$.

C One possible vector to describe this subclass of models defined in table 7.4.1 is given by

$$b_2 = \{\chi^{1,2}\ \chi^{5,6}\ y^{1,2}\ y^{5,6} \mid \bar{y}^{1,2}\ \bar{y}^{5,6}\ \bar{\eta}^2\ \bar{\psi}^{1,\ldots,5}\}. \tag{7.4.8}$$

This vector is identical to equation (6.1.17). We have therefore found either the S^3 or the S^2V subclass of models.

D One possible vector to describe this subclass of models defined in table 7.4.1 is given by

$$b_2 = \{\chi^{1,2}\ \chi^{5,6}\ y^{1,2}\ y^{5,6} \mid \bar{y}^{1,2}\ \bar{y}^{5,6}\ \bar{\eta}^1\ \bar{\eta}^3\}. \tag{7.4.9}$$

This vector is identical to equation (7.4.2). We have therefore found the S^2V subclass of models.

We have shown that in this subclass of models we are not able to generate phenomenologically interesting models. The reasons are that in case **A** we are either not able to reduce the number of generations of one $SO(10)$ gauge group both to 3 or 6 or we have realised a redefinition of the extended S^2V models. In case **B** a $SO(10)$ unification gauge group is not realised. In case **C** and **D** the S^2V models were again realised.

7.4.2 The V^3 free fermionic models

In this section we describe the V^3 models. We show that when an observable $SO(10)$ is realised the V^3 subclass reduces to the S^3 subclass of models.

The V^3 models are initially realised using the two twisting vectors b_1 and b_2 defined as

$$b_1 = \{\chi^{3,4}, \chi^{5,6}, y^{3,4}, y^{5,6} \mid \bar{y}^{3,4}, \bar{y}^{5,6},\ \bar{\eta}^2, \bar{\eta}^3\}, \tag{7.4.10}$$

$$b_2 = \{\chi^{1,2}, \chi^{5,6}, y^{1,2}, y^{5,6} \mid \bar{y}^{1,2}, \bar{y}^{5,6},\ \bar{\eta}^1, \bar{\eta}^3\}. \tag{7.4.11}$$

In this notation vectorial representations are realised on all the three planes where the vectorials of the third plane are realised by means of the vector $b_3 = b_1 + b_2$. However as soon as we separate out $SO(8)$ gauge

groups from the hidden sector we automatically generate spinorial representations of a $SO(8)$, or even a $SO(10)$, gauge group. To see this we isolate one block of theta functions by means of

$$z_2 = \{\bar{\phi}^{5,\ldots,8}\}. \tag{7.4.12}$$

Adding this basis vector gives rise to new massless states of the form

$$b_1 + z_2 = \{\chi^{3,4}, \chi^{5,6}, y^{3,4}, y^{5,6} \,|\bar{y}^{3,4}, \bar{y}^{5,6},\ \bar{\eta}^2, \bar{\eta}^3, \bar{\phi}^{5,\ldots,8}\}. \tag{7.4.13}$$

giving spinorial representations of the $SO(8)$ formed by $\bar{\phi}^{5,\ldots,8}$. The gauge group of this set of basis vectors is a priori $SU(2) \times SU(2) \times SO(28) \to U(1)^3 \times SO(26)$. Separating the theta block we break a priori the group further to $U(1)^3 \times SO(26) \to U(1)^3 \times SO(18) \times SO(8)$. At this level the $SO(10)$ unification group can not be realised.

However, the additional sectors induced by the z_2 vector can enhance $SO(8) \times U(1) \to SO(10)$. This depends on the GSO coefficients of the specific model. If the enhancement is realised the GSO coefficients are $c\binom{z_1}{b_1} = c\binom{z_1}{b_2} = -1$ necessarily. This however removes the vectorial states induced by the sectors b_1 and b_2. We have then effectively realised the S^2V models which are discussed in detail in sections 7.2 and 7.3.

To break $SO(18) \to SO(10) \times SO(8)$ we can separate another $SO(8)$ gauge group. This separation gives us a redefinition of the S^3 models. To show that we define

$$z_1 = \{\bar{\phi}^{1,\ldots,4}\}. \tag{7.4.14}$$

The spinors on the three planes are then realised as

$$B^1_{spinor} = b_1 + x, \tag{7.4.15}$$

$$B^2_{spinor} = b_2 + x, \tag{7.4.16}$$

$$B^3_{spinor} = b_1 + b_2 + x, \tag{7.4.17}$$

where

$$x = 1 + S + \sum_{i=1}^{6} e_i + \sum_{k=1}^{2} z_k. \tag{7.4.18}$$

These models are analysed in detail in [30, 29]. The only difference is that the generalised GSO coefficients are redefined in this subclass of models.

We have therefore shown that the SV^2 and V^3 subclasses either do not contain realistic models or reduce to the S^3 or S^2V models. Because of this we do not give the partition functions for the SV^2 and V^3 models and do not give the chiral and projector operators. These models are also not included in chapter 8.

Part III

Results and Conclusions

Chapter 8

Some Sample $\mathbb{Z}_2 \times \mathbb{Z}_2$ Orbifold Models

In this chapter we give some examples of models in the subclasses S^3 and S^2V that exhibit some interesting features. We focus on these subclasses of models because only these are interesting for phenomenology as explained in chapter 7. We describe their chiral content and their gauge group.

8.1 Three S^3 Models

We apply here the formalism developed in chapter 7 in order to derive sample models in the free fermionic formulation.

The $\mathbb{Z}_2 \times \mathbb{Z}_2$ symmetric orbifold

The simplest example is the symmetric $\mathbb{Z}_2 \times \mathbb{Z}_2$ orbifold. Here we set all the free GSO phases (7.1.35) to zero. The full GSO phase matrix takes

the form ($c\binom{v_i}{v_j} = \exp[i\pi(v_i|v_j)]$) with

$$
(v_i|v_j) \;=\; \begin{array}{c} \\ 1 \\ S \\ e_1 \\ e_2 \\ e_3 \\ e_4 \\ e_5 \\ e_6 \\ b_1 \\ b_2 \\ z_1 \\ z_2 \end{array}
\begin{array}{c}
\begin{array}{cccccccccccc} 1 & S & e_1 & e_2 & e_3 & e_4 & e_5 & e_6 & b_1 & b_2 & z_1 & z_2 \end{array} \\
\left(\begin{array}{cccccccccccc}
1 & 1 & 1 & 1 & 1 & 1 & 1 & 1 & 1 & 1 & 1 & 1 \\
1 & 1 & 1 & 1 & 1 & 1 & 1 & 1 & 1 & 1 & 1 & 1 \\
1 & 1 & 0 & 0 & 0 & 0 & 0 & 0 & 0 & 0 & 0 & 0 \\
1 & 1 & 0 & 0 & 0 & 0 & 0 & 0 & 0 & 0 & 0 & 0 \\
1 & 1 & 0 & 0 & 0 & 0 & 0 & 0 & 0 & 0 & 0 & 0 \\
1 & 1 & 0 & 0 & 0 & 0 & 0 & 0 & 0 & 0 & 0 & 0 \\
1 & 1 & 0 & 0 & 0 & 0 & 0 & 0 & 0 & 0 & 0 & 0 \\
1 & 1 & 0 & 0 & 0 & 0 & 0 & 0 & 0 & 0 & 0 & 0 \\
1 & 0 & 0 & 0 & 0 & 0 & 0 & 0 & 1 & 1 & 0 & 0 \\
1 & 0 & 0 & 0 & 0 & 0 & 0 & 0 & 1 & 1 & 0 & 0 \\
1 & 1 & 0 & 0 & 0 & 0 & 0 & 0 & 0 & 0 & 1 & 1 \\
1 & 1 & 0 & 0 & 0 & 0 & 0 & 0 & 0 & 0 & 1 & 1
\end{array}\right)
\end{array}. \qquad (8.1.1)
$$

This model is equivalent to the model where $\Delta^{(i)} = W^{(i)} = 0$ in equation (7.1.30). All projectors become inactive and thus the number of surviving twisted sector spinorials takes its maximum value which is 48 with all chiralities positive according to equations (7.1.34). Moreover three spinorials and three anti-spinorials arise from the untwisted sector. Following (7.1.8), (7.1.9) the gauge group enhances to $\mathbb{E}_6 \times U(1)^2 \times \mathbb{E}_8$ and the spinorials of $SO(10)$ combine with vectorials and singlets to produce 48+3=51 families (**27**) and 3 anti-families ($\overline{\mathbf{27}}$) of $\mathbb{E}_6$.

A three generation $\mathbb{E}_6$ model

We can obtain a three family $\mathbb{E}_6$ model by choosing the following set of projection coefficients

$$
(v_i|v_j) \;=\; \begin{array}{c} \\ 1 \\ S \\ e_1 \\ e_2 \\ e_3 \\ e_4 \\ e_5 \\ e_6 \\ b_1 \\ b_2 \\ z_1 \\ z_2 \end{array}
\begin{array}{c}
\begin{array}{cccccccccccc} 1 & S & e_1 & e_2 & e_3 & e_4 & e_5 & e_6 & b_1 & b_2 & z_1 & z_2 \end{array} \\
\left(\begin{array}{cccccccccccc}
1 & 1 & 1 & 1 & 1 & 1 & 1 & 1 & 1 & 1 & 1 & 1 \\
1 & 1 & 1 & 1 & 1 & 1 & 1 & 1 & 1 & 1 & 1 & 1 \\
1 & 1 & 0 & 0 & 1 & 0 & 0 & 1 & 0 & 0 & 0 & 0 \\
1 & 1 & 0 & 0 & 0 & 0 & 1 & 0 & 0 & 0 & 0 & 1 \\
1 & 1 & 1 & 0 & 0 & 0 & 1 & 0 & 0 & 0 & 0 & 0 \\
1 & 1 & 0 & 0 & 0 & 0 & 1 & 0 & 0 & 0 & 1 & 0 \\
1 & 1 & 0 & 1 & 1 & 1 & 0 & 1 & 0 & 0 & 0 & 0 \\
1 & 1 & 1 & 0 & 0 & 0 & 1 & 0 & 0 & 0 & 1 & 1 \\
1 & 0 & 0 & 0 & 0 & 0 & 0 & 0 & 1 & 0 & 0 & 0 \\
1 & 0 & 0 & 0 & 0 & 0 & 0 & 0 & 0 & 1 & 0 & 0 \\
1 & 1 & 0 & 0 & 0 & 1 & 0 & 1 & 0 & 0 & 1 & 1 \\
1 & 1 & 0 & 1 & 0 & 0 & 0 & 1 & 0 & 0 & 1 & 1
\end{array}\right)
\end{array}. \qquad (8.1.2)
$$

The full gauge group is $\mathbb{E}_6 \times U(1)^2 \times SO(8)^2$. Three families ($\mathbf{27}$), one from each plane, arise from the sectors $S + b_i + (x), i = 1, 2, 3$. Another set of three families and three anti-families arise from the untwisted sector. The hidden sector consists of nine 8-plets under each $SO(8)$. In addition there exist a number of non-Abelian gauge group singlets. The

model could be phenomenologically acceptable provided one finds a way of breaking $\mathbb{E}_6$. Since it is not possible to generate the $\mathbb{E}_6$ adjoint (not in Kac-Moody level one), we need to realize the breaking by an additional Wilson-line like vector. However, a detailed investigation of acceptable basis vectors, shows that the $\mathbb{E}_6$ breaking is accompanied by truncation of the fermion families. Thus this kind of perturbative $\mathbb{E}_6$ breaking is not compatible with the presence of three generations.

A six generation $\mathbb{E}_6$ model

Similarly a six family $\mathbb{E}_6 \times U(1)^2 \times \mathbb{E}_8$ model can be obtained using the following projection coefficients

$$(v_i|v_j) = \begin{array}{c} \\ 1 \\ S \\ e_1 \\ e_2 \\ e_3 \\ e_4 \\ e_5 \\ e_6 \\ b_1 \\ b_2 \\ z_1 \\ z_2 \end{array} \begin{array}{c} \begin{array}{cccccccccccc} 1 & S & e_1 & e_2 & e_3 & e_4 & e_5 & e_6 & b_1 & b_2 & z_1 & z_2 \end{array} \\ \left(\begin{array}{cccccccccccc} 1 & 1 & 1 & 1 & 1 & 1 & 1 & 1 & 1 & 1 & 1 & 1 \\ 1 & 1 & 1 & 1 & 1 & 1 & 1 & 1 & 1 & 1 & 1 & 1 \\ 1 & 1 & 0 & 0 & 0 & 0 & 1 & 1 & 0 & 0 & 0 & 0 \\ 1 & 1 & 0 & 0 & 1 & 0 & 0 & 1 & 0 & 0 & 0 & 0 \\ 1 & 1 & 0 & 1 & 0 & 0 & 0 & 1 & 0 & 0 & 0 & 0 \\ 1 & 1 & 0 & 0 & 0 & 0 & 1 & 0 & 0 & 0 & 0 & 1 \\ 1 & 1 & 1 & 0 & 0 & 1 & 0 & 0 & 0 & 0 & 0 & 0 \\ 1 & 1 & 1 & 1 & 1 & 0 & 0 & 0 & 0 & 0 & 0 & 1 \\ 1 & 0 & 0 & 0 & 0 & 0 & 0 & 0 & 1 & 0 & 0 & 0 \\ 1 & 0 & 0 & 0 & 0 & 0 & 0 & 0 & 0 & 1 & 0 & 0 \\ 1 & 1 & 0 & 0 & 0 & 0 & 0 & 0 & 0 & 0 & 1 & 1 \\ 1 & 1 & 0 & 0 & 0 & 1 & 0 & 1 & 0 & 0 & 1 & 1 \end{array}\right) \end{array} . \quad (8.1.3)$$

In this model we have six families from the twisted sector, two from each plane together with three families and three anti-families from the untwisted sector, accompanied by a number of singlets and 8-plets of both hidden $SO(8)$'s.

8.2 Two Simple S^2V Models

In this subclass of models we present an example of a model with 32 generations coming from the twisted sector, 16 coming from the first two planes. The second example is a model with 8 generations coming from the twisted sector, 4 coming from each of the first two planes.

The $\mathbb{Z}_2 \times \mathbb{Z}_2$ symmetric orbifold

The simplest example is the symmetric $\mathbb{Z}_2 \times \mathbb{Z}_2$ orbifold. Here we set all the free GSO phases (7.2.8) to zero. This gives a model of 32 generations where 16 are coming from each of the first two planes. The full GSO

phase matrix takes the form ($c\binom{v_i}{v_j} = \exp[i\pi(v_i|v_j)]$)

$$(v_i|v_j) = \begin{array}{c} \\ 1 \\ S \\ e_1 \\ e_2 \\ e_3 \\ e_4 \\ e_5 \\ e_6 \\ b_1 \\ b_2 \end{array} \begin{array}{c} \begin{array}{cccccccccc} 1 & S & e_1 & e_2 & e_3 & e_4 & e_5 & e_6 & b_1 & b_2 \end{array} \\ \begin{pmatrix} 1 & 1 & 1 & 1 & 1 & 1 & 1 & 1 & 1 & 1 \\ 1 & 1 & 1 & 1 & 1 & 1 & 1 & 1 & 1 & 1 \\ 1 & 1 & 0 & 0 & 0 & 0 & 0 & 0 & 0 & 0 \\ 1 & 1 & 0 & 0 & 0 & 0 & 0 & 0 & 0 & 0 \\ 1 & 1 & 0 & 0 & 0 & 0 & 0 & 0 & 0 & 0 \\ 1 & 1 & 0 & 0 & 0 & 0 & 0 & 0 & 0 & 0 \\ 1 & 1 & 0 & 0 & 0 & 0 & 0 & 0 & 0 & 0 \\ 1 & 1 & 0 & 0 & 0 & 0 & 0 & 0 & 0 & 0 \\ 1 & 0 & 0 & 0 & 0 & 0 & 0 & 0 & 1 & 0 \\ 1 & 0 & 0 & 0 & 0 & 0 & 0 & 0 & 0 & 1 \end{pmatrix} \end{array}. \tag{8.2.1}$$

An eight generation $SO(10)$ model

We can obtain an eight generation $SO(10)$ model, four coming from each of the first two planes, by choosing the following set of projection coefficients

$$(v_i|v_j) = \begin{array}{c} \\ 1 \\ S \\ e_1 \\ e_2 \\ e_3 \\ e_4 \\ e_5 \\ e_6 \\ b_1 \\ b_2 \end{array} \begin{array}{c} \begin{array}{cccccccccc} 1 & S & e_1 & e_2 & e_3 & e_4 & e_5 & e_6 & b_1 & b_2 \end{array} \\ \begin{pmatrix} 1 & 1 & 1 & 1 & 1 & 1 & 1 & 1 & 1 & 1 \\ 1 & 1 & 1 & 1 & 1 & 1 & 1 & 1 & 1 & 1 \\ 1 & 1 & 0 & 0 & 0 & 0 & 1 & 1 & 0 & 0 \\ 1 & 1 & 0 & 0 & 1 & 0 & 0 & 1 & 0 & 0 \\ 1 & 1 & 0 & 1 & 0 & 0 & 0 & 1 & 0 & 0 \\ 1 & 1 & 0 & 0 & 0 & 0 & 1 & 1 & 0 & 0 \\ 1 & 1 & 1 & 0 & 0 & 1 & 0 & 0 & 0 & 0 \\ 1 & 1 & 1 & 1 & 1 & 1 & 0 & 0 & 0 & 0 \\ 1 & 0 & 0 & 0 & 0 & 0 & 0 & 0 & 1 & 0 \\ 1 & 0 & 0 & 0 & 0 & 0 & 0 & 0 & 0 & 1 \end{pmatrix} \end{array}. \tag{8.2.2}$$

8.3 Three Extended S^2V Models

In this subclass of models we present a model with 32 positively chiral spinors of the first SO(10), 16 coming from the first two planes and 32 negatively chiral spinors of the second $SO(10)$, again 16 coming from the first two planes. Secondly we present a model that has four generations only of the first $SO(10)$, 2 coming from each of the first two planes and zero net generations of the second $SO(10)$, 2 positive chiral from the first and 2 negative chiral from the second plane.

The $\mathbb{Z}_2 \times \mathbb{Z}_2$ symmetric orbifold

The simplest example is the symmetric $\mathbb{Z}_2 \times \mathbb{Z}_2$ orbifold. Here we set all the free GSO phases (7.3.21) to zero. The full GSO phase matrix takes the form ($c\binom{v_i}{v_j} = \exp[i\pi(v_i|v_j)]$)

$$(v_i|v_j) = \begin{array}{c} \\ 1 \\ S \\ e_1 \\ e_2 \\ e_3 \\ e_4 \\ e_5 \\ e_6 \\ b_1 \\ b_2 \\ z_2 \end{array} \begin{array}{c} \begin{array}{ccccccccccc} 1 & S & e_1 & e_2 & e_3 & e_4 & e_5 & e_6 & b_1 & b_2 & z_2 \end{array} \\ \begin{pmatrix} 1 & 1 & 1 & 1 & 1 & 1 & 1 & 1 & 1 & 1 & 1 \\ 1 & 1 & 1 & 1 & 1 & 1 & 1 & 1 & 1 & 1 & 1 \\ 1 & 1 & 0 & 0 & 0 & 0 & 0 & 0 & 0 & 0 & 0 \\ 1 & 1 & 0 & 0 & 0 & 0 & 0 & 0 & 0 & 0 & 0 \\ 1 & 1 & 0 & 0 & 0 & 0 & 0 & 0 & 0 & 0 & 0 \\ 1 & 1 & 0 & 0 & 0 & 0 & 0 & 0 & 0 & 0 & 0 \\ 1 & 1 & 0 & 0 & 0 & 0 & 0 & 0 & 0 & 0 & 0 \\ 1 & 1 & 0 & 0 & 0 & 0 & 0 & 0 & 0 & 0 & 0 \\ 1 & 0 & 0 & 0 & 0 & 0 & 0 & 0 & 1 & 0 & 0 \\ 1 & 0 & 0 & 0 & 0 & 0 & 0 & 0 & 0 & 1 & 0 \\ 1 & 1 & 0 & 0 & 0 & 0 & 0 & 0 & 0 & 0 & 1 \end{pmatrix} \end{array}. \tag{8.3.1}$$

In this model we find 32 generations of the observable $SO(10)$, 16 coming from each of the first two planes, and 32 anti-generations of the hidden $SO(10)$, 16 coming from each of the first two planes.

A four generation $SO(10)$ model

We can obtain a four generation $SO(10)$ model by choosing the following set of projection coefficients

$$(v_i|v_j) = \begin{array}{c} \\ 1 \\ S \\ e_1 \\ e_2 \\ e_3 \\ e_4 \\ e_5 \\ e_6 \\ b_1 \\ b_2 \\ z_2 \end{array} \begin{array}{c} \begin{array}{ccccccccccc} 1 & S & e_1 & e_2 & e_3 & e_4 & e_5 & e_6 & b_1 & b_2 & z_2 \end{array} \\ \begin{pmatrix} 1 & 1 & 1 & 1 & 1 & 1 & 1 & 1 & 1 & 1 & 1 \\ 1 & 1 & 1 & 1 & 1 & 1 & 1 & 1 & 1 & 1 & 1 \\ 1 & 1 & 0 & 1 & 0 & 0 & 0 & 1 & 0 & 0 & 1 \\ 1 & 1 & 1 & 0 & 1 & 0 & 0 & 0 & 0 & 0 & 0 \\ 1 & 1 & 0 & 1 & 0 & 0 & 0 & 1 & 0 & 0 & 0 \\ 1 & 1 & 0 & 0 & 0 & 0 & 1 & 1 & 0 & 0 & 1 \\ 1 & 1 & 0 & 0 & 0 & 1 & 0 & 1 & 0 & 0 & 1 \\ 1 & 1 & 1 & 0 & 1 & 1 & 1 & 0 & 0 & 0 & 0 \\ 1 & 0 & 0 & 0 & 0 & 0 & 0 & 0 & 1 & 0 & 0 \\ 1 & 0 & 0 & 0 & 0 & 0 & 0 & 0 & 0 & 1 & 0 \\ 1 & 1 & 0 & 0 & 0 & 0 & 0 & 0 & 0 & 0 & 1 \end{pmatrix} \end{array}. \tag{8.3.2}$$

In this model we find two generations of the observable $SO(10)$ coming from each of the first two planes and two generations of the hidden $SO(10)$ coming from the first plane and two anti-generations of the hidden $SO(10)$ coming from the second plane. This model is completely determined at the $N = 4$ level. For more details on this property we refer to section 9.1. Therefore we do not find an enhancement of the $SO(8) \times U(1) \to SO(10)$ and the $SO(8)$ remains completely separate as explained in section 7.3.1.

A six generation $SO(10)$ model

We can obtain a six generation $SO(10)$ model by choosing the following set of projection coefficients

$$(v_i|v_j) = \begin{array}{c} \\ 1 \\ S \\ e_1 \\ e_2 \\ e_3 \\ e_4 \\ e_5 \\ e_6 \\ b_1 \\ b_2 \\ z_2 \end{array} \begin{array}{c} \begin{array}{cccccccccccc} 1 & S & e_1 & e_2 & e_3 & e_4 & e_5 & e_6 & b_1 & b_2 & z_2 \end{array} \\ \begin{pmatrix} 1 & 1 & 1 & 1 & 1 & 1 & 1 & 1 & 1 & 1 & 1 \\ 1 & 1 & 1 & 1 & 1 & 1 & 1 & 1 & 1 & 1 & 1 \\ 1 & 1 & 0 & 0 & 0 & 0 & 0 & 0 & 0 & 0 & 1 \\ 1 & 1 & 0 & 0 & 1 & 0 & 0 & 1 & 0 & 0 & 0 \\ 1 & 1 & 0 & 1 & 0 & 0 & 0 & 1 & 0 & 0 & 1 \\ 1 & 1 & 0 & 0 & 0 & 0 & 1 & 1 & 0 & 0 & 0 \\ 1 & 1 & 0 & 0 & 0 & 1 & 0 & 1 & 0 & 0 & 1 \\ 1 & 1 & 0 & 1 & 1 & 1 & 1 & 0 & 0 & 0 & 0 \\ 1 & 0 & 0 & 0 & 0 & 0 & 0 & 0 & 0 & 0 & 0 \\ 1 & 0 & 0 & 0 & 0 & 0 & 0 & 0 & 0 & 1 & 0 \\ 1 & 1 & 0 & 0 & 0 & 0 & 0 & 0 & 0 & 0 & 1 \end{pmatrix} \end{array}. \tag{8.3.3}$$

In this model we find four generations of the observable $SO(10)$ on the first plane and two generations of the observable $SO(10)$ on the second plane. We find one generation of the hidden $SO(10)$ and one anti-generation of the hidden $SO(10)$ on the first plane. This model is completely determined at the $N = 4$ level. For more details on this property we refer to section 9.1. Therefore, we do not find spinorials of the third hidden $SO(10)$ on the third plane as explained in section 7.3.1.

Chapter 9

General Results

In this chapter we give the general results of the classification. We show how this description uncovers a subset of models that have a well defined $N = 4$ origin. We also highlight the mechanism that realises three generations. We discuss the method we have employed in the classification. We end this section with an overview of the characteristics of realistic models or semi-realistic models in the chiral $\mathbb{Z}_2 \times \mathbb{Z}_2$ free fermionic models with symmetric shifts.

9.1 $N = 4$ Liftable Vacua

In the models considered in sections 8.1, 8.2 and 8.3 we have managed to separate the orbifold twist action (represented here by b_1, b_2) from the shifts (represented by e_i) and the Wilson lines (z_1, z_2). However, these actions are further correlated through the GSO projection coefficients $c\binom{v_i}{v_j}$. Nevertheless, we remark that the twist action can be decoupled from the other two in the case

$$c\begin{bmatrix} b_n \\ z_k \end{bmatrix} = c\begin{bmatrix} b_m \\ e_i \end{bmatrix} = +1 \ , i = 1, \ldots, 6, \ k = 1, 2, \ m, n = 1, 2, 3 \tag{9.1.1}$$

for the S^3 models. The twist action can be decoupled from the other two actions in the case

$$c\begin{bmatrix} b_m \\ e_i \end{bmatrix} = +1 \ , i = 1, \ldots, 6, \ k = 1, 2, \ m, n = 1, 2, 3 \tag{9.1.2a}$$

for the simple S^2V models or

$$c\begin{bmatrix} b_n \\ z_2 \end{bmatrix} = c\begin{bmatrix} b_m \\ e_i \end{bmatrix} = +1\ , i = 1, \ldots, 6,\ m, n = 1, 2, 3 \qquad \text{(9.1.2b)}$$

for the extended S^2V models. The above relation defines a subclass of $N = 1$ four dimensional vacua with interesting phenomenological properties and includes three generation models in the S^3 subclass of models. Due to the decoupling of the orbifold twist action these vacua are direct descendants of $N = 4$ vacua so we refer to these models as $N = 4$ lift-able models. In this subclass of models some important phenomenological properties of the vacuum, as the number of generations, are predetermined at the $N = 4$ level as it is related to the $(e_i\,|e_j\,)$ and $(z_i\,|e_j\,)$ phases in the S^3 subclass of models. In the S^2V subclass of models they are related to the $(e_i\,|e_j\,)$ and also, in the case where we have introduced the z_2 vector, the $(z_2\,|e_j\,)$ phases. The orbifold action reduces the super symmetries and the gauge group and makes chirality apparent, however the number of generations is selected by the $N = 4$ vacuum structure. At the $N = 1$ level this is understood as follows: the $\mathbb{Z}_2 \times \mathbb{Z}_2$ orbifold has 48 fix points in the S^3 subclass and 32 fix points in the S^2V subclass of models. Switching on some of the above phase correspond to a free action that removes some of the fixed points and thus reduces the number of spinorials. Moreover, in the S^3 subclass of models, the chirality of the surviving spinorials is again related as seen by equations (7.1.34) to the $(e_i\,|e_j\,)$ and $(e_i\,|z_k\,)$ coefficients, which are all fixed at the $N = 4$ level. The observable gauge group of liftable models is always $\mathbb{E}_6$ and this can be easily seen by applying (9.1.1) to (7.1.8) and (7.1.9). In the S^2V subclass of models the chirality of the surviving spinorials is related as seen by (7.2.6) and (7.3.15) – (7.3.16) to the $(e_i\,|e_j\,)$ and $(e_i\,|z_k\,)$ coefficients, which are all fixed at the $N = 4$ level.

Typical examples of liftable vacua in the S^3 subclass of models are the three and six generation $\mathbb{E}_6 \times U(1)^2 \times SO(8)^2$ models presented in section 8.1. A careful counting, taking into account some symmetries among the coefficients, shows that this class of models consists of 2^{20} models, or 2^{21} if we include $(b_1\,|b_2\,)$. Typical examples of liftable vacua in the simple and extended S^2V models are presented in equation (8.2.2) and (8.3.2) respectively. A careful counting, taking into account some symmetries among the coefficients, shows that the simple S^2V class consists of 2^{10} models, or 2^{11} if we include $(b_1\,|b_2\,)$. The extended S^2V class consists of 2^{15} models, or 2^{16} if we include $(b_1\,|b_2\,)$. All these vacua are interesting because they have a clear geometrical interpretation.

From the orbifold description we learn that all breakings of the hidden and observable gauge group are induced using Wilson lines. From the

$4D$ point of view the internal gauge group is broken in a similar fashion using Wilson lines. The twisted planes in equation (6.2.7) describe the removal of the free moduli using twists. When a group is broken using Wilson lines the field corresponding to this Wilson line obtains a nonzero VEV. The fixing of the moduli using twists can be interpreted as the removal of the quantum fluctuations of the fields identified with the Wilson lines. These Wilson lines become discrete Wilson lines and the VEV becomes a fixed value.

In the extended S^2V models we find that enhancement of $SO(8)\times U(1) \rightarrow SO(10)$ is possible only at the $N = 1$ level as is explained in section 7.3.1. The models that exhibit this type of enhancement are therefore not liftable to a $N = 4$ theory.

9.2 The Method of Classification

As we discussed in chapter 7 and 8, the free GSO phases of the $N = 1$ partition function control the number of chiral generations in a given model. In chapter 7 we have given analytic formulas that enable the calculation of the number of generations for any given set of phases. To gain an insight into the structure of this class of vacua we can proceed with a computer evaluation of these formulas and thus classify the space of these vacua with respect to the number of generations. This also allows detailed examination of the structure of these vacua and in particular how the generations are distributed among the three orbifold planes. The main obstacle to this approach is the huge number of vacua under consideration. As a first step in this direction, we restrict to the class of liftable vacua that is physically appealing and contains representative models with the right number of generations. As stated in section 9.1 the liftable S^3 subclass consists in principle of 2^{21} models or less in the S^2V subclass of models. Their complete classification takes a few minutes on a personal computer using an appropriate computer program. The program is written in FORTRAN and goes over all GSO coefficients. It takes into account the constraints that are required for liftablility. For each configuration of GSO coefficients it uses equation (7.1.29) for the S^3 models, equation (7.2.7) for the simple S^2V models and equations (7.3.18) and (7.3.19) for the extended S^2V models to calculate the number of generations. The program gives for each plane the total number of generations and the total number of anti-generations. If this model has been found already by permuting the three twisted planes the model is dropped from the end result while if it is a new

model, this model is recorded. At the end we have acquired a complete list of all models that are physically inequivalent. We have required in the program that the models exhibit $N = 1$ supersymmetry.

We have first analysed the S^3 subclass of models. The different configurations are used to calculate the number of generations using formulae (7.1.27) – (7.1.29). For the analysis of the gauge group we use formulae (7.1.8) – (7.1.11). The results are presented in Tables B.1.1 – B.1.4. In these tables we list the number of generations coming from the twisted sectors. They are listed per plane. The number of positive chiral generations is separated from the number of negative chiral generations on each plane. The total number is then listed before listing the total net number of generations. As the sign of the chirality is determined by the coefficient $(b_1\,|b_2\,)$, as is clear from equations (7.1.34), we have listed models that have a positive net number of generations. In order to maintain a complete separation of the hidden gauge group we have set $(z_1\,|z_2\,) = 1$. The tables are ordered by the total net number of chiral states.

We find that there are no liftable models with a $SO(10)$ observable gauge group, which is always extended to $\mathbb{E}_6$, and the states from the vector x are not projected out. Since the models admit a geometrical interpretation, it means that they must descend from the ten dimensional $\mathbb{E}_8 \times \mathbb{E}_8$ heterotic–string on $\mathbb{Z}_2 \times \mathbb{Z}_2$ Calabi–Yau threefold.

In a small number of all the models the hidden gauge group is enhanced to $SO(8)\times SO(8) \to SO(16)$. We find that a fraction of the liftable models are enhanced to $SO(8) \times SO(8) \to \mathbb{E}_8$. We find that the 24 generations NAHE model as explained in section 5.4 is present in table B.1.1.

Since the total number of different models is relatively small in the S^2V subclass of models we can do a complete classification of these models. The results of the classification of the simple S^2V models are listed in table B.2.1. The models listed in chapter 8 are liftable. We have listed these models due to their clear $N = 4$ origin. Since the extended S^2V subclass of models do not give phenomenologically interesting models we have not listed the physically different models we find in this subclass. We do find however that we cannot reduce the number of families down to 3, i.e. 2 on one plane and 1 on the second plane. We are able to reduce the number of generations down to 4, or two on each plane, but at the cost of introducing another $SO(10)$ gauge group with spinorials on the first two planes. In the subclass of liftable extended S^2V models we find that it is not possible to have only spinorial representations of the first $SO(10)$ in the massless spectrum. An example of the models which

have net zero generations from the second $SO(10)$ is given in equation (8.3.2).

9.3 Reduction of Generations and the Internal Manifold

In chapter 6 we discussed a direct translation between the bosonic formulation and the fermionic formulation of the heterotic string compactifications. $\mathbb{Z}_2 \times \mathbb{Z}_2$ orbifold compactifications are relevant for this thesis. These orbifolds contain three twisted sectors, or three twisted planes. A priori we may have the possibility that all three twisted planes produce spinorial $SO(10)$ representations. We refer to this subclass of models as S^3 models. The alternatives are models in which spinorial representations may be obtained from only two, one, or none of the twisted planes, and the others produce vectorial representations. We refer to these cases as S^2V, SV^2 and V^3 models, respectively. The NAHE set is an element of the S^3 subclass of the chiral $\mathbb{Z}_2 \times \mathbb{Z}_2$ models. The S^3 subclass allows, depending on the one–loop GSO projection coefficients, the possibility of spinorials on each plane. In specific models in this subclass each Standard Model family is obtained from a distinct orbifold plane. Such models therefore produce three generation models and may be phenomenologically interesting. The only other phenomenologically viable option can intuitively come from the subclass S^2V models as this class of models may intuitively contain a model with for example 2 generations coming from the first plane and 1 generation coming from the second plane and none from the third. However, we find that the S^2V subclass of models do not give phenomenologically interesting models as is seen in chapter 7 and 8. The SV^2 class of models cannot produce a physical model because it is not possible to reduce the number of families to 3 as they would have to be coming from one plane and 3 cannot be written as a power of 2. Similarly the V^3 subclass of models will not contain phenomenologically interesting models.

Since the projectors are constructed using the complete separation of the internal manifold we see that three generation models are only possible when

$$\Gamma_{6,6} \;=\; \Gamma^3_{2,2} \;\longrightarrow\; \Gamma^6_{1,1}. \tag{9.3.1}$$

These $\Gamma_{1,1}$ internal parts do not describe a complex manifold. They describe internal real circles. If we use solely complex manifolds, of the type $\Gamma_{6,6} = \Gamma^3_{2,2}$, and using only symmetric shifts, we find that there are

no 3 generation models. We therefore conclude that the net number of generations can never be equal to three in the framework of $\mathbb{Z}_2 \times \mathbb{Z}_2$ Calabi–Yau compactifications. This implies the necessity of non zero torsion in CY $\mathbb{Z}_2 \times \mathbb{Z}_2$ compactifications in order to obtain semi–realistic three generation models. This is one of the main results of the analysis and it reveals, at least in the context of the three generation free fermionic models, that the geometrical structures that underly these models may not be simple Calabi–Yau manifolds, but it corresponds to geometries that are yet to be defined.

In the realistic free fermionic models the reduction of the number of families together with the breaking of the observable $SO(10)$ is realized by isolating full multiplets at two fixed points on the internal manifold. In reducing the number of families down to one, different component of each family are attached to the two distinct fixed points. We remove one full multiplet and simultaneously break the $SO(10)$ symmetry. We therefore keep a full multiplet on each twisted plane. In the $SO(10)$ models described here a whole 16 or $\overline{16}$ of $SO(10)$ is attached to one fixed point. We are therefore not able to break the $SO(10)$, and simultaneously preserve the full Standard Model multiplets. For this reason we find that the observable $SO(10)$ cannot be broken perturbatively in this class of three generation models, and may only be broken non perturbatively. It is therefore not possible to reduce both the number of families down to 3 and break the observable gauge group $SO(10)$ down to its subgroups perturbatively.

We conclude that there is a method to reduce the number of generations from 48 to 3. Since we need 4 projectors we need to separate the hidden gauge group using $SO(8)$ characters

$$\Gamma_{0,8} \to \Gamma_{0,4}\, \Gamma_{0,4} \tag{9.3.2}$$

and we need to break the internal complex manifold to an internal real manifold

$$\Gamma_{6,6} \to \left[\Gamma_{1,1}\, \Gamma_{1,1}\right]^3 . \tag{9.3.3}$$

If we reduce the number of generations to 3 we cannot break the $SO(10)$ observable group to its subgroups, while maintaining a full multiplet. The $SO(10)$ observable gauge group cannot therefore be broken perturbatively. We can reduce the number of generations from 48 to 6 using 3 projectors. This entails that we can choose either to separate the hidden gauge group using $SO(16)$ characters, or to leave the internal manifold complex.

We argued above that we cannot break $SO(10)$ down to a subgroup perturbatively, while reducing the number of generations to 3. If we want

to break the $SO(10)$ symmetry perturbatively, and keep a full $SO(10)$ multiplet from a given twisted plane, we can only reduce the number of generations to 6. This can be achieved if we define three different projectors like the ones defined in equations (7.1.27). We are therefore left with two options. First, we can use $SO(16)$ characters for the separation of the hidden gauge group. We have then constructed only one projector which leaves us no other option than to break the complex structure using symmetric shifts

$$\Gamma_{6,6} \to \Gamma^6_{1,1}. \tag{9.3.4}$$

Second, we can use $SO(8)$ characters for the separation of the hidden gauge group. In doing so we have constructed two projectors. The third can be realized by the symmetric shifts that leave the complex structure of the internal manifold intact

$$\Gamma_{6,6} \to \Gamma^3_{2,2}. \tag{9.3.5}$$

We have therefore concluded the classification of the chiral $\mathbb{Z}_2 \times \mathbb{Z}_2$ free fermionic models with symmetric shifts. In this chapter we have shown how liftable models appear in the models discussed. We have elaborated on the method we have used to classify all the models. Although we have not listed all models of the S^3 subclass we are able to derive some general properties of these additional models. We have shown that in this class of models we do not find realistic three generation models with a Calabi-Yau compactification.

Chapter 10

Discussion

In this chapter we give a short summary of the issues discussed in this thesis. We end with a discussion on the realistic free fermionic models and give some suggestions for further research.

In this thesis we have classified the chiral content of the heterotic $\mathbb{Z}_2 \times \mathbb{Z}_2$ orbifolds. This classification was possible since we can choose *any* point in the moduli space to describe the chiral content as explained in section 3.4. This choice gave us the opportunity to describe the chiral content of the heterotic $\mathbb{Z}_2 \times \mathbb{Z}_2$ orbifolds in the free fermionic construction. In this thesis we presented a direct translation between symmetric shifts in the orbifold construction to symmetric shifts in the free fermionic construction. As the hidden $\mathbb{E}_8$ gauge group is broken to $SO(8) \times SO(8)$ in the realistic free fermionic models we have included this in our classification. The classification of the chiral content therefore includes all models where symmetric shifts are realised on the internal space and where the hidden gauge group is broken to $SO(8) \times SO(8)$ at *any* point in the moduli space.

We have started by giving an overview of the general construction of string models in chapter 2. We gave an introduction to the orbifold description of string theory in chapter 3. We set the string on a circle after which we expanded to the general manifold. We then introduced shifts and ended this chapter with a discussion of $\mathbb{Z}_2$ twists. In this chapter we have shown that the twisted sector *does not* depend on the moduli of the internal space. This is an essential ingredient that has allowed this classification. In chapter 4 we constructed the partition function of the heterotic string. We isolated some constraints on the partition

function due to modular invariance of the theory. This lead to the formulation of the free fermionic string. Since bosons can only be interchanged with free fermions at the maximal symmetry point, the target space in the free fermionic construction is inherently at the maximal symmetry point in the moduli space. In chapter 5 we discuss the practicalities of constructing a free fermionic model and its spectrum. We isolate some sectors that are relevant for the remainder of the thesis. Two semi-realistic models are discussed in detail.

In chapter 6 we use the orbifold description developed in chapter 3 to isolate the free parameters of the $\mathbb{Z}_2 \times \mathbb{Z}_2$ orbifold with symmetric shifts. We discuss the translation of the orbifold description to the free fermionic description. We have specified the basis vectors for the free fermionic formulation that describe a shift on the internal space. We have shown that the basis vectors that induce the twist on the internal space are completely fixed by requiring spinorial representations. In chapter 7 we use the free fermionic language to derive formulas that describe the chiral content of the $\mathbb{Z}_2 \times \mathbb{Z}_2$ orbifold with symmetric shifts using the methods we explained in chapter 5. Using these formulas we have written a computer program in FORTRAN to analyse all heterotic $\mathbb{Z}_2 \times \mathbb{Z}_2$ orbifold models. Using this computer program we gave some sample models in chapter 8. In chapter 9 we discussed the general results we obtained from the classification.

In chapter 5 we have discussed two semi-realistic models. Similarly realistic models can be constructed using the NAHE set basis vectors. All these models have one feature in common, which is their $\mathbb{Z}_2 \times \mathbb{Z}_2$ orbifold origin. In chapter 9 we came to the conclusion that there are no three generation models with a $\mathbb{Z}_2 \times \mathbb{Z}_2$ Calabi-Yau space. The realistic free fermionic models do however exhibit three generations. We have shown in section 5.4 that the last vector γ that realises the reduction of the number of generations to three, cannot be written as a linear combination of symmetric shifts. This vector necessarily induces a different type of reduction than the one we have described in this thesis.

In the free fermionic formulation the moduli of the internal manifold are all fixed to the maximal symmetry point in the moduli space. In the orbifold description we have left all the moduli untouched. It may therefore be the case that the vector that breaks the observable $SO(10)$ and simultaneously reduces the number of generations to three requires the moduli to be fixed at the maximal symmetry point. Research in this direction may prove very interesting and may shed some light on the dynamical mechanism that singles out the vacuum we observe in nature.

In this thesis we have focused on the chiral content of the $\mathbb{Z}_2 \times \mathbb{Z}_2$ fermionic models of the heterotic string. It is fairly easy to extend this analysis to the vectorial sector. Similarly the total $U(1)$ charge can be calculated as a function of the free GSO coefficients. In chapter 7 we have isolated the GSO coefficients that completely determine the chiral content. It is therefore believed that the remaining coefficients determined the other sectors of the model. Furthermore, as we have explained, some very interesting results are to be expected from analysing the dual descriptions of the free fermionic formulation of the heterotic string. This should be possible as the complete structure of partition function is known at the level of the $\mathbb{Z}_2 \times \mathbb{Z}_2$ orbifold with symmetric shifts. Likewise we can analyse threshold corrections, helicity supertraces and other properties of the semi-realistic models.

Having given an overview of the thesis together with some suggestions for future work, we have come to a closure.

Part IV

Appendix

Appendix A.1. The Spectrum of the Model Without Enhanced Symmetry

Appendix A.1. The Spectrum of the Model Without Enhanced Symmetry

SEC	$SU(4) \times SU(2)$	Q_R	Q_1	Q_2	Q_4	Q_5	$SU(2)_3 \times SU(2)_6$	$SU(4)_H \times SU(2)_{H_3} \times SU(2)_{H_1} \times SU(2)_{H_2}$	Q_7	Q_8
b_1	$(\bar{4},1)$	4	-2	0	-2	0	$(1,1)$	$(1,1,1,1)$	0	0
	$(\bar{4},1)$	4	2	0	2	0	$(1,1)$	$(1,1,1,1)$	0	0
	$(\bar{4},1)$	-4	-2	0	-2	0	$(1,1)$	$(1,1,1,1)$	0	0
	$(\bar{4},1)$	-4	2	0	2	0	$(1,1)$	$(1,1,1,1)$	0	0
b_2	$(\bar{4},1)$	4	0	-2	0	2	$(1,1)$	$(1,1,1,1)$	0	0
	$(\bar{4},1)$	4	0	2	0	-2	$(1,1)$	$(1,1,1,1)$	0	0
	$(\bar{4},1)$	-4	0	-2	0	2	$(1,1)$	$(1,1,1,1)$	0	0
	$(\bar{4},1)$	-4	0	2	0	-2	$(1,1)$	$(1,1,1,1)$	0	0
b_3	$(4,2)$	0	0	0	0	0	$(1,2)$	$(1,1,1,1)$	0	0
$S + b_1 + b_2 +$	$(1,1)$	0	2	-2	0	0	$(1,1)$	$(1,1,1,2)$	0	0
$\alpha + \beta$	$(1,1)$	0	-2	2	0	0	$(1,1)$	$(1,1,2,1)$	0	0
	$(1,1)$	0	-2	2	0	0	$(1,1)$	$(1,1,1,2)$	0	0
	$(1,1)$	0	2	-2	0	0	$(1,1)$	$(1,1,2,1)$	0	0
$b_3 + \beta + 2\gamma$	$(1,1)$	0	0	0	-2	2	$(2,1)$	$(1,1,1,1)$	4	0
	$(1,1)$	0	0	0	2	2	$(1,2)$	$(1,1,1,1)$	4	0
	$(1,1)$	0	0	0	-2	-2	$(1,2)$	$(1,1,1,1)$	4	0
	$(1,1)$	0	0	0	2	-2	$(2,1)$	$(1,1,1,1)$	4	0
	$(1,1)$	0	0	0	-2	2	$(2,1)$	$(1,1,1,1)$	-4	0
	$(1,1)$	0	0	0	2	2	$(1,2)$	$(1,1,1,1)$	-4	0
	$(1,1)$	0	0	0	-2	-2	$(1,2)$	$(1,1,1,1)$	-4	0
	$(1,1)$	0	0	0	2	-2	$(2,1)$	$(1,1,1,1)$	-4	0
$S + 2\gamma$	$(1,1)$	4	0	0	0	0	$(1,1)$	$(4,2,1,1)$	0	4
	$(1,1)$	-4	0	0	0	0	$(1,1)$	$(\bar{4},2,1,1)$	0	-4
$1 + S + b_3 +$	$(1,2)$	0	2	2	0	0	$(1,1)$	$(1,1,2,1)$	0	0
$\alpha + \beta + 2\gamma$	$(1,2)$	0	-2	-2	0	0	$(1,1)$	$(1,1,2,1)$	0	0
$1 + b_1 +$	$(4,1)$	0	0	0	0	0	$(2,1)$	$(1,1,1,2)$	0	0
$b_2 + 2\gamma$										
$1 + S + b_1 +$	$(1,2)$	0	0	0	4	0	$(1,1)$	$(1,1,1,2)$	0	0
$b_2 + b_3 + 2\gamma$	$(1,2)$	0	0	0	-4	0	$(1,1)$	$(1,1,1,2)$	0	0

Table A.1.1: The spectrum of the model described in table 5.3.1 and matrix (5.3.6), which does not exhibit an enhanced symmetry.

SEC & Field	$SU(4)$ $\times SO(5)$	Q_R	Q_1	Q_2	Q_3	Q_4	Q_5	Q_6	$SU(4)_H \times SU(2)_{H_3} \times SU(2)_{H_2}$	Q_7	Q_8
0:											
ϕ_1, $\bar{\phi}_1$	**(1,1)**	**0**	**0**	∓ 1	∓ 1	**0**	**0**	**0**	$(1,1,1)$	**0**	**0**
ϕ_2, $\bar{\phi}_2$	**(1,1)**	**0**	**0**	± 1	∓ 1	**0**	**0**	**0**	$(1,1,1)$	**0**	**0**
ϕ_3, $\bar{\phi}_3$	**(1,1)**	**0**	∓ 1	**0**	∓ 1	**0**	**0**	**0**	$(1,1,1)$	**0**	**0**
ϕ_4, $\bar{\phi}_4$	**(1,1)**	**0**	± 1	**0**	∓ 1	**0**	**0**	**0**	$(1,1,1)$	**0**	**0**
ϕ_5, $\bar{\phi}_3$	**(1,1)**	**0**	∓ 1	∓ 1	**0**	**0**	**0**	**0**	$(1,1,1)$	**0**	**0**
ϕ_6, $\bar{\phi}_6$	**(1,1)**	**0**	∓ 1	± 1	**0**	**0**	**0**	**0**	$(1,1,1)$	**0**	**0**
b_1	$(\bar{4},1)$	**-4**	**2**	**0**	**0**	**2**	**0**	**0**	$(1,1,1)$	**0**	**0**
	$(\bar{4},1)$	**4**	**2**	**0**	**0**	**-2**	**0**	**0**	$(1,1,1)$	**0**	**0**
	$(\bar{4},1)$	**4**	**-2**	**0**	**0**	**2**	**0**	**0**	$(1,1,1)$	**0**	**0**
	$(\bar{4},1)$	**-4**	**-2**	**0**	**0**	**-2**	**0**	**0**	$(1,1,1)$	**0**	**0**
b_2	$(\bar{4},1)$	**4**	**0**	**-2**	**0**	**0**	**-2**	**0**	$(1,1,1)$	**0**	**0**
	$(\bar{4},1)$	**-4**	**0**	**-2**	**0**	**0**	**2**	**0**	$(1,1,1)$	**0**	**0**
	$(\bar{4},1)$	**-4**	**0**	**2**	**0**	**0**	**-2**	**0**	$(1,1,1)$	**0**	**0**
	$(\bar{4},1)$	**4**	**0**	**2**	**0**	**0**	**2**	**0**	$(1,1,1)$	**0**	**0**
$b_3 \oplus b_3 +$	$(4,4)$	**0**	**0**	**0**	**2**	**0**	**0**	**-2**	$(1,1,1)$	**0**	**0**
$\zeta + 2\gamma$	$(4,4)$	**0**	**0**	**0**	**2**	**0**	**0**	**2**	$(1,1,1)$	**0**	**0**
$S + 2\gamma$:	$(1,1)$	**-4**	**0**	**0**	**0**	**0**	**0**	**0**	$(6,1,1)$	**4**	**0**
	$(1,1)$	**4**	**0**	**0**	**0**	**0**	**0**	**0**	$(6,1,1)$	**-4**	**0**
S_1, $\bar{S}_1$	$(1,1)$	∓ 4	**0**	**0**	**0**	**0**	**0**	**0**	$(1,1,1)$	∓ 4	± 8
S_2, $\bar{S}_2$	$(1,1)$	∓ 4	**0**	**0**	**0**	**0**	**0**	**0**	$(1,1,1)$	∓ 4	∓ 8

Table A.2.1: The spectrum of the model described in table 5.3.2 and matrix (5.3.12), which does exhibit an enhanced symmetry.

SEC & Field	$SU(4)$ $\times SO(5)$	Q_R	Q_1	Q_2	Q_3	Q_4	Q_5	Q_6	$SU(4)_H \times SU(2)_{H_3} \times SU(2)_{H_2}$	Q_7	Q_8
$b_2+\alpha+2\gamma$											
S_3, $\bar{S}_3$	$(1,1)$	0	0	∓ 2	0	∓ 2	∓ 2	∓ 2	$(1,1,1)$	∓ 4	0
S_4, $\bar{S}_4$	$(1,1)$	0	0	∓ 2	0	∓ 2	± 2	∓ 2	$(1,1,1)$	± 4	0
S_5, $\bar{S}_5$	$(1,1)$	0	0	∓ 2	0	∓ 2	∓ 2	± 2	$(1,1,1)$	∓ 4	0
S_6, $\bar{S}_6$	$(1,1)$	0	0	∓ 2	0	∓ 2	± 2	± 2	$(1,1,1)$	± 4	0
S_7, $\bar{S}_7$	$(1,1)$	0	0	∓ 2	0	± 2	∓ 2	∓ 2	$(1,1,1)$	± 4	0
S_8, $\bar{S}_8$	$(1,1)$	0	0	∓ 2	0	± 2	± 2	∓ 2	$(1,1,1)$	∓ 4	0
S_9, $\bar{S}_9$	$(1,1)$	0	0	∓ 2	0	± 2	∓ 2	± 2	$(1,1,1)$	± 4	0
S_{10}, $\bar{S}_{10}$	$(1,1)$	0	0	∓ 2	0	± 2	± 2	± 2	$(1,1,1)$	∓ 4	0
$S+b_2+$	$(1,1)$	2	0	2	2	0	-2	0	$(4,1,1)$	0	0
$b_3+\alpha+$	$(1,1)$	2	0	-2	2	0	2	0	$(4,1,1)$	0	0
$\beta \pm \gamma$	$(1,1)$	2	0	-2	2	0	2	0	$(1,2,1)$	-2	0
	$(1,1)$	2	0	2	2	0	-2	0	$(1,2,1)$	-2	0
	$(1,1)$	-2	0	-2	2	0	-2	0	$(\bar{4},1,1)$	0	0
	$(1,1)$	-2	0	2	2	0	2	0	$(\bar{4},1,1)$	0	0
	$(1,1)$	-2	0	2	2	0	2	0	$(1,2,1)$	2	0
	$(1,1)$	-2	0	-2	2	0	-2	0	$(1,2,1)$	2	0

Table A.2.2: Table A.2.1 continued

SEC	$SU(4)\times$ $SO(5)$	Q_R	Q_1	Q_2	Q_3	Q_4	Q_5	Q_6	$SU(4)_H \times SU(2)_{H_3}$ $SU(2)_{H_2}$	Q_7	Q_8
$S+b_1+b_3+$	$(1,1)$	2	-2	0	2	-2	0	0	$(4,1,1)$	0	0
$\alpha+\beta\pm\gamma$	$(1,1)$	2	2	0	2	2	0	0	$(4,1,1)$	0	0
	$(1,1)$	2	2	0	2	2	0	0	$(1,2,1)$	-2	0
	$(1,1)$	2	-2	0	2	-2	0	0	$(1,2,1)$	-2	0
	$(1,1)$	-2	2	0	2	-2	0	0	$(\bar{4},1,1)$	0	0
	$(1,1)$	-2	-2	0	2	2	0	0	$(\bar{4},1,1)$	0	0
	$(1,1)$	-2	-2	0	2	2	0	0	$(1,2,1)$	2	0
	$(1,1)$	-2	2	0	2	-2	0	0	$(1,2,1)$	2	0
$S+b_1+b_2+$ $\alpha+\beta\oplus$	$(1,4)$	0	-2	-2	0	0	0	0	$(1,1,2)$	0	0
$S+b_1+b_2+$ $\alpha+\beta+\zeta+2\gamma$	$(1,4)$	0	2	2	0	0	0	0	$(1,1,2)$	0	0
$1+b_1+$	$(1,1)$	2	0	2	2	0	-2	0	$(1,1,2)$	0	0
$\alpha+\beta\pm\gamma$	$(1,1)$	2	0	-2	2	0	2	0	$(1,1,2)$	0	0
	$(1,1)$	-2	0	-2	2	0	-2	0	$(1,1,2)$	0	0
	$(1,1)$	-2	0	2	2	0	2	0	$(1,1,2)$	0	0
$1+b_2+$	$(1,1)$	2	2	0	2	2	0	0	$(1,1,2)$	0	0
$\alpha+\beta\pm\gamma$	$(1,1)$	2	-2	0	2	-2	0	0	$(1,1,2)$	0	0
	$(1,1)$	-2	-2	0	2	2	0	0	$(1,1,2)$	0	0
	$(1,1)$	-2	2	0	2	-2	0	0	$(1,1,2)$	0	0

Table A.2.3: Table A.2.2 continued

	1		2		3		total		net
No.	+	−	+	−	+	−	+	−	
1	16	0	8	0	8	0	32	0	32
2	8	0	8	0	8	0	24	0	24
3	8	0	8	0	4	0	20	0	20
4	8	0	6	2	4	0	18	2	16
5	8	0	4	0	4	0	16	0	16
6	12	4	4	0	4	0	20	4	16
7	8	0	8	0	4	4	20	4	16
8	6	2	4	0	4	0	14	2	12
9	4	0	4	0	4	0	12	0	12
10	8	0	2	0	2	0	12	0	12
11	4	0	4	0	2	0	10	0	10
12	4	0	4	0	3	1	11	1	10
13	6	2	4	0	2	0	12	2	10
14	4	4	4	0	4	0	12	4	8
15	4	0	4	0	2	2	10	2	8
16	4	0	3	1	2	0	9	1	8
17	4	0	2	0	2	0	8	0	8
18	6	2	3	1	2	0	11	3	8
19	6	2	2	0	2	0	10	2	8
20	10	6	2	0	2	0	14	6	8
21	6	2	4	0	2	2	12	4	8
22	3	1	3	1	2	0	8	2	6
23	3	1	2	0	2	0	7	1	6
24	2	0	2	0	2	0	6	0	6
25	4	0	2	2	2	0	8	2	6
26	4	0	2	0	1	1	7	1	6
27	4	0	1	0	1	0	6	0	6
28	6	2	1	0	1	0	8	2	6
29	3	1	3	1	1	0	7	2	5
30	2	0	2	0	1	0	5	0	5

Table B.1.1: Inequivalent liftable S^3 models with a $\mathbb{E}_6 \times U(1)^2 \times SO(8) \times SO(8)$ gauge group. The chiral content of each model is listed per plane and numbered, $+$ lists all the positive chiral states per plane while $-$ lists all the negative states per plane. The total sum of all the planes is then listed and subsequently the net total number of chiral states. The list is ordered by the total net number of chiral states.

	1		2		3		total		net
No.	+	−	+	−	+	−	+	−	
31	3	1	2	0	1	0	6	1	5
32	3	1	2	0	2	2	7	3	4
33	2	2	2	0	2	0	6	2	4
34	4	4	2	0	2	0	8	4	4
35	4	0	2	2	2	2	8	4	4
36	3	1	2	0	1	1	6	2	4
37	2	0	2	0	1	1	5	1	4
38	2	0	1	0	1	0	4	0	4
39	3	1	1	0	1	0	5	1	4
40	1	1	3	1	3	1	7	3	4
41	2	0	1	0	1	1	4	1	3
42	3	1	1	1	1	0	5	2	3
43	1	0	1	0	1	0	3	0	3
44	2	0	1	1	1	1	4	2	2
45	2	0	2	0	1	3	5	3	2
46	2	2	2	0	1	1	5	3	2
47	1	1	1	0	1	0	3	1	2
48	2	2	1	0	1	0	4	2	2
49	4	4	1	0	1	0	6	4	2
50	1	1	1	1	3	1	5	3	2
51	1	1	1	0	1	1	3	2	1
52	1	1	0	1	3	1	4	3	1
53	2	2	2	2	2	2	6	6	0
54	2	0	2	2	1	3	5	5	0
55	2	2	1	1	1	1	4	4	0
56	4	4	2	2	2	2	8	8	0
57	4	4	1	1	1	1	6	6	0
58	1	1	1	1	1	1	3	3	0
59	2	2	2	2	1	1	5	5	0
60	1	3	1	0	1	0	3	3	0
61	4	4	4	4	4	4	12	12	0

Table B.1.2: Table B.1.1 continued.

	1		2		3		total		net
No.	+	−	+	−	+	−	+	−	
1	16	0	8	0	8	0	32	0	32
2	8	0	8	0	8	0	24	0	24
3	8	0	6	2	4	0	18	2	16
4	8	0	4	0	4	0	16	0	16
5	12	4	4	0	4	0	20	4	16
6	8	0	8	0	4	4	20	4	16
7	6	2	4	0	4	0	14	2	12
8	4	0	4	0	4	0	12	0	12
9	4	4	4	0	4	0	12	4	8
10	4	0	4	0	2	2	10	2	8
11	4	0	3	1	2	0	9	1	8
12	4	0	2	0	2	0	8	0	8
13	6	2	3	1	2	0	11	3	8
14	6	2	2	0	2	0	10	2	8
15	10	6	2	0	2	0	14	6	8
16	6	2	4	0	2	2	12	4	8
17	3	1	3	1	2	0	8	2	6
18	3	1	2	0	2	0	7	1	6
19	2	0	2	0	2	0	6	0	6
20	3	1	2	0	2	2	7	3	4
21	2	2	2	0	2	0	6	2	4
22	4	4	2	0	2	0	8	4	4
23	4	0	2	2	2	2	8	4	4
24	3	1	2	0	1	1	6	2	4
25	2	0	2	0	1	1	5	1	4
26	1	1	3	1	3	1	7	3	4
27	2	0	1	1	1	1	4	2	2
28	1	1	1	1	3	1	5	3	2
29	2	2	2	2	2	2	6	6	0
30	2	0	2	2	1	3	5	5	0
31	2	2	1	1	1	1	4	4	0
32	4	4	2	2	2	2	8	8	0
33	4	4	1	1	1	1	6	6	0
34	1	1	1	1	1	1	3	3	0
35	4	4	4	4	4	4	12	12	0

Table B.1.3: Inequivalent liftable S^3 models with a $\mathbb{E}_6 \times U(1)^2 \times SO(16)$ gauge group. The chiral content of each model is listed per plane and numbered, $+$ lists all the positive chiral states per plane while $-$ lists all the negative states per plane. The total sum of all the planes is then listed and subsequently the net total number of chiral states. The list is ordered by the total net number of chiral states.

	1		2		3		total		net
No.	+	−	+	−	+	−	+	−	
1	16	0	16	0	16	0	48	0	48
2	12	4	8	0	8	0	28	4	24
3	8	0	8	0	8	0	24	0	24
4	10	6	4	0	4	0	18	6	12
5	6	2	6	2	4	0	16	4	12
6	6	2	4	0	4	0	14	2	12
7	4	0	4	0	4	0	12	0	12
8	3	1	3	1	3	1	9	3	6
9	4	4	2	2	2	2	8	8	0
10	4	4	4	4	4	4	12	12	0
11	2	2	2	2	2	2	6	6	0

Table B.1.4: Inequivalent liftable S^3 models with a $\mathbb{E}_6 \times U(1)^2 \times \mathbb{E}_8$ gauge group. The chiral content of each model is listed per plane and numbered, $+$ lists all the positive chiral states per plane while $-$ lists all the negative states per plane. The total sum of all the planes is then listed and subsequently the net total number of chiral states. The list is ordered by the total net number of chiral states.

	1		2		total		net
No.	+	−	+	−	+	−	
1	16	0	16	0	32	0	32
2	12	4	8	0	20	4	16
3	8	0	8	0	16	0	16
4	10	6	4	0	14	6	8
5	6	2	6	2	12	4	8
6	4	0	4	0	8	0	8
7	3	1	3	1	6	2	4
8	8	8	8	8	16	16	0
9	4	4	4	4	8	8	0
10	2	2	2	2	4	4	0
11	0	0	0	0	0	0	0

Table B.2.1: Inequivalent simple S^2V models. The chiral content of each model is listed per plane and numbered, $+$ lists all the positive chiral states per plane while $-$ lists all the negative states per plane. The total sum of all the planes is then listed and subsequently the net total number of chiral states. The list is ordered by the total net number of chiral states.

Bibliography

[1] G. ALTARELLI AND M. W. GRUNEWALD, *Precision electroweak tests of the standard model*, hep-ph/0404165, (2004).

[2] C. ANGELANTONJ AND A. SAGNOTTI, *Open strings*, Phys. Rept., 371 (2002), pp. 1–150.

[3] I. ANTONIADIS AND C. BACHAS, *4-D fermionic superstrings with arbitrary twists*, Nucl. Phys., B298 (1988), p. 586.

[4] I. ANTONIADIS, C. BACHAS, C. KOUNNAS, AND P. WINDEY, *Supersymmetry among free fermions and superstrings*, Phys. Lett., B171 (1986), p. 51.

[5] I. ANTONIADIS, C. P. BACHAS, AND C. KOUNNAS, *Four-dimensional superstrings*, Nucl. Phys., B289 (1987), p. 87.

[6] I. ANTONIADIS, J. R. ELLIS, J. S. HAGELIN, AND D. V. NANOPOULOS, *Gut model building with fermionic four-dimensional strings*, Phys. Lett., B205 (1988), p. 459.

[7] ——, *The flipped $SU(5) \times U(1)$ string model revamped*, Phys. Lett., B231 (1989), p. 65.

[8] I. ANTONIADIS, G. K. LEONTARIS, AND J. RIZOS, *A three generation $SU(4) \times O(4)$ string model*, Phys. Lett., B245 (1990), pp. 161–168.

[9] Z. BERN, *Perturbative quantum gravity and its relation to gauge theory*, Living Rev. Rel., 5 (2002), p. 5.

[10] G. B. CLEAVER, D. J. CLEMENTS, AND A. E. FARAGGI, *Flat directions in left-right symmetric string derived models*, Phys. Rev., D65 (2002), p. 106003.

[11] G. B. CLEAVER, A. E. FARAGGI, AND D. V. NANOPOULOS, *String derived* MSSM *and M-theory unification*, Phys. Lett., B455 (1999), pp. 135–146.

[12] G. B. CLEAVER, A. E. FARAGGI, D. V. NANOPOULOS, AND J. W. WALKER, *Phenomenological study of a minimal superstring standard model*, Nucl. Phys., B593 (2001), pp. 471–504.

[13] G. B. CLEAVER, A. E. FARAGGI, AND S. NOOIJ, NAHE*-based string models with* $SU(4) \times SU(2) \times U(1)$ $SO(10)$ *subgroup*, Nucl. Phys., B672 (2003), pp. 64–86.

[14] G. B. CLEAVER, A. E. FARAGGI, AND C. SAVAGE, *Left-right symmetric heterotic-string derived models*, Phys. Rev., D63 (2001), p. 066001.

[15] B. T. CLEVELAND ET AL., *Measurement of the solar electron neutrino flux with the homestake chlorine detector*, Astrophys. J., 496 (1998), pp. 505–526.

[16] J. R. ELLIS, A. E. FARAGGI, AND D. V. NANOPOULOS, *M-theory model-building and proton stability*, Phys. Lett., B419 (1998), pp. 123–131.

[17] A. ERDLYI ET AL., *Higher transcendental functions*, vol. 2, Mc Graw-Hill Book Company, 1953.

[18] A. E. FARAGGI, *Construction of realistic standard - like models in the free fermionic superstring formulation*, Nucl. Phys., B387 (1992), pp. 239–262.

[19] ——, *Fractional charges in a superstring derived standard like model*, Phys. Rev., D46 (1992), pp. 3204–3207.

[20] ——, *Hierarchical top - bottom mass relation in a superstring derived standard - like model*, Phys. Lett., B274 (1992), pp. 47–52.

[21] ——, *A new standard - like model in the four-dimensional free fermionic string formulation*, Phys. Lett., B278 (1992), pp. 131–139.

[22] ——, *Aspects of nonrenormalizable terms in a superstring derived standard - like model*, Nucl. Phys., B403 (1993), pp. 101–121.

[23] ——, *Custodial nonabelian gauge symmetries in realistic superstring derived models*, Phys. Lett., B339 (1994), pp. 223–231.

[24] ——, $\mathbb{Z}_2 \times \mathbb{Z}_2$ *orbifold compactification as the origin of realistic free fermionic models*, Phys. Lett., B326 (1994), pp. 62–68.

[25] ——, *Superstring phenomenology: Present and future perspective*, hep-ph/9707311, (1997).

[26] ——, *Toward the classification of the realistic free fermionic models*, Int. J. Mod. Phys., A14 (1999), pp. 1663–1702.

[27] ——, *Phenomenological aspects of M-theory*, hep-th/0208125, (2002).

[28] ——, *Phenomenological survey of M-theory*, hep-th/0307037, (2003).

[29] A. E. FARAGGI, C. KOUNNAS, S. E. M. NOOIJ, AND J. RIZOS, *Towards the classification of $\mathbb{Z}_2 \times \mathbb{Z}_2$ fermionic models*, hep-th/0311058, (2003).

[30] ——, *Classification of the chiral $\mathbb{Z}_2 \times \mathbb{Z}_2$ fermionic models in the heterotic superstring*, Nucl. Phys., B695 (2004), pp. 41–72. hep-th/0403058.

[31] ——, *Classification of the chiral $\mathbb{Z}_2 \times \mathbb{Z}_2$ fermionic models in the heterotic superstring II*, In preparation and to be sent to Nucl. Phys. B, (2004).

[32] A. E. FARAGGI AND D. V. NANOPOULOS, *Naturalness of three generations in free fermionic $\mathbb{Z}_2^n \times \mathbb{Z}_4$ string models*, Phys. Rev., D48 (1993), pp. 3288–3296.

[33] A. E. FARAGGI, D. V. NANOPOULOS, AND K. YUAN, *A standard like model in the 4-D free fermionic string formulation*, Nucl. Phys., B335 (1990), p. 347.

[34] S. FERRARA, L. GIRARDELLO, C. KOUNNAS, AND M. PORRATI, *Effective lagrangians for four-dimensional superstrings*, Phys. Lett., B192 (1987), p. 368.

[35] ——, *The effective interactions of chiral families in four- dimensional superstrings*, Phys. Lett., B194 (1987), p. 358.

[36] S. FERRARA AND C. KOUNNAS, *Extended supersymmetry in four-dimensional type II strings*, Nucl. Phys., B328 (1989), p. 406.

[37] S. FERRARA, C. KOUNNAS, M. PORRATI, AND F. ZWIRNER, *Effective superhiggs and $StrM^2$ from four-dimensional strings*, Phys. Lett., B194 (1987), p. 366.

[38] ——, *Superstrings with spontaneously broken supersymmetry and their effective theories*, Nucl. Phys., B318 (1989), p. 75.

[39] Y. FUKUDA ET AL., *Evidence for oscillation of atmospheric neutrinos*, Phys. Rev. Lett., 81 (1998), pp. 1562–1567.

[40] P. H. GINSPARG, *Applied conformal field theory*, in Fields, strings, critical phenomena : proceedings, E. Brezin and J. Zinn-Justin, eds., Les Houches Summer School in Theoretical Physics, North-Holland, 1988, p. 640. hep-th/9108028.

[41] M. B. GREEN, *Supersymmetrical dual string theories and their field theory limits: A review*, Surveys High Energ. Phys., 3 (1984), pp. 127–160.

[42] M. B. GREEN AND J. H. SCHWARZ, *Anomaly cancellation in supersymmetric D=10 gauge theory and superstring theory*, Phys. Lett., B149 (1984), pp. 117–122.

[43] M. B. GREEN, J. H. SCHWARZ, AND E. WITTEN, *Superstring theory*, vol. 1: Introduction of Cambridge Monographs On Mathematical Physics, Cambridge University Press, 1987.

[44] ——, *Superstring theory*, vol. 2: Loop amplitudes, anomalies and phenomenology of Cambridge Monographs On Mathematical Physics, Cambridge University Press, 1987.

[45] A. GREGORI, C. KOUNNAS, AND P. M. PETROPOULOS, *Non-perturbative triality in heterotic and type II $N = 2$ strings*, Nucl. Phys., B553 (1999), pp. 108–132.

[46] A. GREGORI, C. KOUNNAS, AND J. RIZOS, *Classification of the $N = 2$, $\mathbb{Z}_2 \times \mathbb{Z}_2$-symmetric type II orbifolds and their type II asymmetric duals*, Nucl. Phys., B549 (1999), pp. 16–62.

[47] D. J. GROSS, J. A. HARVEY, E. J. MARTINEC, AND R. ROHM, *The heterotic string*, Phys. Rev. Lett., 54 (1985), pp. 502–505.

[48] K. HAGIWARA ET AL., *Review of particle physics*, Phys. Rev., D66 (2002), p. 010001.

[49] P. HORAVA AND E. WITTEN, *Eleven-dimensional supergravity on a manifold with boundary*, Nucl. Phys., B475 (1996), pp. 94–114.

[50] ——, *Heterotic and type I string dynamics from eleven dimensions*, Nucl. Phys., B460 (1996), pp. 506–524.

[51] H. KAWAI, D. C. LEWELLEN, AND S. H. H. TYE, *Construction of fermionic string models in four- dimensions*, Nucl. Phys., B288 (1987), p. 1.

[52] S. V. KETOV, *Conformal field theory*, Singapore: World Scientific, 1995.

[53] E. KIRITSIS, *Introduction to non-perturbative string theory*, hep-th/9708130, (1997).

[54] ——, *Introduction to superstring theory*, Leuven University Press, 1998. hep-th/9709062.

[55] E. KIRITSIS AND C. KOUNNAS, *Perturbative and non-perturbative partial supersymmetry breaking:* $N = 4 \to N = 2 \to N = 1$, Nucl. Phys., B503 (1997), pp. 117–156.

[56] E. KIRITSIS, C. KOUNNAS, P. M. PETROPOULOS, AND J. RIZOS, *Universality properties of* $N = 2$ *and* $N = 1$ *heterotic threshold corrections*, Nucl. Phys., B483 (1997), pp. 141–171.

[57] ——, *String threshold corrections in models with spontaneously broken supersymmetry*, Nucl. Phys., B540 (1999), pp. 87–148.

[58] G. K. LEONTARIS AND J. RIZOS, $N = 1$ *supersymmetric* $SU(4) \times SU(2)_L \times SU(2)_R$ *effective theory from the weakly coupled heterotic superstring*, Nucl. Phys., B554 (1999), pp. 3–49.

[59] J. L. LOPEZ, *Supersymmetry: From the fermi scale to the planck scale*, Rept. Prog. Phys., 59 (1996), pp. 819–865.

[60] J. L. LOPEZ, D. V. NANOPOULOS, AND K. YUAN, *The search for a realistic flipped* $SU(5)$ *string model*, Nucl. Phys., B399 (1993), pp. 654–690.

[61] ——, *Moduli and kähler potential in fermionic strings*, Phys. Rev., D50 (1994), pp. 4060–4074.

[62] J. D. LYKKEN, *Four-dimensional superstring models*, hep-ph/9511456, (1995).

[63] B. M. MCCOY AND T. T. WU, *The two-dimensional Ising model*, Harvard University Press, 1973.

[64] K. S. NARAIN, *New heterotic string theories in uncompactified dimensions* < 10, Phys. Lett., B169 (1986), p. 41.

[65] K. S. NARAIN, M. H. SARMADI, AND E. WITTEN, *A note on toroidal compactification of heterotic string theory*, Nucl. Phys., B279 (1987), p. 369.

[66] S. E. M. NOOIJ, *Change of topology in string theory*, Master's thesis, University of Amsterdam, June 2001.

[67] J. POLCHINSKI, *String theory*, vol. 2: Superstring theory and beyond, Cambridge University Press, 1998.

[68] ——, *String theory*, vol. 1: An introduction to the bosonic string, Cambridge University Press, 1998.

[69] F. QUEVEDO, *Lectures on superstring phenomenology*, hep-th/9603074, (1996).

[70] P. RAMOND, *Journeys beyond the standard model*, Frontiers in Physics, Westview Press, 2004.

[71] A. N. SCHELLEKENS, *Introduction to conformal field theory*, Fortsch. Phys., 44 (1996), pp. 605–705.

[72] J. H. SCHWARZ, *Superstring theory*, Phys. Rept., 89 (1982), pp. 223–322.

[73] P. K. TOWNSEND, *Four lectures on M-theory*, hep-th/9612121, (1996).